T2R2 東京科学大学 リサーチリポジトリ
Science Tokyo Research Repository

論文 / 著書情報
Article / Book Information

題目(和文)	
Title(English)	Shape-changing and Variable-stiffness Interface using Pneumatic Actuators
著者(和文)	Jefferson Pardomuan
Author(English)	Pardomuan Jefferson
出典(和文)	学位:博士(学術), 学位授与機関:東京工業大学, 報告番号:甲第12594号, 授与年月日:2023年9月22日, 学位の種別:課程博士, 審査員:小池 英樹,三宅 美博,德永 健伸,金﨑 朝子,下坂 正倫
Citation(English)	Degree:Doctor (Academic), Conferring organization: Tokyo Institute of Technology, Report number:甲第12594号, Conferred date:2023/9/22, Degree Type:Course doctor, Examiner:,,,,
学位種別(和文)	博士論文
Type(English)	Doctoral Thesis

Powered by T2R2 (Science Tokyo Research Repository)

Doctoral Dissertation

Shape-changing and Variable-stiffness Interface using Pneumatic Actuators

Tokyo Institute of Technology

School of Computing

Department of Computer Science

Name : Jefferson Pardomuan

Supervisor : Professor Hideki Koike

Submission Date : August 2023

Acknowledgments

I would like to express my deepest gratitude to Professor Hideki Koike, for all the guidance, constant supervision, and feedback throughout my study and research. Further, I want to thank Shio Miyafuji, Erwin Wu, and Nobuhiro Takahashi for their ongoing support, and encouragement.

I would also like express much appreciation to the School of Computing of the Tokyo Institute of Technology for providing such excellent facilities and a wonderful working environment for me to undertake my study.

Many thanks also to my fellow lab members within the Koike Lab for all the support and friendship during my study. Particular thanks are extended to Jana Howard, Daichi Saito, Liao Chen, Luna Takagi, Yuka Tashiro, and Eri Nagatomo for their input and discussion on this project.

Special thanks to the Indonesian community at Reformed Evangelical Church in Tokyo for their friendships that made Tokyo feel like home.

Finally, I would like to thank my wife Febrina and my daughter Astrella for their unconditional love and support during my study at the Tokyo Institute of Technology. I would not have been able to complete this thesis without their unconditional love, support, and encouragement.

Abstract

Shape-changing interface is an ongoing multi-disciplinary study that has great promise for future application. Despite the possibilities, entry to shape-changing interface research is challenging due to the required knowledge of both complex electronics and mechanical engineering. These complexities increase exponentially when physical properties such as variable-stiffness are added into the systems. This research focuses on the development of a framework for prototyping shape-changing and variable-stiffness interfaces using pneumatic actuation. The aim is to facilitate the creation of interfaces that are intuitive, lightweight, cost-effective, and easily scalable.

The first part of this study introduces ClaytricSurface, a novel approach to 2.5D modeling with variable stiffness capabilities. This system adapts to various modeling tasks by adjusting its stiffness to match the requirements. It also provides dynamic haptic feedback, simulating different brush types in paint applications. While ClaytricSurface is effective for manual shape modeling, it lacks self-actuation capabilities.

To address the limitations of ClaytricSurface, the second part introduces ASTRE, a programmable shape-changing and variable stiffness mechanism. This novel concept utilizes mechanical constraints to modify the behavior of pneumatic artificial muscles (PAMs) and achieves a breakthrough by simplifying the combination of shape deformation and stiffness tuning in shape-changing interfaces.

The third part leverages the benefits of the ASTRE mechanism as a prototyping tool for shape-changing interfaces. Two methods are proposed: the ASTRE Toolkit, which enables constructive assembly of truss structures, and VabricBeads, which explores fabric structures design and implementations. These prototyping tools facilitate an intuitive, convenient, and rapid prototyping process, with low-cost materials and accessible fabrication tools.

Finally, the thesis summarizes its contributions, discusses design implications, and highlights future research directions for the proposed shape-changing and variable-stiffness prototyping framework. By addressing the complexity barriers and providing accessible tools, this research aims to empower designers and researchers to explore the possibilities of shape-changing interfaces and pave the way for their widespread adoption.

Contents

List of Figures

List of Tables

Chapter 1

Background

1.1 Shape-changing Interface Overview

The shape-changing interface represents a groundbreaking technology that has the potential to transform the paradigm of human-computer interaction. It presents a wide range of advantages, including enhanced user experiences through novel and intuitive interactions. This type of interface possesses the capability to adapt to various environments and tasks, allowing for personalized customization. Moreover, it opens up new avenues for design, enabling dynamic functionality and serving as visually appealing aesthetics [6].

The idea of the shape-changing interface can be traced back to Sutherland's Ultimate Display [188] that was published in 1965. He describes display interfaces that incorporate our perceptual motor skills, enabling a direct interaction similar to our interactions with the physical world. These interfaces capitalize on our haptic and kinaesthetic senses, leveraging our innate understanding of physical 3D forms [6]. The concept of shape-changing interface also has roots in Tangible User Interfaces (TUI) where users can interact with computers through physical embodiments of information [70]. It also has roots in Organic User Interface (OUI), where the computer interface uses a non-planar display as a primary means of input-output. When OUIs have the ability to become the data on display through deformation, either via manipulation or actuation [65].

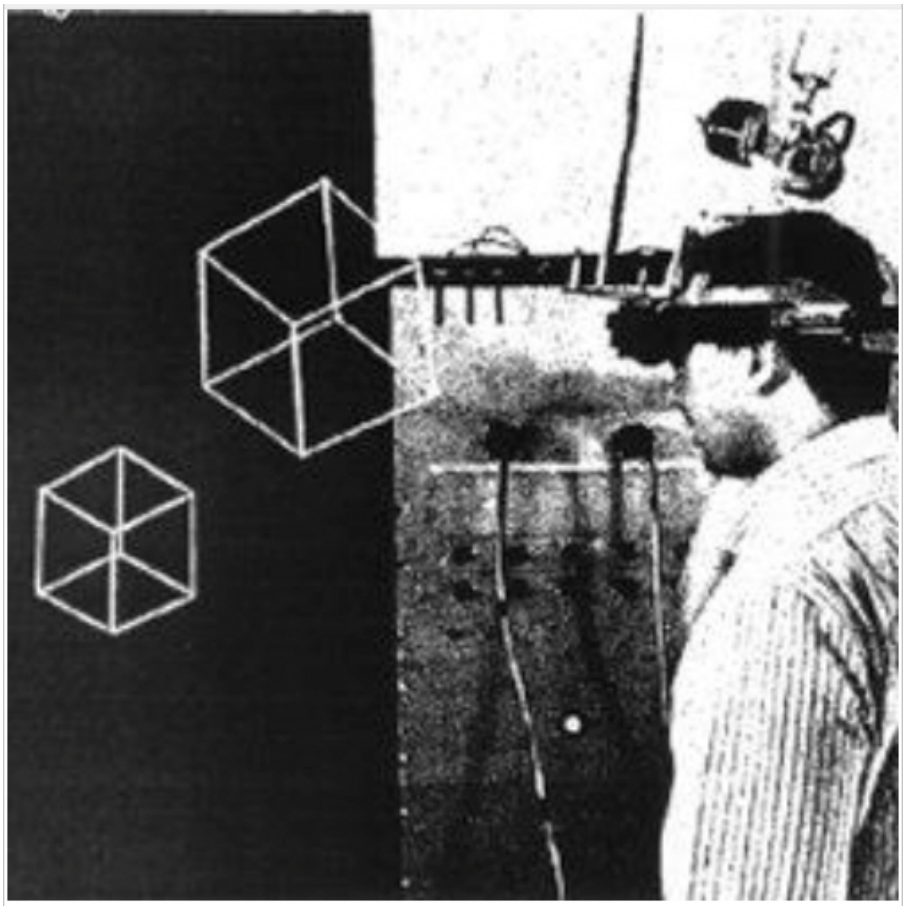

Figure 1.1: Sutherland's vision on Ultimate Display'1965 [188]

1.2 Deformation Properties of Shape-changing interface

Based on the deformation properties, shape-changing interfaces can be classified into passive and active shape-change.

1.2.1 Passive Shape-change

Passive shape-change refers to shape deformation that resulted from the user's direct physical manipulation. This concept often intersects with Tangible User Interfaces, where users can interact with digital information through physical objects

Figure 1.2: IlluminatingClay: an early example of passive shape-changing interfaces[152]

[155].

Previous works have proposed the utilization of continuous tangible material (such as clay, sand, and cloth) for rapid modeling of landscape design [69, 152] and visualize time distortion [21]. By incorporating digital input-output, these studies successfully enhanced passive materials, leading to intuitive and immersive interactions. Furthermore, advancements in digital fabrication technologies have enabled researchers to investigate shape transformations in customized deformable objects [68, 83, 160, 181] and adaptable structures [52, 64, 185]. These studies have laid the groundwork for interaction techniques facilitated by the concept of a non-rigid interface.

To further enhance the interaction capabilities of passive shape-change interfaces, previous studies have introduced the concept of variable-stiffness interface [42, 61, 120, 144, 217]. This approach focuses on modifying the physical properties, specifically the stiffness, of the interface. Although it doesn't directly alter

the shape of the interface, it significantly impacts its malleability, affordance, and adaptability. This concept holds promise for various areas of HCI research, although its exploration has been limited due to challenges related to design complexity and scalability [3].

1.2.2 Active Shape-change

Active shape-change refers to the self-actuated interface that can dynamically change the shapes and structures. The most typical active shape-changing interface is the pin-array display [43, 53, 71, 154, 193], wherein rods are vertically actuated to form a 2.5D surface. Recent development in pin-array displays proposed modular reconfigurable display [59] and swarm robot embedded with haptic display [190, 191]. Materiable [132] demonstrates the feasibility of rendering various material properties (flexibility, elasticity, and viscosity) through direct touch interaction and dynamic pin controls. Nevertheless, certain limitations, such as responsivity and surface stiffness, arise from the constraints of the actuator used in rigid bodies.

To achieve a programmable shape-changing material using digital fabrication, Tibbit et al. proposed 4D printing concept [203]. It refers to the process of utilizing smart materials that are initially fabricated through 3D printing, which subsequently exhibit changes in their shape or properties over time in response to external stimuli such as heat, humidity, light, or chemicals [76, 186, 199, 214]. These studies presented self-assembling and adaptive structures that have potential applications in robotics, architecture, and biomedical [30, 50, 203]. The typical limitations of 4D printed interfaces include non-reversible and slow actuation speed, which is not suitable for interactive applications.

In order to achieve both the convenience of digital fabrication with responsive shape-changing capabilities, previous studies also explored novel fabrication techniques. These techniques include 3D printed inflatables [84, 225], heat sealing [157, 169], machine knitting [4, 85], and electronic printing [8, 213]. These studies have demonstrated the efficiency of prototyping using computer-aided design tools

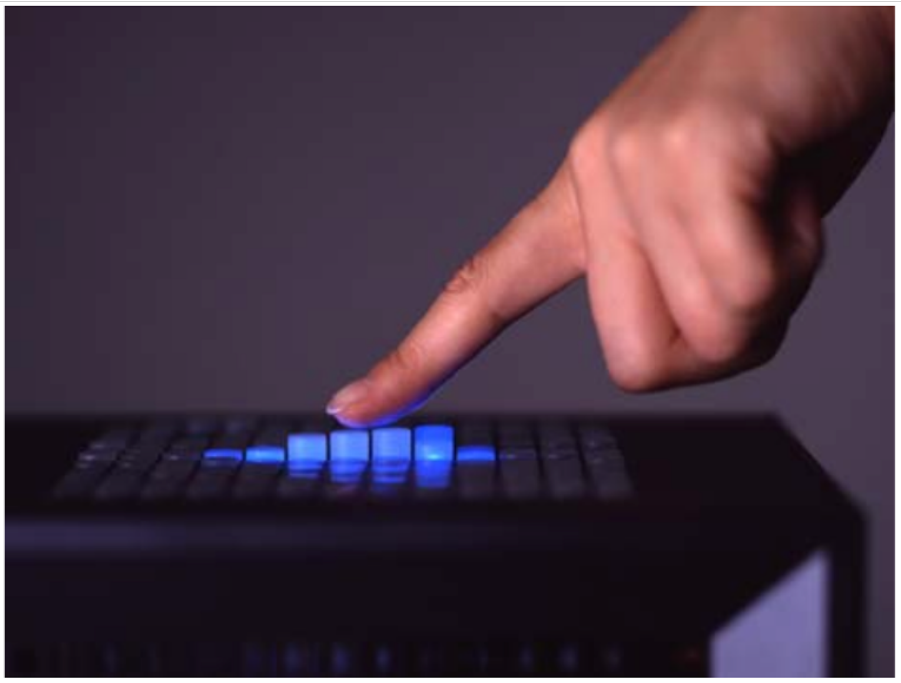

Figure 1.3: Lumen: an example of active shape-change pin array display[154]

and digital fabrication technologies. However, most of these approaches were designed with predetermined actuated shapes, which limits their application to specific scenarios.

1.2.3 Soft Shape-changing Interface

The rigid nature of electronic components, actuators, and bodies in shape-changing interfaces has posed limitations on their form, function, and interaction capabilities [65]. Consequently, researchers have explored the concept of bioinspired interfaces by integrating soft actuation elements, leveraging advancements in soft robotics [158]. Previous studies have proposed various approaches for achieving active shape-change, including the use of soft bodies [4, 27, 103], soft actuator technologies [2, 157, 213, 227], flexible sensors [51, 220], and flexible electronics [82, 90, 96]. Several limitations of soft interface are including a lack of control precision, limited load-bearing forces, and manual fabrication complexity. These

limitations arise from the inherent characteristics of soft materials and the associated design and fabrication processes [221].

1.3 Research Motivation

Based on the above background, shape-changing interfaces show great potential in advancing the state of current interaction technology. However, shape-changing interfaces are still confined to research purposes owing to their design complexity, fabrication cost, and mass production difficulty.

1.3.1 Technological Challenge of Shape-changing Interfaces

Alexander et. al. proposed a total of 12 grand challenges in shape-changing interfaces that are categorized into technological, behavioral, design, and societal challenges [6]. In this research, our main focus was on addressing technological challenges, particularly in the development of toolkits for prototyping shape-changing hardware.

Shape-changing interfaces are a subset of robotic systems that particularly address shape creation and haptic feedback. As a result, it is possible for such shape-changing hardware to have a relatively large number of degrees of freedom and a mechanical structure that transforms actuation into a constrained form [180]. This complexity can make the prototyping of shape-changing interfaces challenging, as it requires expertise in both electronics and mechanical engineering, which goes beyond the knowledge typically required in other areas of interactive computing, such as software programming or basic electronics [6].

1.3.2 Toolkits for Prototyping Shape-changing Interface

To address this challenge, several works have proposed physical toolkits for rapid prototyping of shape-changing interfaces [22, 38, 39, 136, 147, 148, 212]. These tools

Figure 1.4: Topobo: an early example of shape-changing prototyping toolkit[148]

enable designers to experiment with shape-changing interfaces and make real-time iterations. Another approach to rapid prototyping involves the use of computer-aided design tools, which support the design decision process and facilitate the creation of physical simulations of the final products [4, 60, 84]. Each of these toolkits is covering different techniques to choose from, making it difficult to navigate through all the options. Designers have to consider factors like feasibility, functionality, manufacturing processes, and costs. Additionally, there is no standardized or widely adopted method for prototyping shape-changing interfaces, so designers often need to experiment and customize their own solutions.

1.3.3 Pneumatic Actuation for Prototyping Shape-changing Interface

Pneumatic actuation offers several advantages for prototyping shape-changing interfaces, including low cost, intuitive application, safety, and convenience of fabrication. Previous studies have leveraged these properties and proposed various

fabrication techniques, such as 3D printing [41, 84], heat sealing [143, 169], laser cutting [224], blow molding [127, 215], and modular assemblies [22, 55], for prototyping pneumatic interfaces. Pneumatic actuators provide soft and compliant properties that are well-suited for prototyping soft shape-changing interfaces. However, despite their popularity, pneumatic actuators require an external source for inflation and deflation. As a result, pneumatic actuators must be connected to inflexible, noisy, and bulky pumps and valves through the tubing. This configuration also generates noise and reduces portability.

1.3.4 Variable-stiffness for Prototyping Shape-changing Interface

The stiffness properties of a shape-changing interface play a critical role in shape precision, deformation responsivity, ergonomics, and haptic feedback. The ability to adjust interface stiffness allows for increased variation in interaction and application, which proves advantageous in prototyping shape-changing interfaces [6, 184]. Researchers can benefit from this capability as it reduces the need for extensive fabrication and design iterations, leading to more efficient development processes. Previous research has explored the concept of vacuum jamming [42, 120, 144, 217] as a means to pneumatically adjust the malleability and stiffness of interfaces. However, these methods are limited to passive shape-change, relying heavily on user manipulation to induce desired transformations.

Building upon these foundations, the primary motivation of this research is to streamline the fabrication process and design iteration of pneumatic shape-changing interfaces. Our goal is to offer accessible tools, techniques, and design guidelines while demonstrating diverse application examples. Specifically, we concentrate on variable-stiffness interfaces and aim to make significant advancements by enabling active shape-change capabilities.

1.4 Organization

The organization of this thesis is as follows :

Chapter 1: Provides an introduction to the research, including background information and research motivation.

Chapter 2: Reviews related work in shape-changing mechanisms, variable-stiffness mechanisms, and shape-changing interface prototyping tools.

Chapter 3: Presents the research proposal, frameworks, and goals of the study.

Chapter 4: Introduces the ClaytricSurface system, which is an interactive 2.5D modeling tool capable of passive shape-change and dynamic stiffness control.

Chapter 5: Presents the ASTRE mechanism as a solution for active shape-change and variable-stiffness capabilities. It showcases a comprehensive exploration of the design and methods. Provides technical investigations to examine the mechanical characteristics of the ASTRE mechanism.

Chapter 6: Introduces the AstreToolkit, a prototyping tool that utilizes the ASTRE mechanism and employs a constructive assembly concept to streamline the prototyping process.

Chapter 7: Presents VabricBeads, a design exploration for shape-changing and variable-stiffness fabric. Explores interaction techniques and applications for fabric forms.

Chapter 8: Discusses the research contribution, findings, insights, limitations, and potential future work.

Chapter 9: Provides a summary of the entire research study.

The relevant publication list for this thesis is following:

1. ClaytricSurface: An Interactive Deformable Display with Dynamic Stiffness Control, IEEE Computer Graphics and Applications, Vol.34, No.3, pp.59-67, 2014. (Chapter 4)

2. ASTRE: Prototyping Technique for Modular Soft Robots With Variable Stiffness, in IEEE Access, vol. 10, pp. 80495-80504, 2022. (Chapter 5)

3. Constructive Assembly Tools for Shape-changing and Variable Stiffness Interface, 11 pages, (To be submitted) (Chapter 6)

4. Variable Stiffness Fabric using Beads and Artificial Muscle, 10 pages, (To be submitted) (Chapter 7)

Chapter 2

Related Work

2.1 Shape-changing Interface Mechanism

When classified by their underlying mechanisms, shape-changing interfaces can be broadly categorized into four groups: electromechanical, fluid-actuated, smart materials, and electromagnetic [194].

Electromechanical

The electromechanical mechanism relies on electric motors, such as DC, stepper, and servo motors, to generate motion. Many previous works in pin-array displays have utilized electromechanical actuators for actuation purposes [43, 59, 71, 193]. These actuators enable dynamic motion and offer fast actuation speeds, reaching up to 983 mm/s [194]. While pin-array displays primarily use motors for linear actuation, various interfaces also employ them for other types of deformations, such as tilt and rotation [5, 104, 131, 164, 202]. The use of motors in these interfaces allows for easy implementation in mobile and self-contained applications, thanks to the use of batteries. However, it is important to note that the weight of the motor becomes more prominent, especially when significant force is required. Additionally, motors can also be utilized for indirect actuation through tendon wires to achieve soft body deformations, as demonstrated by Togler et al. [204].

Fluid actuated

Fluid actuators can be categorized into pneumatic actuators, which utilize air pressure [53], and hydraulic actuators, which rely on liquid pressure [225]. While

hydraulic actuators are capable of generating higher forces compared to pneumatic actuators, they present more complex control requirements and slower actuation speeds. In recent years, there has been a significant increase in the use of pneumatic actuators, driven by advancements in soft robotics research [6].

Pneumatic actuators find application in flexible interfaces that offer diverse geometries, miniaturized forms, and stretchable properties [84, 87, 112, 127, 215, 224, 227]. These actuators enable the development of interfaces that can adapt to various shapes and sizes, allowing for enhanced versatility and interaction possibilities.

Shape Memory Materials (SMMs)

Shape memory materials refers to materials that can undergo changes in their spatial properties in response to external stimuli, such as electric current. One commonly used smart material for shape actuation is Shape Memory Alloy (SMA). SMA finds application in pin-array displays to reduce their form factors, enabling compact designs [154]. Additionally, SMA wires are utilized in various soft deformable interfaces, benefiting from their compliant and flexible nature [25, 27, 195, 208]. However, SMA-based actuation does have certain limitations, including high energy consumption and slow response time. Alternative types of stimuli, such as heat [76] and humidity [110], have also been explored for shape actuation in research endeavors.

Electromagnet

Similar to electric motors, magnetism has been employed in previous works to generate motion in diverse applications. One notable example is Mudpad [73, 133], which utilizes a magnetic field to transform Magnetorheological (MR) fluid, enabling changes in the physical properties of displays. Another approach involves manipulating ferromagnetic objects [159, 183] to induce shape changes. Additionally, TableHop [166] incorporates transparent electrodes to create small deformations and provide vibrotactile feedback on the display surface. These magnetic-based mechanisms offer unique possibilities for interactive displays and shape-changing interfaces.

2.2 Variable-stiffness Mechanism

The ability to control stiffness plays a vital role in providing haptic feedback, controlling deformability, and offering customizable affordances within interfaces. Although vacuum jamming has been extensively studied to enhance interaction in shape-changing interfaces [42, 120, 144], there is a gap in the literature regarding investigations into novel variable-stiffness mechanisms. In contrast, the field of soft robotics research has primarily concentrated on developing innovative mechanisms to achieve variable-stiffness properties [222].

Jamming mechanism

Jamming is a structural phenomenon that can significantly alter the mechanical properties of a material. Typically, a jamming structure is composed of elements with low effective stiffness and damping. When a pressure gradient, such as vacuum, is applied to the structure, it induces an increase in the kinematic and frictional coupling, resulting in a substantial alteration of its mechanical behavior [3, 105]. Previous research has explored the use of jamming in various structures, such as granular, fiber, or layer [7, 15, 42, 144], to attain different material properties.The vacuum-actuated jamming structure offers advantages such as consistent isotropic pressure and a scalable fabrication process. However, it does require an external membrane, which can introduce design complexities for system integration. Additionally, vacuum actuation has an upper limit on the achievable vacuum pressure, which imposes constraints on the range of attainable stiffness [3].

Other techniques for implementing jamming mechanisms include mechanical methods such as clamps, meshes, and tendons [74, 140, 168], as well as magnetically induced jamming [10, 35]. Mechanical actuation methods are particularly appealing as they enable directional control of the applied pressure, which is advantageous for achieving localized stiffness control. Furthermore, unlike other methods, mechanical actuation does not have a fundamental physical upper limit on the applied pressure, allowing for greater flexibility in achieving desired stiffness levels

[3].

Electro Active Polymers (EAPs)

Electroactive Polymers (EAPs) are a class of materials that can undergo deformation in response to an applied electric potential between two electrodes. Previous works in HCI field have explored the use of EAPs for various applications, including bio-inspired shape-changing interfaces and small form-factor devices [45, 157]. In the field of soft robotics, EAPs have been utilized for variable-stiffness mechanisms in applications such as robotic grippers and medical rehabilitation devices [20, 111, 156]. Although EAPs hold great potential as silent and self-contained actuators. However, there are still challenges to overcome in terms of high-voltage control, fabrication processes, and material characteristics.

Electro and Magneto-rheological Materials (ERM/MRM)

ERM/MRM fluids have the ability to modify their rheological properties in response to the application of a magnetic or electric field [19, 114]. These fluids find particular suitability in automotive applications, such as adaptive bumper and shock absorber systems, as well as in damping control for adaptive orthotic devices [222].

Low Melting Point Alloys/Polymers (LMPA/LMPP)

Low Melting Point Alloys (LMPAs) or Low Melting Point Metals (LMPMs) are materials that exhibit rapid changes in stiffness when exposed to external stimuli, such as heat. In robotics, researchers have explored the use of cost-effective and easily obtainable materials like wax [26] and Galium [176]. These materials possess the unique property of solidifying at low temperatures and becoming more flexible when heated to higher temperatures. In previous work, LMPAs have been employed to secure the joints of metamaterial structures, allowing for shape alterations in their flexible state [153]. One limitation of LMPA/LMPP material is its slow transition speed, particularly when not employing cooling elements. This can impact the responsiveness and speed of shape changes in the structures.

Shape Memory Materials (SMMs)

Shape memory materials, such as Shape Memory Alloys (SMA), not only possess the ability to change their spatial properties but also exhibit variations in stiffness when subjected to external stimuli. These changes in stiffness are a result of phase transitions and glass transitions within the material, leading to alterations in its mechanical characteristics. In the field of soft and wearable robotics, researchers have explored the application of fabrics embeded with Shape Memory Materials (SMMs) to manipulate and adjust their mechanical properties [24, 49, 232]. Utilizing SMMs in these applications offers several advantages, including ease of implementation and the ability to achieve desired shape changes. However, it is important to note that the maximum range of stiffness achievable with SMMs may be lower compared to other mechanisms.

2.3 Prototyping and Fabrication Tools

Recent advancements in computational design and digital fabrication have shown promising potential in streamlining the prototyping process of shape-changing interfaces. Previously high-cost tools such 3D printers and laser cutters have become more accessible and open-source, enabling researchers to hack and modify such tools. Several toolkits that have been proven effective in facilitating the prototyping of shape-changing interfaces include design tools, rapid fabrication tools, and physical design tools.

Design Tools

Computer-Aided Design (CAD) tools have played a crucial role in the design of shape-changing interfaces, providing designers with the ability to create, modify, and simulate digital models. Recent advancements in this field have introduced powerful design tools that offer features such as parametric design [46, 68], interactive simulations [55, 142], and automatic model optimization [60, 125]. These tools have found specific applications in various design contexts, including kinematic structures [28, 100], deployable structures [145, 178, 231], and soft robots

[16, 115]. By leveraging these tools, designers can rapidly iterate on and evaluate designs before moving on to the fabrication stage. However, it is important to acknowledge that a domain gap still exists between computer simulations and physical prototypes. Furthermore, previous studies have demonstrated that physical tools are often preferred in certain design scenarios, particularly in collaborative works [109].

Rapid Fabrication Tools

In the field of HCI, Fused Deposition Modeling (FDM) 3D printing has emerged as a popular and accessible fabrication technology. It's low-cost nature and wide availability have facilitated various applications, including rapid prototyping of structures [125, 126], dynamic mechanical devices [60, 100, 101], novel sensing techniques [79, 97, 172, 200], 4D printing [76, 186, 199, 214], and pneumatically actuated interfaces [84, 149, 173, 211]. In order to push the boundaries of 3D printing even further, researchers have proposed hybrid fabrication approaches that combine 3D printing with other crafting techniques, such as bead assembling [185], blow molding [215], and fabric weaving [34]. By harnessing the convenience and versatility of 3D printing, researchers have been able to explore various aspects, including materials, structures, shapes, interactions, and dynamics. However, it is important to note that 3D printing is a time-consuming process, which limits real-time structure iteration.

Physical Design Tools

To enable design tools with physical interaction, previous studies have investigated the utilization of constructive assembly. This approach involves the use of Tangible User Interfaces (TUIs) where modular parts and interactive units are interconnected to create larger constructions [99]. By employing constructive assembly, designers can manipulate and interact with physical components to explore various design possibilities and rapidly prototype complex structures or systems [31, 55, 59, 102, 126, 134, 148, 164, 175]. This approach offers a tangible and intuitive means of engaging with design tools, bridging the gap between digital and

physical realms in the design process. Many of these studies provide a user-friendly and intuitive toolkit adoption. However, to replicate the toolkit itself, most studies still requires an experienced fabricator in term of electrical and mechanical engineering.

2.4 Research Positioning

In this research, our primary goal is to develop prototyping frameworks that combine active deformation and variable stiffness functionalities in shape-changing interfaces. The proposed mechanism introduced in ASTRE (Chapter 5) represents a substantial advancement compared to previous methods for implementing shape-changing interfaces. Specifically, our mechanism allows for simultaneous changes in both the shape and stiffness, all within a single integrated system. Figure 2.1 shows a visual representation of the positioning of our proposal in relation to prior works.

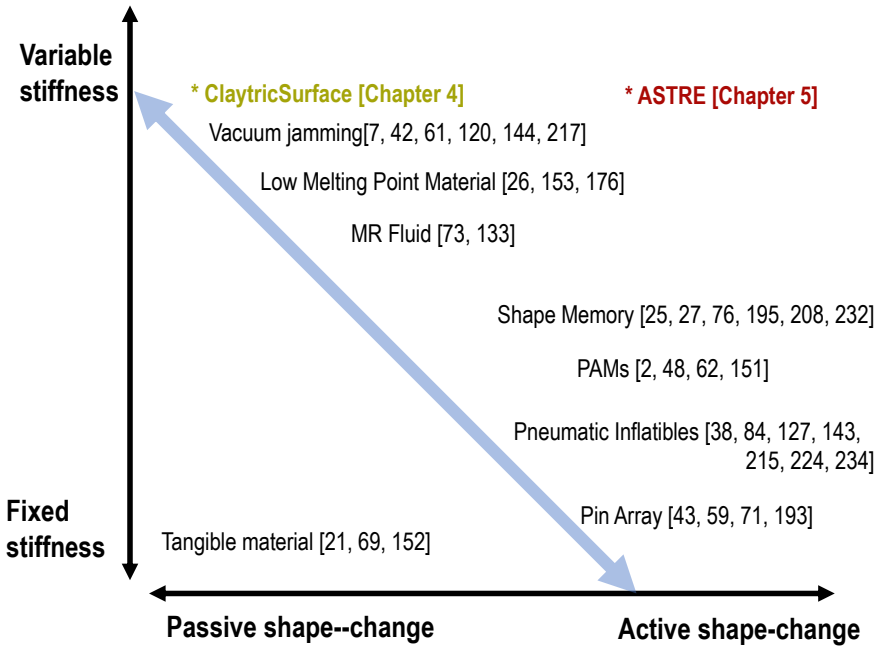

Figure 2.1: Research positioning in the shape-changing and variable-stiffness interface categories.

Chapter 3

Research Proposal

3.1 Pneumatic Actuator Overview

Pneumatic actuators play a vital role in converting air pressure energy into mechanical force, enabling the operation of a wide range of tools and machinery through positive pressure (compressed) energy. Additionally, negative pressure (decompressed) pneumatic systems, commonly known as vacuum, have found practical applications in various domains including electronics, food preservation, and medical treatments. The focus of this research is specifically on leveraging the advantages of both compressed and vacuum-based pneumatic actuation for the development of shape-changing interfaces with variable-stiffness capabilities. This study aims to explore new possibilities and advancements in interaction, especially for prototyping purposes.

3.1.1 Compressed Air Actuator

In the field of HCI and robotics research, pneumatic actuation has gained popularity due to its notable advantages, including compliant properties, rapid response time, lightweight nature, and energy efficiency [223]. Previous studies have highlighted the development of wearable devices with inflatable actuators, showcasing their potential to enhance user activities such as grasping, navigation, and communication [33, 38, 112, 235]. Despite their effective actuation force, inflatable actuators often suffer from the limitation of bulky inflated forms, which can restrict

user motion and mobility.

To overcome the limitations associated with inflatable actuators, researchers have shifted their attention to thin Pneumatic Artificial Muscles (PAMs), which offer a unique combination of flexibility and high-force capabilities [95]. Several works have explored the use of PAMs for applications such as haptic interface [196, 236] and shape-changing fabric [2, 151]. In this research, we also investigate the potential of PAMs as actuators; however, our primary focus lies in exploring the programmability of mechanical constraints to influence the overall shape and stiffness of the interface. By leveraging the mechanical constraint concept, we aim to expand the design possibilities and improve user experiences.

When considering the design of pneumatic interfaces, previous works have primarily focused on the programmability of structures to achieve specific shape deformations [37, 84, 112, 119, 127, 135, 143, 145, 178, 201, 215, 224]. These studies have showcased the potential of computational design in streamlining the fabrication of specialized form factors for customized interactions. Furthermore, they have demonstrated the simplicity of pneumatic actuator design, often achieved using a single type of flexible material, in contrast to other dynamic actuators such as Shape Memory Materials [8, 213], which require composite layers of materials.

In terms of fabrication methods, previous research in pneumatic interfaces has explored innovative techniques such as knitting, heat sealing, and 3D printing [41, 84, 112, 127, 143, 215, 224]. These studies have demonstrated the potential of pneumatic interfaces for rapid prototyping, thanks to the simplified and time-efficient fabrication techniques they employ. In this thesis, we propose a novel fabrication technique that combines Pneumatic Artificial Muscles (PAMs) with 3D-printed mechanical reinforcement. While our technique involves manual threading work, it offers certain advantages. We utilize commercial PAMs that exhibit high-pressure durability and increased strength, making our actuators more reliable compared to those created using 3D-printed or heat-sealed inflated membranes, which are often dependent on specific materials and machines for their performance.

In comparison to pneumatic actuators, hydraulic actuators offer the advantage of generating higher forces using the same tube diameter [2, 113, 225]. However, the scalability of hydraulic actuators presents a significant challenge as they require large liquid reservoirs and become increasingly heavy when scaled up. Previous research has addressed the issue of scalability and demonstrated the implementation of large-scale pneumatic structures [92, 135, 169, 189]. These interfaces have found applications in various domains, including human-scale furniture and large-scale kinetic structures, reaching impressive heights of up to 4 meters. On the other hand, there has also been an exploration of small-scale pneumatic interfaces [2, 58, 107], focusing on tangible and haptic applications at the millimeter scale. In line with these efforts, our research intentionally leverages pneumatic actuators to develop highly scalable interfaces that can be scaled up or down based on design requirements.

3.1.2 Vacuum Actuator

Vacuum is a commonly utilized medium in both HCI [42, 61, 144, 217] and soft robotics [7, 15, 128] research for implementing jamming mechanisms. These studies have effectively demonstrated the simplicity, feasibility, and reliability of jamming using vacuum. However, there are certain limitations associated with vacuum-based actuation, including relatively low actuation speed and potential issues with the durability of soft membranes. In recent developments in soft robotics, vacuum actuation has been explored for deformable robot arms and grippers [40, 72, 81]. Nevertheless, these initial studies have indicated that vacuum-based deformation exhibits lower strength and speed compared to compressed air actuators.

Our research is a pioneering study that focuses on the utilization of the granular jamming technique to control the compliant deformation of shape displays (Chapter 4). Additionally, we introduce the novel concept of stiffness control using compressed air actuation, specifically through the implementation of Pneumatic Artificial Muscle and 3D printed mechanical constraints (Chapter 5).

3.2 Research Approach

This research aims to build a framework that systematically guides the design and prototyping of shape-changing and variable-stiffness interfaces using pneumatic actuators. Figure 3.1 a illustrates the basic frameworks of this research.

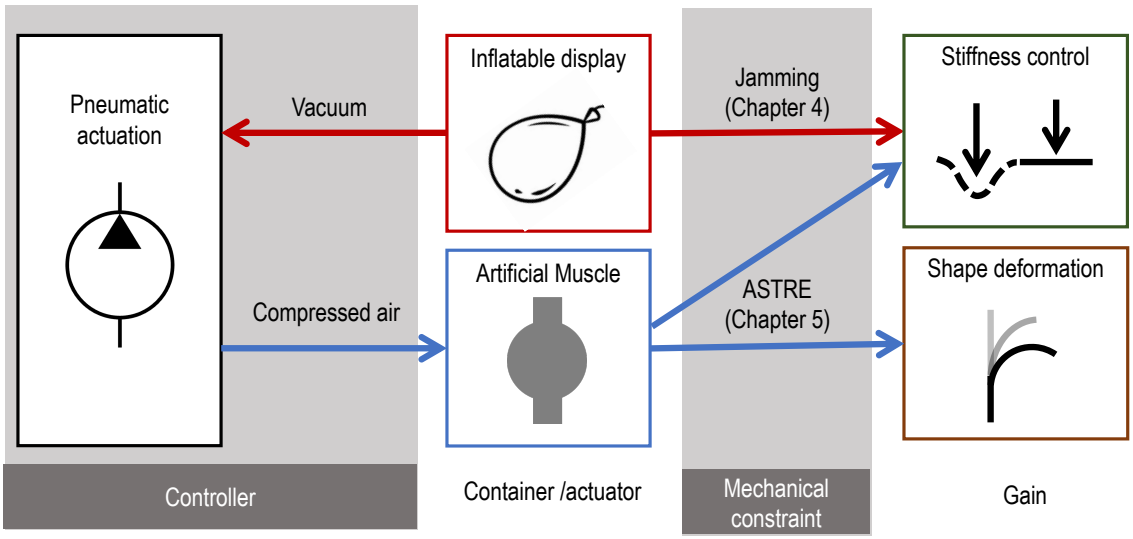

(a) Framework overview: Consist of controller, actuator, mechanical constraint, and gain.

Pneumatic	Vacuum	Compressed air	
Actuator	* Chapter 4 Inflatable	* Chapter 5 Artificial Muscle (PAMs)	
Mechanical constraint	Granullar Jamming	• Locking • Malleable • Brake	• Bending • Twisting • Contractible
Gain	Stiffness control		Shape deformation

(b) Three types of mechanical constraint: Stiffness control using granular jamming, deformation control using PAMs, and stiffness control using PAMs.

Figure 3.1: The research framework

Pneumatic control

Pneumatic control involves the utilization of pneumatic energy sources, such as compressed air or vacuum, to operate entire systems. It also includes actively regulating the air pressure to activate the actuators. The key components of pneumatic control include the compressor/vacuum pump, valve, and regulator.

Actuator

The actuator is responsible for converting energy and signals from the pneumatic control system into mechanical force. Within this framework, two types of actuators are utilized: inflatable actuators and artificial muscles. Inflatable actuators convert vacuum energy into a shrinking force (mechanical coupling), while artificial muscles generate both contraction force and radial expansion by utilizing compressed air.

Mechanical constraint

Mechanical constraint refers to physical attachments that restrict the motion of the actuators. This framework introduces the concept of programmable mechanical constraints as its primary novelty. In Chapter 4, we present the jamming mechanism as a mechanical constraint that induces stiffness changes in vacuum actuators. Additionally, in Chapter 5, we propose the ASTRE mechanism, capable of inducing stiffness changes and shape deformations through artificial muscle actuation. Figure 3.1b provides further details on our proposed programmable mechanical constraints.

Gain

Gain refers to the final mechanical output of the framework. In this research, the gain can manifest as stiffness changes or shape deformations, depending on the actuator and mechanical constraint employed. Shape deformations can include bending, twisting, or contraction, while stiffness control can be achieved through locking, malleable, or rotational brake behaviors.

3.2.1 Stiffness Control Using Granular Jamming

Stiffness control plays a crucial role in providing tactile feedback, deformability, and adjustable affordances. In this research, we employ the vacuum-jamming technique to enable dynamic changes in the stiffness of the interface, transitioning it between soft and stiff states. Additionally, we incorporate graphical input-output capabilities to support various applications, including modeling and drawing tasks.

While significant contributions have been made to enhance usability in modeling and sculpting, it is important to note that the current system lacks self-actuated deformation capabilities. This limitation hinders the potential benefits of providing programmable shape changes, dynamic haptic feedback, and adaptive shape interaction

3.2.2 Deformation Control Using PAMs

In the follow-up research, we explore the capabilities of active shape deformation using artificial muscle actuation. Artificial muscles are selected due to their soft, lightweight, and high-strength properties. We propose three types of modules to translate the contraction force of PAMs into bending, twisting, and contraction deformations. The type of deformation is determined by the specific mechanical constraint, and the amount of deformation can be actively controlled through air pressure or programmed by adjusting the constraint parameters.

3.2.3 Stiffness Control Using PAMs.

Although we can incorporate shape-changing properties of PAMs with a vacuum jamming mechanism, similar to previous work by Yang et al. [226], the resulting systems become exceedingly complex with multiple layers of membranes. This complexity reduces usability and increases fabrication intricacy. In this research, we propose a novel variable-stiffness mechanism that utilizes PAMs and mechanical constraints. This approach offers a more practical system as both the shape-

changing mechanism and the proposed variable-stiffness mechanism share similar material properties and can be actuated within the same pressure ranges.

3.2.4 Framework Contribution

In general, the contribution of this framework can be summarized as follow :

- Novel concept: We introduce a novel concept that combines shape-changing and variable-stiffness capabilities using pneumatic actuators and programmable mechanical constraints. This concept provides enhanced capabilities for pneumatic interfaces, allowing for dynamic shape changes and adaptable stiffness.
- Standardized platform: We develop a standardized platform for physical prototyping and fabrication of shape-changing interfaces. This platform simplifies the implementation process and enables researchers and designers to easily create and iterate on prototypes.
- Design tool: We provide a design tool that offers exploration guidance and application examples. This tool assists novice users in understanding and learning the workflow of the framework.

Chapter 4

ClaytricSurface: An Interactive Deformable Display with Dynamic Stiffness Control

4.1 Overview

Conventional displays' rigid, planar physical limitations bring about many restrictions when users interact with data involving 3D shapes or tactile information. For example, viewing or altering a 3D shape on a planar display requires complex GUI operations such as frequent viewpoint changes or vertex operations. A Virtual Reality (VR) head-mounted display can show a 3D object in VR space, but physical contact with the object is impossible.

To introduce direct user interaction with 3D data, researchers have explored non-planar or deformable displays that let users mold or directly modify the data like modifying a physical object [65]. Flexible materials such as cloth [21], elastomer [170], sand and clay [69, 152] have been utilized as display surface to provide an organic element with the surface input/output methods. These displays generally show images on a tangible surface or convex shape, and the users can touch or deform the shape freely with their hands. However, the surface material's limitations restrict the shapes that can be produced. Similarly, physical parameters of the surface such as stiffness or smoothness can be changed only by modifying

the underlying hardware configuration. Thus, interaction methods that the same system could provide to the user were limited.

This research focuses on creating displays that can dynamically change surface stiffness from soft to hard and vice versa. Toward that end, we developed ClaytricSurface, a flexible shape-deformable display that supports different interactivity styles. By enabling controllable stiffness, this surface can function both as a traditional rigid planar surface and as a flexible-shaped surface. Moreover, adjusting the degree of surface softness allows for the generation of various touch sensations and tactile feedback.

We developed a 3D modeling application to demonstrate the usability of the ClaytricSurface system. Our system utilizes touch input to control the softness, enabling users to experience immediate changes in softness while making adjustments on the fly. When the display is in a soft state, users can significantly deform the surface shape, allowing for greater flexibility and exploration. In a malleable clay-like state, users can create more intricate and detailed shapes. Finally, when the display is in a stiff state, it maintains its shape even when external forces (such as touch input) are applied. This range of variable-stiffness capabilities provides users with versatile and responsive control over the surface, enhancing the overall user experience and creative possibilities in the 3D modeling application.

4.2 Related Work

4.2.1 Shape-changing Interface with Programmable Material Properties

Previous research has explored the concept of programmable material properties, including viscosity. One such example is MudPad [73], a haptic display that can induce localized viscosity changes on multitouch screens. It utilizes an array of electromagnets to actuate magnetorheological (MR) fluid overlaid on the surface.

This technology enables a wide range of viscosity levels, from fluid-like water to viscous-like peanut butter. Another example is HapticCanvas [228], which employs dilatant fluid to provide users' fingers with variable fluid resistance, creating a sensation of "sliminess." These previous works enable the manipulation of viscosity to offer haptic feedback. However, it's important to note that both of these research projects utilize fluid as the display medium. Consequently, the shape change experienced by the user is not retained since the fluid will return to a flat surface after manipulation.

4.2.2 Jamming in Robotics

Previous research has explored the utilization of vacuum jamming as a mechanism for controlling stiffness in soft robotics. This approach has found applications in various domains, owing to its ability to fix shape and regulate rigidity solely through air pressure. For instance, Brown et al. [7, 17] introduced a robotic gripper that can grasp diverse objects without the need for complex mechanical structures. The gripper comprises an inflatable membrane filled with granular materials, which conform to the shape of an object when pressed, and firmly grip the object when the gripper is jammed using a vacuum. Another example is JSEL, a ball-shaped robot capable of locomotion [182]. It consists of cellular compartments (cells) along its outer perimeter, each filled with a jamming (granular) material. Combined with a balloon-like actuator, the robot can modulate and deform its shape to facilitate rolling locomotion. Jamming techniques have also been explored for medical devices that require both softness for careful navigation within the body and rigidity for stable surgical platforms [106]. These earlier studies have primarily focused on the capabilities of jamming techniques for fixing the shape of robots [7, 106] and controlling shape deformation [182]. However, the deformability of jamming interfaces resulting from user manipulation, dynamic changes in stiffness, and user interfaces for controlling stiffness have yet to be thoroughly investigated.

4.2.3 Jamming in HCI

Vacuum jamming has also been explored in the field of Human-Computer Interaction (HCI) research. Mitsuda et al. [122] proposed a wearable haptic interface that enhances human movement with sensations like contacting a wall or moving in water within virtual reality systems. This interface consists of flexible tubes filled with Styrofoam particles, which can be worn on the user's arm. The tubes can be jammed to restrict user motion while they are immersed in VR environments. Another example is Hovermsh by Mazzone et al. [120], where they introduced a concept for a shape-changing display. The display utilizes cubical meshes (cells) filled with Styrofoam particles as the display surface, along with an inner layer of inflatable chambers. Similar to JSEL [182], HoverMesh can be deformed by inflating or deflating the inner chambers while jamming or unjamming the cells. Jamming User Interfaces [42] is a relevant work in this research area, published after the initial proposal systems [118]. It explores multiple applications of vacuum jamming as user interfaces, including a malleable surface where shape deformations are detected using optical sensing through the transparent display's rear, variable-stiffness feedback for mice, and touch input mounted on the back surface of a tablet, enhancing scrolling or dragging gestures with haptic and tactile feedback. Compared to previous jamming research, this particular study focuses on the control of deformability in shape-changing interfaces, surface sensing techniques, and complementary methods for modeling applications.

4.2.4 3D Modeling Tools

To address the design challenge of creating a freeform model, numerous prior works have explored the use of sketch-based 3D modeling approaches [138]. One notable system is Teddy [67], an interactive system that utilizes sketching techniques for expressive design of 3D objects. By sketching a 2D outline, the system automatically generates a corresponding 3D model based on the sketch silhouettes.

While these techniques effectively streamline the rough 3D modeling process, they face limitations when it comes to creating small and intricate parts due to the constraints of tablet touch-input and 2D viewing.

To overcome such limitations, several studies have proposed combining physical tools with 3D sensors and graphical output to facilitate a tangible modeling experience [69, 152]. These approaches leverage physical manipulation for the rapid and intricate creation of physical models, while also benefiting from the advantages of digital models, including interactivity, scalability, and reproducibility [70]. Motivated by these previous works, we also developed a tangible display that incorporates both touch input and graphical output. However, our focus extends beyond existing research by specifically investigating the impact of variable-stiffness on modeling tasks. We explore properties such as the relationship between shape deformability and stiffness level, as well as the accuracy of depth-based touch detection on surfaces with varying shapes and stiffness levels.

4.3 Mechanical Constraint of Vacuum Jamming

In the development of ClaytricSurface, our focus was on utilizing vacuum jamming techniques [217] to control display surface stiffness. The display is made from a stretchy inflatable pouch that can endure vacuum pressure. When an empty pouch is applied with a vacuum, the pouch will shrink until no space remains inside. However, when a pouch filled with small particles gets vacuumed, it will exhibit jamming behavior (Figure 4.1). These small particles act as a mechanical constraint to alter vacuum-sucking forces into frictional forces between the particles.

In atmospheric pressure, the particles inside the pouch exhibit smooth sand-like properties. However, as the air inside the pouch is depressurized, spaces between the particles are also reduced resulting in increases in the surface's stiffness. With further reduction in the air pressure (approaching vacuum levels), the pouch becomes rigid with minimal flexibility. ClaytricSurface leverages this principle to enable

real-time pressure control, allowing for dynamic changes in the display's shape and stiffness. This capability enables seamless transitions from a soft to a hard surface.

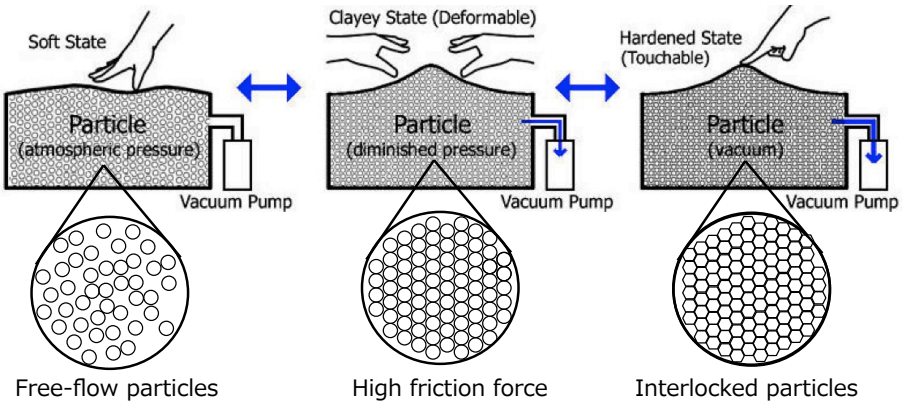

Figure 4.1: Vacuum jamming based stiffness control.

4.3.1 Granular Media used in Jamming Mechanism

Basically, all granular materials (particles) exhibit the phenomenon of jamming, although the strength of this effect can vary depending on the size, shape, and compressibility of the particles. This strength can be quantified by the flexural modulus, which measures a material's resistance to deformation under load. While the flexural modulus is important for defining the maximum stiffness of a jammed state in a display, another crucial factor is the softness of the display in an unjammed state. The softness determines the expressiveness of the shapes that can be formed on the display.

A parameter that characterizes how granular media flow or behave in a liquid-like manner is known as the angle of repose. This refers to the maximum angle to the horizontal at which granular particles will remain without sliding. In our research, we referenced previous works such as the material review presented in [11, 182]. Based on this literature, we selected 1 mm diameter polystyrene particles as the material for our study. These particles possess desirable properties such as being lightweight, smooth, round, and small in size.

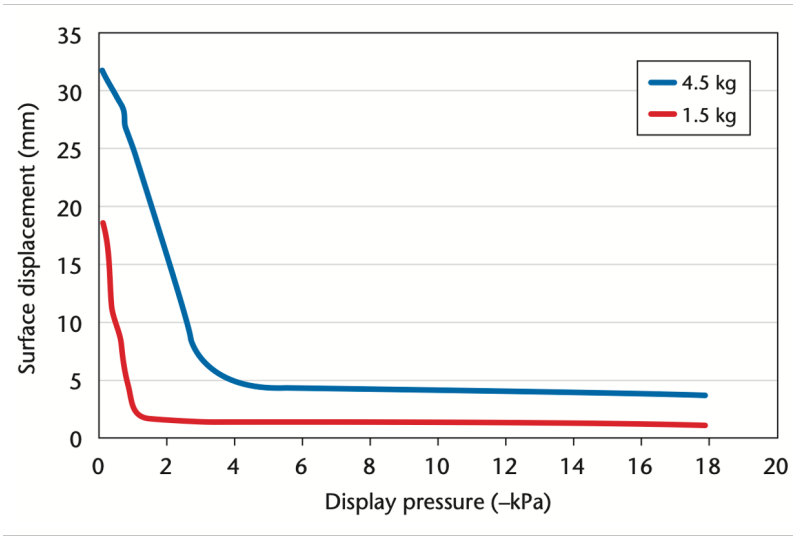

Figure 4.2: Display displacement versus internal pressure. The results reflected our system's limits: when the pressure fell below a threshold, the display didn't become any hard

4.3.2 Pressure and Stiffness Relation in Jamming Mechanism

Here investigated the relationship between the pressure, and the surface deformation due to external force. We changed the pressure from –18.00 kPa (the maximum vacuum) to 0 kPa, in steps of 0.12 kPa. At each step, we applied a constant force simulating a finger touch on the surface and measured the displacement. We considered two pressing modes: light touch and hard press. To simulate a light touch, we added a 1.5 kg weight to the rod; for a hard press, we used a 4.5 kg weight. We applied this force for 5 seconds, recording the rod's displacement for each measurement.

Figure 4.2 shows the results. The display became harder as the internal pressure decreased. However, a displacement of approximately 2 to 5 mm typically occurred even at minimum pressure. Essentially, this displacement arose from the particles' and surface fabric's softness. These characteristics reflected our system's limits: when the pressure fell below a threshold, the display didn't become any harder.

To eliminate this limitation, we've considered using alternative materials for the particles and surface fabric. Also, the displacement was significantly smaller when the display pressure was below –2.00 kPa for weak presses or –4.00 kPa for strong presses. So, to achieve the plateau, we would choose –4.00 kPa, which we can easily do with an inexpensive vacuum pump (US$10). This suggests that the cost for substantial shape changes induced by finger pressing is insubstantial because the vacuum pressures aren't great.

4.4 System Hardware

Figure 4.3 depicts our prototype's hardware configuration, which comprises three main units. The display unit (particle table)is a 655×505×35 mm box filled with 1 mm expanded polystyrene particles covered and sealed with non-breathing spandex. The spandex has vertical and horizontal elasticity. To increase air tightness, we attached a rubber sheet to the back of the spandex. The display has three nozzles: one for compression, one for decompression, and one that's connected to a pneumatic pressure sensor by 4 mm inner-diameter tubing. The pressure control unit consists of the pressure sensor, two solenoid valves, a vacuum pump, and a vacuum regulator. The sensor can measure relative pressure from 0 kPa (atmospheric pressure) to –24.50 kPa. One of the valves connects the display to the pump; the other connects the display to the open air. The pump is a linear motor piston pump with a speed of 40 liters per minute and a maximum vacuum of –33.30 kPa. The pump is noisy; however, we suppressed the noise by placing the pump in a sealed housing and relocating this system away from the display unit. The vacuum regulator controls the vacuum speed. The projector-and-depth-camera unit is approximately one meter above the display. The projector projects colors onto the display in conjunction with the user's touch input; the camera (a Microsoft Kinect) detects finger touches, as we explain later.

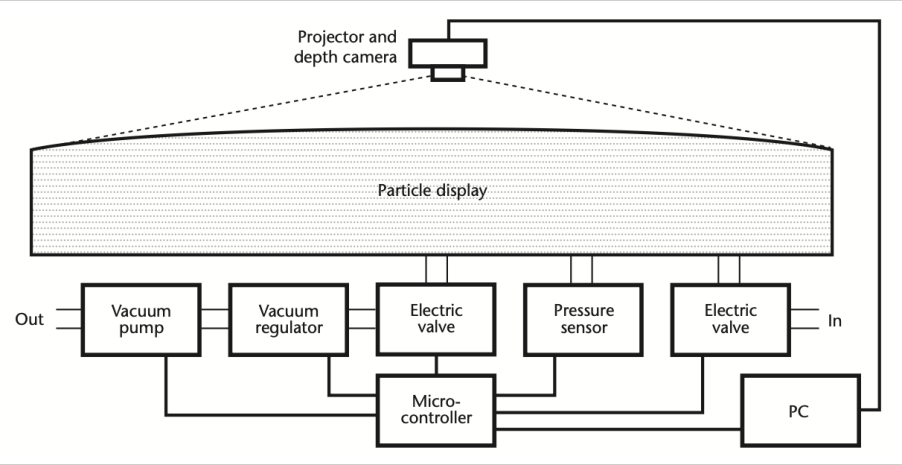

(a) ClaytricSurface's configuration.

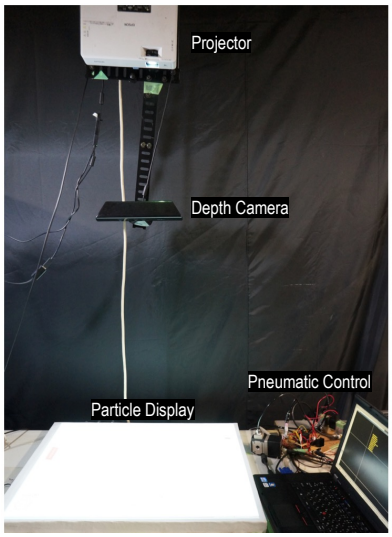

(b) ClaytricSurface's hardware

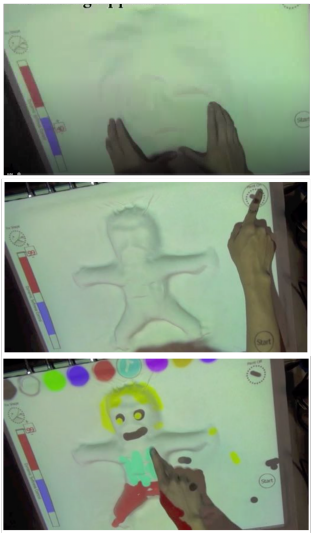

(c) Projected GUI on ClaytricSurface's

Figure 4.3: ClaytricSurface's hardware configuration and projected GUI

4.5 Input Detection

We have implemented multitouch finger input and stylus-based input.

4.5.1 Touch Detection

The depth camera can capture only the finger's upper surface because the finger pad, the area that normally touches the surface, is obscured. So, the system iden-

tifies the approaching contact by determining whether the finger is within 15 mm (the normal fingertip thickness) of the display's surface.

ClaytricSurface first stores the surface depth data to use in forming an image of the initial background. By comparing that image with the one built from the current input depth obtained from the camera, the system detects the hand and fingers. It subtracts the current background and depth images and binarizes the area that appears to be from 5 to 15 mm from the surface. It takes into account noise in the depth image and fingertip thickness (see Figure 4.4a). It determines the touch location by calculating the centroid of each region in the binarized image (see 4.4a) 3b).

When the surface is soft, user contact can change the surface shape and thus the initial background depth data. So, ClaytricSurface updates the background depth accordingly. To do this, it first detects the user's hand region by detecting objects within 400 mm from the surface. Next, it checks whether this region crosses the display boundary because the user's hands extend from outside the display. It then creates an exclusion mask using the minimum bounding rectangles of the hand region (see Figure 4.4c). For each frame, the background depth image updates from the previous depth image.

4.5.2 Stylus Input

For stylus input, we use an induction-based tablet that can sense a stylus coil up to 2 cm overhead. We place the tablet under the display, which is 1 cm thick. The tablet can locate stylus touches through the display even when the surface isn't flat (see Figure 4.5).

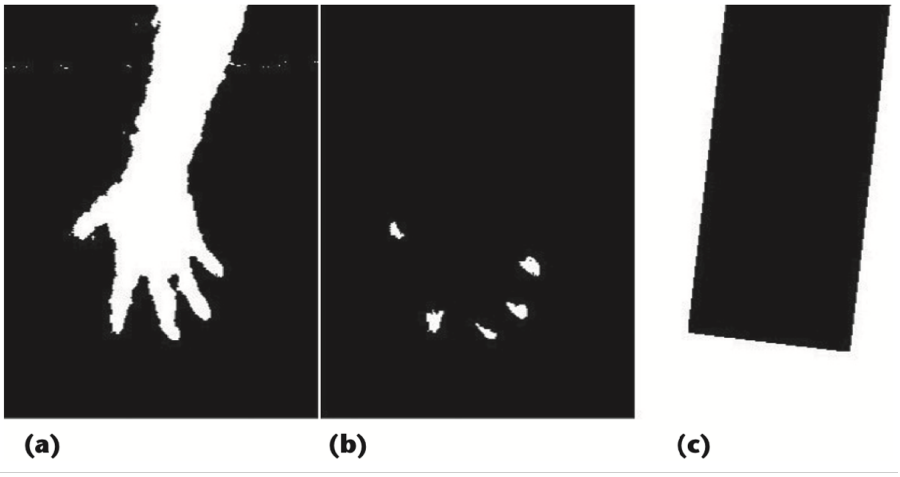

Figure 4.4: Touch detection. (a) The user's hand detected in the target region. (b) The area touched by the fingertips. (c) The exclusion mask, which uses the minimum bounding rectangles of the hand region. Because the camera can only capture the finger's upper surface, the system identifies the approaching contact by determining whether the finger is within 15 mm of the display's surface.

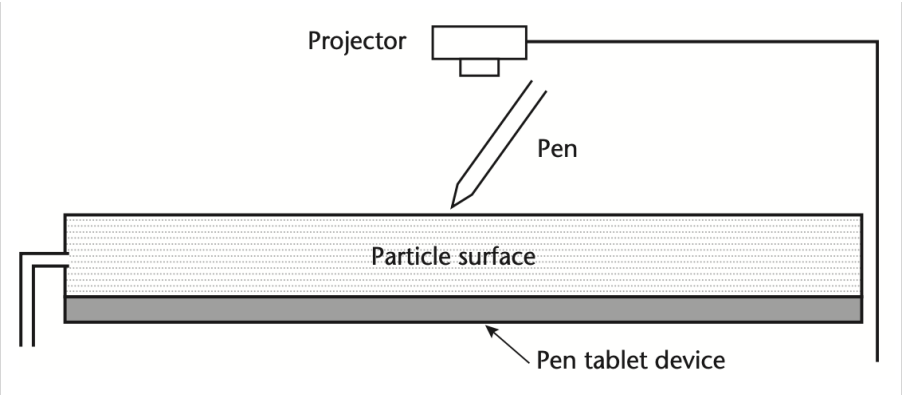

Figure 4.5: Stylus input employs a tablet beneath the display. Because the display is only 1 cm thick, the device can locate stylus contact even when the surface isn't flat.

4.6 Peripheral Technologies

4.6.1 Vacuum-Molding Tool

With a prepared mold, users can easily copy and form a detailed 3D shape (see Figure 4.6). When the display is soft, the user places the mold over the desired

location on the display. A pump connected to the mold evacuates the air between the mold and the display, pulling the surface into the mold and creating the desired shape (see Figure 4.6c). Hardening the display in this state maintains the molded shape.

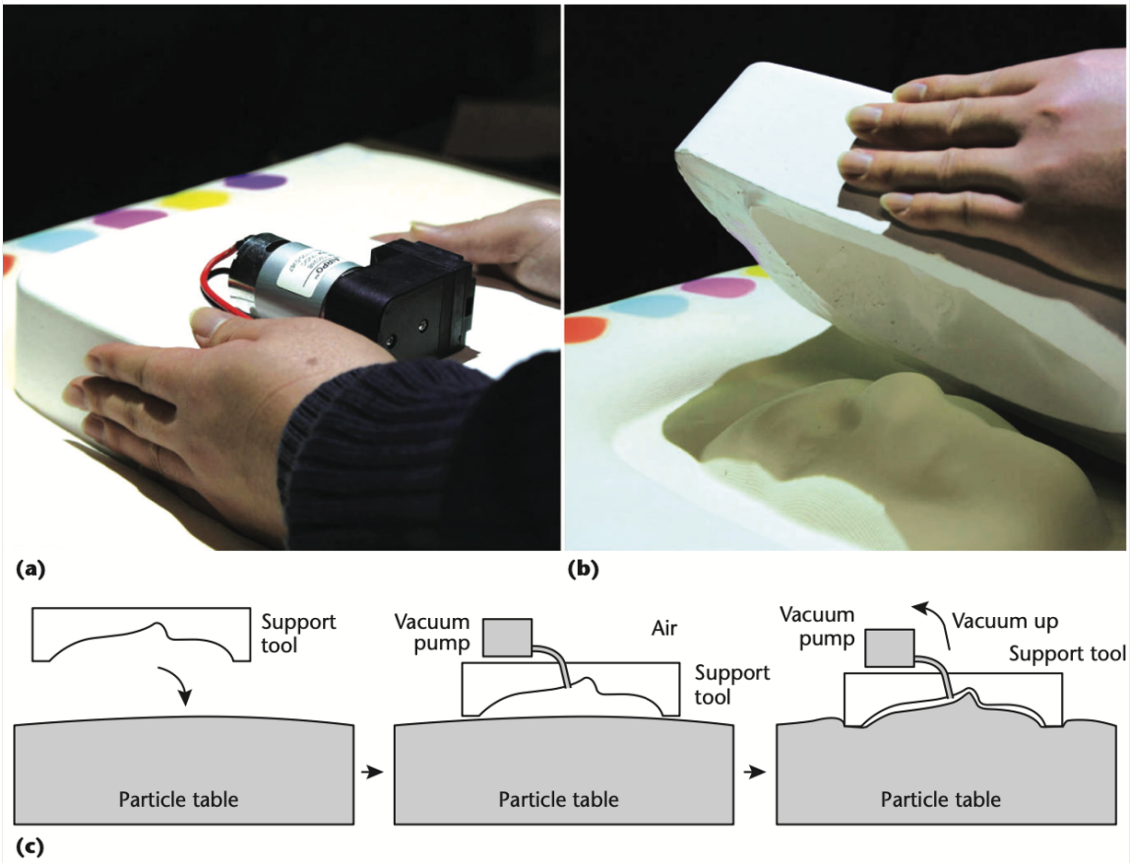

Figure 4.6: A vacuum-molding tool. (a) Placing the tool over the display. (b) The molded display. (c) The vacuum-molding principle. This tool lets users easily copy and form a detailed 3D shape.

4.6.2 Automatic Stiffness Control

We created three simple gesture-based methods to support modeling. First, with hardening assistance, if both of the user's hands touch the surface for three seconds when the system is soft, the pressure automatically changes to –5.00 kPa. The

second method lets users create a tall shape. It activates if the user decreases the pressure by more than 0.30 kPa (by pulling up the surface). The surface continues to harden even after the user removes his or her hands. The third method employs an accelerometer to provide an automatic reset function. When the user shakes the display, pressure increases, returning it to the default setting (like erasing with the Etch A Sketch toy). We also added gradual surface hardening and hardening after a countdown. These two modes simulate clay production processes (curing and drying), adding entertainment elements to the modeling process.

4.7 Application

To demonstrate our system, we developed two design applications.

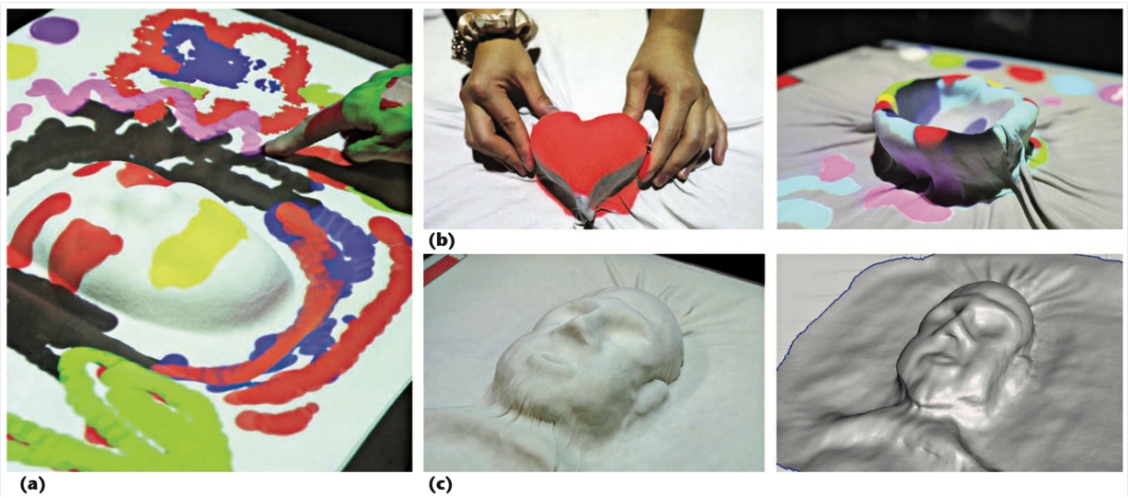

Figure 4.7: The modeling application. (a) A user creating a shape. (b) Two created shapes. (c) A created shape and the scanned model of that shape. Users can make shapes directly by hand rather than employing the complex keyboard-and-mouse actions that 3D-modeling programs require.

4.7.1 Modeling Application

This application (see Figure 4.7) demonstrates ClaytricSurface's potential for entertainment purposes. Users can make shapes directly by hand rather than employing the complex keyboard-and-mouse actions that 3D-modeling programs require. Users can also apply textures by simply touching the shape directly, much like sculpting. In addition, users can "fingerprint" colors, which the system projects onto the display (see Figure 4.7a). Modeling with ClaytricSurface differs substantially from conventional modeling. For example, users can't employ cut-and-paste. However, they can easily make models while transitioning between surface states. That is, they can make a rough model on the soft surface and add details using the hardened surface. The modeling support, peripherals, and reset function we described before are available in this application. In addition, users can easily capture a created shape and convert it to 3D CAD data using the depth camera (see Figure 4.7c), for seamless 3D printing. (We implemented the capture and conversion using the Microsoft Kinect Software Development Kit.)

4.7.2 Paint Application

We also developed a paint application using dynamic stiffness control and the stylus input we described before (see Figure 4.8). With the slider, users can set the display's stiffness so that they can make a 1 to 1.5 cm high 3D texture by hand. On the basis of the system's tactile feedback, they can use the stylus to simulate different brush types. Furthermore, as they apply pressure with the stylus, its trajectory creates a 3D path on the surface. Users can feel this trajectory, offering possible applications for visually impaired users.

Figure 4.8: A person using the paint application. On the basis of the tactile feedback, users can employ the stylus to simulate different brush types

4.8 User Experiments

4.8.1 Deformabilty and Stiffness Level

We conducted an evaluation to examine the relationship between surface deformability during modeling operations and the appropriate stiffness level of the surface. The operations were categorized into three types: "Rough shape," "Detailed shape," and "Tall shape with overhang." We designed an experiment to determine the suitable hardness (pressure) range for each activity. For the experiment, we recruited eight participants (six males and two females) aged between 19 and 24 years. Their task was to replicate three different objects using the ClaytricSurface system. The sample objects included a Triangle (representing a rough shape), a Face (representing a detailed shape), and a Bowl (representing a shape with an overhang). These objects are depicted in Figure 4.9.

We examined the range of stiffness (pressure values) used by the participants

while creating shapes on the ClaytricSurface. The results of this experiment are presented in Figure 4.10 a. The graph displays the average pressure values used by each participant to replicate the three different shapes, along with the standard deviation. From the findings, we observed that participants tended to use lower softness values (-1kPa) when modeling the Triangle, while higher softness values (-2.6kPa) were employed for the face shapes. The highest average pressure value recorded was (-4kPa) for overhung shapes. These results confirm our previous technical evaluation on displacement and pressure relations, where the display does not stiffen beyond the (-4kPa) thresholds. Based on these results, we conclude that the effective pressure range for the modeling application is 0 to (-4kPa), which can be achieved using an inexpensive vacuum pump.

To further enhance the modeling stiffness control, we incorporated a color range indicator into the control slider, as shown in Figure 4.10b. This visual cue assists users in selecting the optimal hardness value suitable for the specific modeling task, and it also helps them reset details without changing the overall shapes by providing a pressure threshold reference. The color range includes blue for rough shape modeling and red for detailed shape modeling. Additionally, we introduced a button as a replacement for the slider to automatically select the pressure range for rough or detailed shape modeling.

(a) Sample object

(b) Created models by users

Figure 4.9: Three models used in user evaluation on stiffness level and deformability: triangle, face, bowl

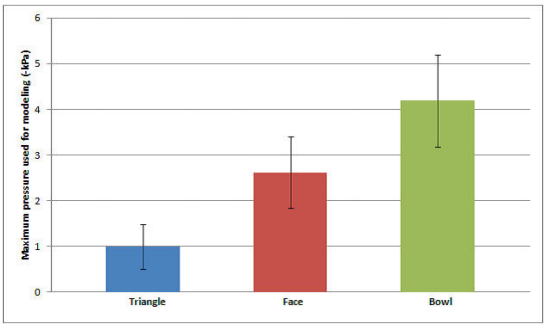

(a) Average pressure value with standard deviation

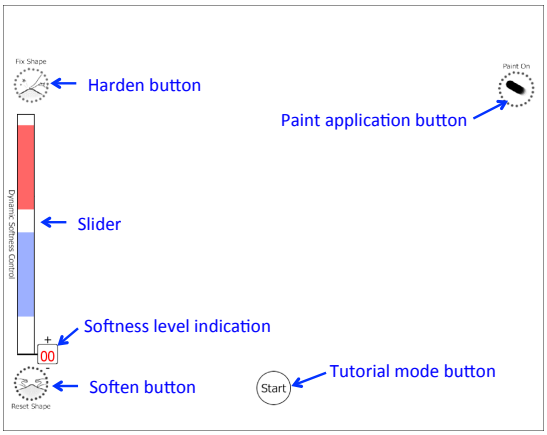

(b) Projected color range on the slider

Figure 4.10: User evaluation results on stiffness level and deformability experiments

4.8.2 Touch Detection Accuracy

We evaluated the detection accuracy for finger touches on four surface shapes: soft flat, rigid flat, rigid convex hemispheroidal, and rigid concave hemispheroidal. The hemispheroidal surfaces were 5 cm high and 15 cm in diameter (see Figure 4.11).

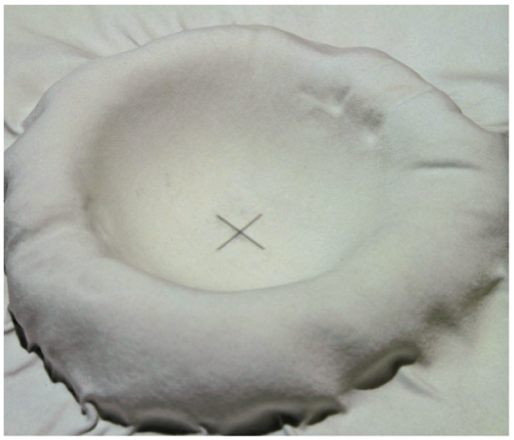

(a) Concave

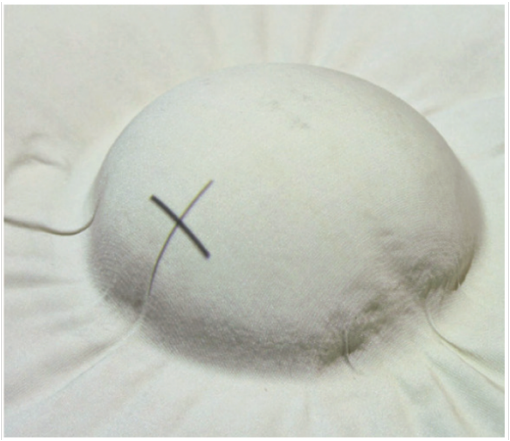

(b) Convex

Figure 4.11: Hemispheroidal surfaces for evaluation. The participants had to touch targets that appeared on the surface in random order.

The participants were the 10 students we mentioned before (one was female and one was lefthanded); all had experience with touch devices. They touched an X-marked target that appeared at nine fixed locations on the display surface in random order, first with their right hand and then with their left. Eight targets were on a ring with a 50-mm radius (linear distance) from the ninth, central target (see Figure 6a). On the convex and concave surfaces, the targets were at approximately a 45-degree zenith angle. This procedure produced 432 pointing trials (4 surfaces $\times$ 2 hands $\times$ 9 targets $\times$ 6 trials) per participant.

To minimize the influence of other potential factors, we took three measures. First, to ensure the contact point wasn't occluded, we had the participants touch the target without bending the index finger. Second, to avoid misdetection from inadvertent motion during touching, we had the participants hold the finger still after touching. We then recorded the location 200 ms after the first contact. A buzzer signaled the completion of the data taking and informed the participant of a successful measurement.

Finally, to control parallax issues, we had the participants keep their heads steady above the surface so that the whole target area was clearly visible. Figure 6a shows the recorded touchpoints. The red points were with the right hand; the blue points were with the left. Confidence ellipses enclose 95 percent of the points. The contact points for all the targets yielded an offset of 3.9 mm (a 1.7-mm standard deviation) biased to the right of the target's center. No perceptible offset difference existed between right and left-hand touches.

Figure 4.12b displays the minimum GUI button diameter needed to cover 95 percent of the touch points for each surface. We also grouped the targets on the hemispheroidal surfaces on the basis of slope type (uphill or downhill) and calculated the button diameter. We found that both the offset (11.7 mm) and minimum button sizes (16–25 mm) for rigid surfaces agreed with previous research on touch detection using a depth camera.3

On the basis of Figure 4.12b, the flat, soft surface was the least accurate, with

a minimum button diameter of 30.2 mm. Finger presses made the surface under the fingertip stick out. We determined that this resulted from a miscalculation of the touch area because the system wasn't updating the surface obscured by the user's hand. However, with a little training, users can achieve more accurate touch detection by adjusting their touch strength according to the surface hardness.

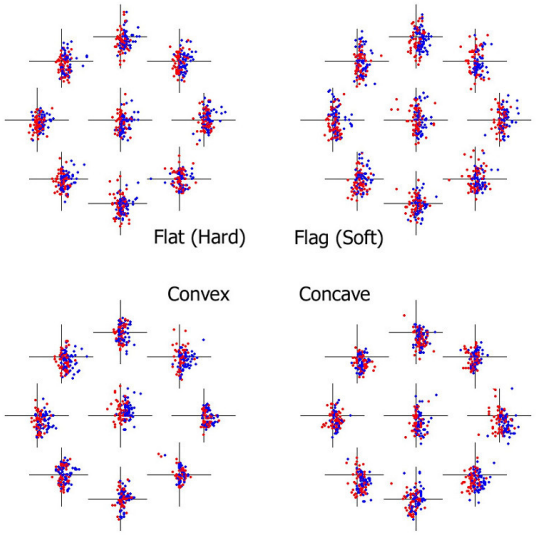

(a) The recorded touch points, with 95 percent confidence ellipses.

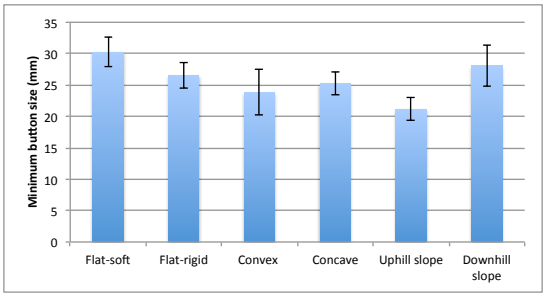

(b) The minimum GUI button diameter needed to cover 95 percent of the touch points for each surface.

Figure 4.12: Touch detection evaluation results. The error bars denote the standard deviation across all trials.

The accuracy was slightly higher with convex surfaces than with concave surfaces (23.9 versus 25.2 mm). Also, accuracy was higher with uphill slopes than with downhill slopes (21.1 versus 28.0 mm). As we mentioned before, our system determines touch in a region from 5 to 15 mm from the surface. When the user's finger touches an uphill slope, this region is smaller owing to the finger's angle of incidence. When the finger touches a downhill slope, the touch region becomes larger, and the centroid shifts away from the real touch point.

To improve touch detection accuracy, one approach that can be considered is the introduction of multiple cameras. Utilizing multiple cameras from different

angles can provide a more comprehensive view of the user's interactions, potentially reducing occlusion and enhancing overall touch detection precision. However, it is important to acknowledge the limitations of depth camera-based touch detection, which is around 21.1 mm in our system. To overcome this limitation and achieve further accuracy improvements, an embedded capacitive touch sensor can be a more effective solution. Prior research, as demonstrated by [42], has shown the effectiveness of capacitive touch sensors in enhancing touch detection precision and sensitivity.

4.9 Discussion

Here we examine aspects of ClaytricSurface that deserve further comment or need improvement.

4.9.1 User Feedback

We conducted a study to observe how first-time users performed with ClaytricSurface. Seven participants operated our modeling application and provided feedback. Some participants commented that controlling the hardness was initially difficult because the relation between the hardness and the slider wasn't clear. However, after a few attempts to manipulate the slider and obtain a feel for the hardness using touch, those participants were able to use the application to shape a model and add texture. Participants also suggested that color-coding the slider to indicate the appropriate hardness for different tasks—blue for rough shaping and red for detailing—would help users choose surface malleability. Finally, most participants stated that the tactile feedback when the hardness changed dynamically was appealing, making the surface feel more organic than artificial.

4.9.2 The Particles and Surface Fabric

Particle size is significant in determining tactile characteristics. A small, light particle is a good filler. The particle's size and the surface fabric's thickness affect the created shape's resolution and detail. Small particles and a thin surface material will let users create finer, more detailed shapes. Also, if an external force is applied to the display, the smaller, lighter particles react more smoothly, giving the models a more aesthetic look and feel. This also reduces the load on the user's finger during long-term use of the system. In addition, light particles prevent the surface from collapsing under its own weight. If the display pressure decreases, the spaces between the particles next to the surface fabric will fill with the shapes of other particles. If the particles are too large, the texture will be visually unpleasing (similar to goose bumps), and fingers will experience increased friction when stroking the display. The particle size also affects the air volume in the display. Smaller particles reduce the display's overall volume shrinkage under decompression and increase the response time to internal pressure changes. However, display volume changes due to compression aren't visually noticeable. We plan to investigate using nonspherical particles to create various friction levels and provide different and unique tactile sensations. We demonstrated our prototype over five days (approximately five hours per day) at an international conference. The particles and display surface sustained no substantial damage. A slight darkening and stretching of the fabric occurred, along with increased air leakage, which we considered to be due to the fabric's deterioration and general wear and tear. The maintenance in this case isn't difficult because the fabric is inexpensive and easily replaced.

4.9.3 Responsiveness

The responsiveness to pressure control depends on the air volume (the display size) and the vacuum pump's displacement. The prototype takes about three seconds to go from soft to hard. Although current linear piston pumps have enough

decompression capability to harden the surface, we found that the decompression speed was unacceptable owing to the pumps' low displacement. So, we plan to combine the current vacuum pump with other types of pumps such as an air blower, which offers high (fast) displacement. In addition, we could combine a vacuum tank and an air compressor to decrease the response time when stiffness changes. A high-response pressure control could generate even more tactile sensations owing to haptic vibrations from rapid pressure changes.

4.9.4 Shape Modeling

Our system's shape-modeling capability has limitations stemming from the limited quantity of particle filler and the surface fabric's area and flexibility. For example, if the user makes a large convex shape in one part of the display, he or she must gather a large number of particles. This prevents the user (or another user) from creating shapes at another part of the display. In the prototype, a shape's maximum height is approximately 15 cm. When creating a tall convex shape, users must pull the surface fabric with substantial force. However, the system can't both decrease the surface stiffness and maintain the shape's height. To fix this, we'll need more flexible cloth. However, this might lead to decreased surface elasticity caused by permanent fabric stretching and decreased durability. So, we're developing mechanisms to dynamically change both the surface volume and area. The display's hardness also depends on the particle layer's thickness. If the user makes a detailed shape with parts less than 3 cm wide, the shape might be easily deformed inadvertently by hand or under gravity, even if the display is at its hardest. To make modeling easier and more efficient, the vacuum-molding tool provides some primitive shapes (circle, rectangle, and triangle) as a base design. In particular, if the target shape is clearly specified, the system can have a preset shape to aid modeling. Users then only need to change the preset shape's details. Furthermore, the system can project geometric information such as dimensions or the current height onto the shape to aid modeling navigation.

4.9.5 Self-deformation

While vacuum jamming is effective in controlling the surface stiffness properties, it should be noted that jamming alone cannot generate external forces on the surface material to enable shape deformation. Consequently, although users have the freedom to fix or modify the surface shape, the shaping process itself relies entirely on manual manipulation. Other research studies have also utilized the vacuum jamming method on deformable interfaces and demonstrated self-actuated surface deformation by combining it with additional actuators, such as pressured cells and cylinder pistons, as shown in Hovermesh [120] and Haptic Jamming [179]. However, these methods come with their own challenges. Firstly, they often involve complex system designs that are difficult to implement. Secondly, they may result in resolution degradation due to separated mesh structures. In our future work, we aim to develop a novel mechanism that enables both shape deformation and stiffness change within a single system, addressing these limitations.

Chapter 5

ASTRE: Programmable Shape-changing and Variable-stiffness Mechanism using Artificial Muscle

5.1 Overview

Soft actuators offer several advantages over traditional rigid actuators, particularly in terms of human interaction safety and environmental adaptability. These actuators are also lightweight, consume less energy, and can mimic biological motions. Whitesides et al. have highlighted the significance of soft actuators in serving as intermediaries between humans, rigid robots, and computer systems, emphasizing their future importance [221].

Recently, many solutions for soft actuator fabrication have been proposed, however, the majority of the soft actuator is built using elastomeric materials such as silicone rubbers [174]. Common techniques include mixing polymer and catalyst, degassing, molding, and adhesion of different layers. This sequence of processes is difficult because experience and know-how are needed to handle issues, such as removing air bubbles and molding small air channels. To cope with this drawback, we proposed ASTRE : a soft actuator novel mechanism using a combination of Pneumatic Artificial Muscle(PAMs) and 3D printed mechanical constraint. This technique enhances the inherent contraction deformation of Pneumatic Artificial

Muscles (PAMs) by enabling programmed shape changes and adjustable stiffness. By eliminating processes such as molding, curing, and adhesion, it effectively reduces fabrication time and effort. Moreover, it achieves this with a reduced number of materials and equipment, while maintaining a diverse set of features.

In this research, we proposed a novel shape-changing and variable-stiffness mechanism using a composite of soft PAMs and 3D printed structures. The printed structures functioned as programmable mechanical constraints to alter PAMs contraction and radial expansion behavior into both shape deformation and stiffness changes. We leverage both shape and stiffness tuning capabilities as a framework for prototyping shape-changing interfaces. We explore the possible features and utilization of such an interface and synthesize a design space based on our exploration.

In summary, the contributions of this research are listed as follows:

1. Democratization of novel mechanism to program deformation and stiffness using PAMs and 3D printed constraint.

2. Showcase of the 3D printed module design for shape-changing and variable-stiffness mechanisms.

3. Technical evaluation to demonstrate the dynamic of our proposed mechanisms.

5.2 Related Work

5.2.1 Soft Actuator in Robotics

The soft actuator has become the main focus for the advancement of soft robotics research [206]. Previous works have proposed various types of material utilized for soft actuators such as silicon/PDMS [139, 192], film [143, 157], gel [78, 137, 216], fiber [56, 163], paper [8, 213] and composite such as PAMs [2, 95]. These works have opened up new technology to achieve a compliant robot with lightweight,

and energy-efficient traits. Various research especially has focused on fluid-driven actuator [95, 137, 139, 192, 223], due to the convenient fabrication, simple control, and intuitive mechanism.

5.2.2 Soft Actuator in HCI

Soft actuators in HCI research also serve new types of interactions that previously cannot be achieved by rigid actuators (e.g. motors). Previous works have proposed various utilization of soft actuators for input devices [87, 91], wearables [85, 86, 94], aesthetic [169, 215, 227], and large-scale interface [135, 189]. Soft actuators are especially functional for shape-changing interfaces due to the capabilities of a seamless transition in shape-deformation [141]. It allows an organic-like interaction that can enhance user affective and intuitiveness. The proposed actuation in this research can be categorized into linear scaling, bending, and twisting.

5.2.3 Soft and Variable-stiffness Actuator

While achieving a flexible body is the primary objective of a soft actuator, it also presents a significant challenge when it comes to positioning control. To address this challenge, variable-stiffness has emerged as one of the most effective solutions, drawing inspiration from natural examples like octopus arms and elephant trunks [116]. Among the various techniques for achieving variable-stiffness in soft actuators, the vacuum jamming technique is the most commonly employed, encompassing granular, layered, and fiber jamming [7, 15, 88]. Another approach involves the use of Low Melting Point Materials (LMPMs), such as wax, and Low Melting Point Alloys (LMPAs), which can be activated using external stimuli like heat and electric power [26, 176]. However, these stiffness control techniques are inherently complex due to the challenges associated with managing different power sources for actuation and stiffness adjustment (e.g., compressors and vacuum pumps).

Previous works have also explored the utilization of bead jamming [32, 74, 88],

which operates on a similar principle to vacuum jamming. In this approach, a tendon actuator is employed as a coupling force to induce jamming between beads arranged in a series. Building upon this concept, we have incorporated these mechanisms into PAMs actuators. Additionally, we have investigated the programmability of this mechanism by adjusting the mechanical constraint parameters.

5.2.4 PAMs based Soft Actuator

Pneumatic artificial muscles(PAMs) such as the McKibben actuator, since patented in the 1950s have been used in many robotics applications [206]. In recent studies, PAMs have been widely used for wearable soft robot actuators because of their lightweight and high-efficiency properties [48, 62, 196]. Although some of these previous works also utilized 3D-printed mechanical constraints to control PAMs deformation, this study is the first to focus on various mechanical constraint designs, especially for variable-stiffness mechanism.

5.3 Proposal of Mechanical Constraint Mechanism for PAMs Actuator

PAMs is a tendon shape actuator that consists of an inner tube and sleeve. When actuated PAMS exhibits two types of forces which are radial expansion and linear contraction. Both of these forces are dependent on the diameter of the tubes, the weaving angle of the sleeve, and the pressure of the air inside the tube. In this research, we propose a set of mechanical constraint mechanisms to alter either/both PAMs radial expansion and linear contraction force into various shape deformation and haptic/stiffness properties.

In this research, we utilized four basic mechanisms consisting of bilayer bending, spring mechanism, beads jamming, and rotational brake. We based these mechanisms on previous works on robotics and shape-changing interfaces, however, we

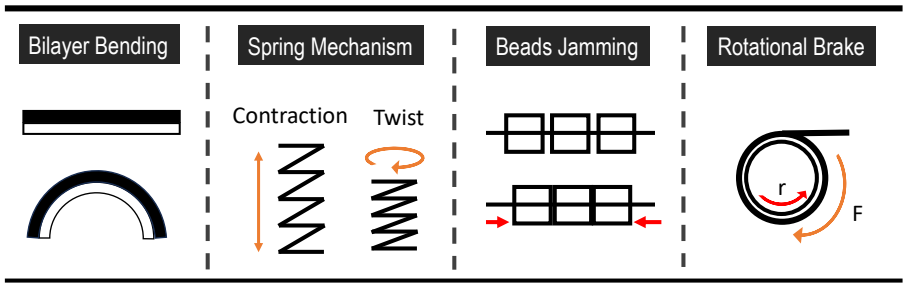

Figure 5.1: Four types of basic mechanisms that serve as the foundation for primitive modules.

present novelties in the combination of such mechanisms with PAMs actuators. In addition, we also leverage the mechanism into various programmable shape-deformation and variable-stiffness behavior, showcasing the efficiency of the proposed techniques.

5.3.1 Bilayer Bending Mechanism

One commonly employed approach for achieving bending deformation in materials involves the integration of a composite with two layers of different materials into a bilayer structure. This configuration allows for bending to occur by leveraging the differential expansion or contraction between the layers upon actuation while maintaining consistent strain at the layer interface [210]. The magnitude of the bending angle can be customized based on factors such as material stiffness, layer thickness, and applied strain. Moreover, intentional design choices can enable the material to exhibit surface wrinkling effects instead of conventional bending. Previous studies have explored the application of this approach using various actuators, including Shape Memory Alloys (SMA) [129], wire tendons [204], inflatables [129], and PAMs [2, 207]. However, the parametric programming of bending angles through the manipulation of mechanical constraints, particularly in the context of PAMs actuators has not yet been conducted.

5.3.2 Spring Mechanism

A spring is an elastic structure that is specifically engineered to store and release mechanical energy, while also providing redundancy to support a diverse range of deformations caused by external forces. In our research, we focus on the utilization of helical springs, which possess an elongated shape and the ability to withstand both contraction and twisting loads. Similar to the bending mechanism, the stiffness of springs can be adjusted based on factors such as shear modulus, wire thickness, number of coils, and coil diameter [60]. These parameters play a crucial role in determining the extent of spring deformation and its response to external forces.

5.3.3 Beads Jamming

Similar to vacuum jamming, bead jamming also consists of a collection of elements (beads) that the kinematic and frictional coupling increase when tension is applied, resulting in altered mechanical properties [3]. While vacuum jamming requires an external membrane, which can create design complications for system integration. The material of the membrane also can have a significant influence on a jamming structure's performance. In this research, we utilize bead jamming [32, 74] where each bead is connected using a shrinkable tendon to induce the jamming phenomenon. This mechanism can improve the limitation of interface design and can be combined with a deformation mechanism to enable shape-changing while stiffening the structures.

5.3.4 Rotational Brake

The rotational brake mechanism is employed to introduce frictional forces that effectively reduce or halt rotational motion. By regulating the level of friction, this mechanism can provide users with a sensation of stiffness change when they apply external forces to the system. In our approach, we utilize the radial expansion force of Pneumatic Artificial Muscles (PAMs) to generate and manipulate the frictional

force exerted on the mechanical constraint. This allows us to achieve precise control over the rotational brake and enable the desired stiffness modulation in response to user interaction.

5.4 Primitive Modules

Utilizing the four basic mechanisms, we propose six types of modules that can be classified into shape-changing and variable-stiffness modules. Figure 5.2 shows the 3D model and the difference between the actuated and unactuated states.

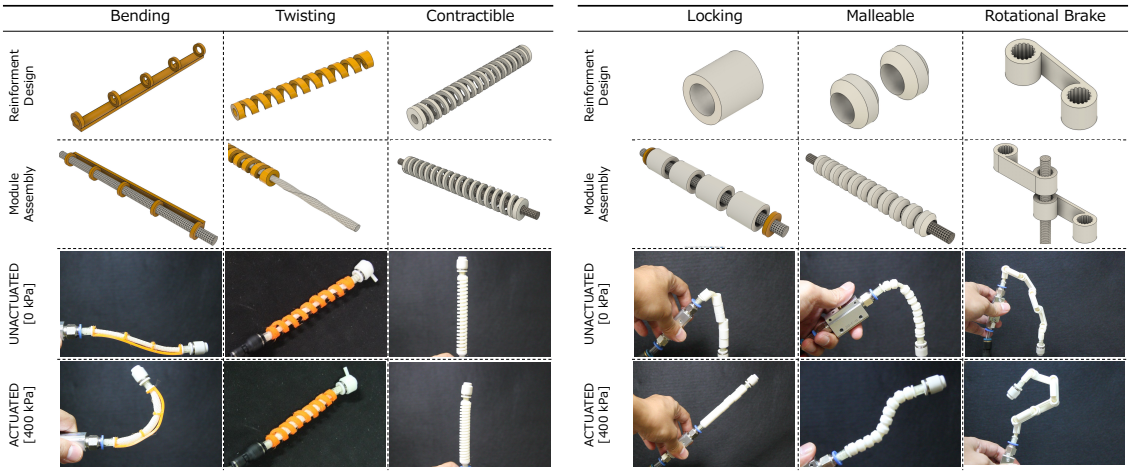

(a) Shape-changing modules (b) Variable-stiffness module

Figure 5.2: Two types of ASTRE modules

5.4.1 Shape-changing Modules

The shape-changing modules induce deformation by altering the contraction force of the PAMs actuator into three types of motion. The motion is determined by mechanical constraints and can be controlled by adjusting the air pressure and module parameter. The three deformations module are:

1. **Bending module** utilizing bilayer actuation phenomenon. It provides a curve and angle for shape deformation purposes. It exhibits a straight shape

normally and bends when actuated. The basic design is a flexible constraint layer with rings along the layer acting as a guide rail for the PAMs actuator. It also can be designed to be normally curved, providing smaller or larger amplitude angles.

2. **Twisting module** was based on the torsion behavior of a helical spring. We twisted the PAMs, insert them inside 3D printed spring, and fix both PAM's ends into the spring. This mechanism resulted in twisting deformation when actuated and reverse twisting when unactuated. We printed the module using TPU filament on an FDM printer.

3. **Contractible module** was also based on the spring mechanism. Although PAMs can contract without mechanical constraint, the spring structure serves as a damper to store the compression energy and exert opposing forces. The spring constraint also adds some rigidity to the PAMs soft body, while still allowing flexibility in deformation.

5.4.2 Variable-stiffness Modules

The variable-stiffness modules transform the physical properties by altering the contraction and radial expansion of the PAMs using mechanical constraints. Both the contraction and expansion ratios are influenced by the air pressure. Thus, the stiffness of each module could be controlled by adjusting the air pressure. Three types of variable-stiffness are:

1. **Locking module** was based on the beaded jamming mechanism [74]. The module is soft and flexible normally and becomes rigid when actuated. We design the module as an array of beads with PAMs threaded inside. When actuated, the contraction force of the PAMs pulls and compresses the beads making them locked with each other.

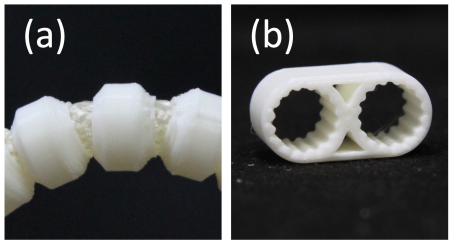

Figure 5.3: (a) The bulge between malleable modules. (b) Gear tooth to increase brake torque

2. **Malleable module** exhibits unique behavior that allows the structure to retain its shape after being bent by an external force. The module is flexible when unactuated and becomes deformable when actuated. Similarly to the locking module, the malleable module utilizes beads jamming with PAMs threaded inside. However, the beads in the malleable module have smaller holes. When the module is bent(see Figure 5.3(a)) the PAMs bulge out on a small gap between the modules. This bulge allows the module to retain its shape, even when the bending force is released. We design a chamfer on malleable beads, to allow a greater range of deformability.

3. **Brake module** is based on a hinge structure with PAMs threaded as its shafts. In a normal state, the hinge can rotate freely. However, when the PAMs are expanded inside the hinge, they rub together and resist rotation. We added a gear tooth to the hole to increase the brake torque(see Figure 5.3(b))

5.5 Shape Deformation and Stiffness Tunning Mechanism

Here we conduct a preliminary experiment to understand the basic PAMs mechanism, shape-changing mechanism, and variable-stiffness mechanism.

5.5.1 Basic PAMs Mechanism

PAMs were originally invented by Dr. O. Häfner, and further developed by Dr. Joseph Laws McKibben for use in practical applications in 1952[121]. The PAMs we use in this research are made of a flexible tube (silicon) enclosed in a braided sleeve (Aramid). When the tube is pressurized, due to the constraint by the braids, any volumetric expansion from the tube translates into a contraction deformation(Figure 5.4). In this research, we used PAMs actuator that is produced by S-muscle co [165]. There are three types of size variations consisting of 1.8 mm, 3 mm, and 5 mm in outer diameter. However, to simplify the evaluation of this preliminary work, we conducted all experiments using 5 mm PAMs. We use 0.4 MPa as maximum pressure to prolong the PAMs usage lifetime, as the PAMs need to be repeatedly used.

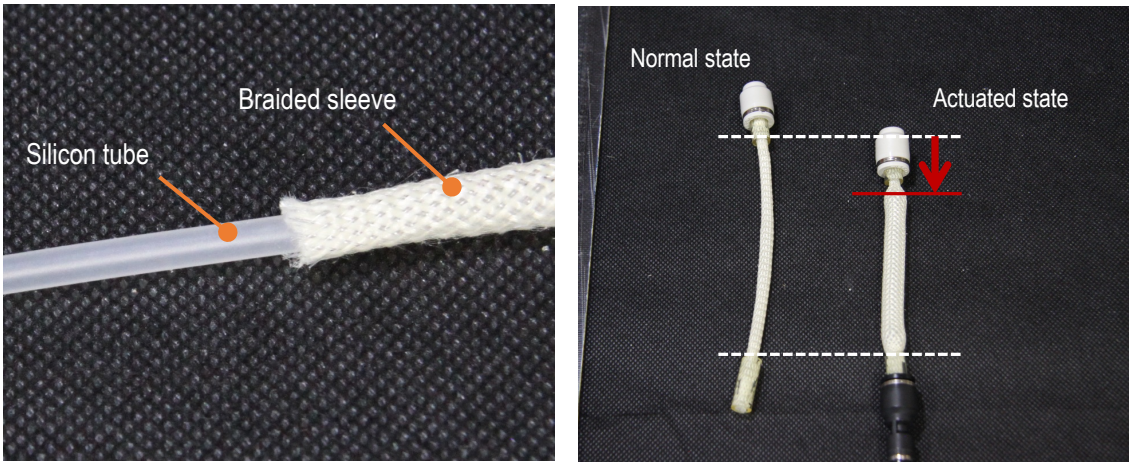

(a) Basic PAMs structure (b) PAMs on normal and actuated state

Figure 5.4: Illustration of basic PAMs structures and actuation mechanism

Contraction Ratio Characteristics

Figure 5.5a shows the relationship between the contraction ratio and air pressure. It shows non-linear increases in the contraction ratio along with the increases in air pressure. It also shows a maximum contraction ratio of 20% under an air pressure

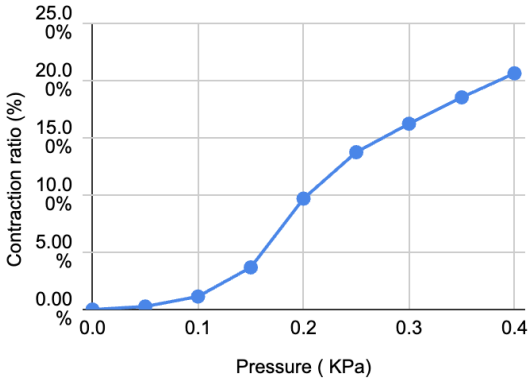

(a) PAMS Contraction ratio

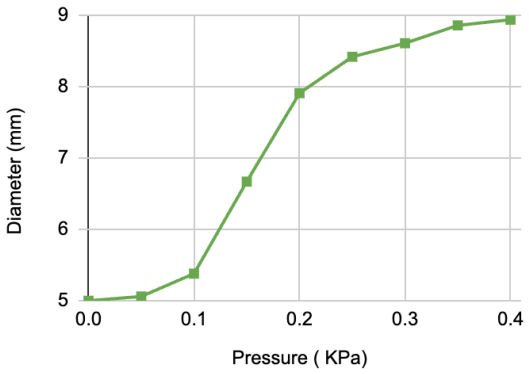

(b) PAMs Diameter

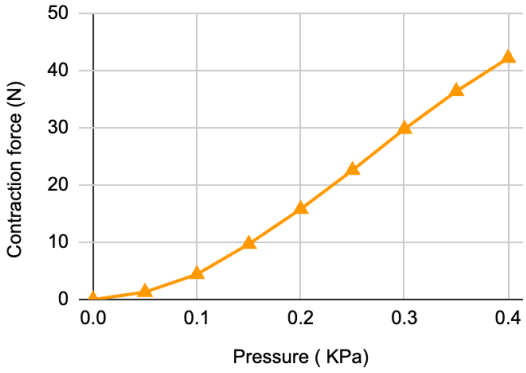

(c) PAMs Contraction force

Figure 5.5: Basic PAMs characteristics related to air pressure

of 0.4MPa.

Radial Expansion Characteristics

Figure 5.5b shows the relationship between PAMs diameter and air pressure. It shows non-linear increases similar to the contraction ratio graph. The maximum expanded diameter is 9 mm (180% expansion) at 0.4MPa.

Contraction Force Characteristics

Figure 5.6c shows the relationship between Contraction force and air pressure. It shows a similar relatively linear relationship, with a maximum contraction force

is 42N at 0.4MPa.

5.5.2 Shape Deformation Mechanism

We are able to alter the compression force into three types of deformation bending, twisting, and contractible. Due to the compression force correspondence with the air pressure, therefore the deformation is directly related to the pressure. Although precision control of deformation is difficult due to the motion hysteresis and the tube material fatigue. However, the relative relations is remaining the same.

Bending Characteristics

Figure 5.6 shows the relationship between bending angle and air pressure. It shows non-linear increases in bending angle along with increases in air pressure. It also shows a maximum bending angle of 150° under an air pressure of 0.4MPa.

Twisting Characteristics

Here we conduct an experiment where we change the air pressure and measure the twisting angle at 1080° winding (Figure 5.6b. It shows an asymptotic behavior of bending angle to a constant value as the pressure increases. It shows a maximum twist angle of 425° under an air pressure of 0.4MPa. However, further adjustments on winding can be made to create different twisting behavior.

Contractible Characteristics

Figure 5.6c shows the relationship between the contraction ratio of the contractible module and air pressure. Similar to the basic PAMs, it shows non-linear increases in contraction ratio along with air pressure. However, the maximum contraction ratio is less than 20% due to the contractible module's spring stiffness.

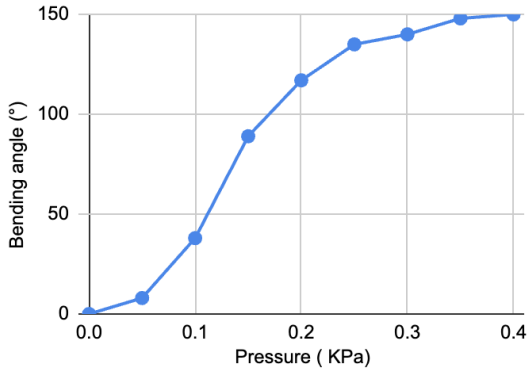

(a) Bending angle

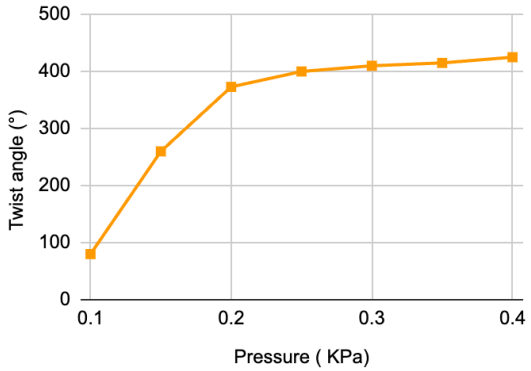

(b) Twisting angle (at 1080° winding)

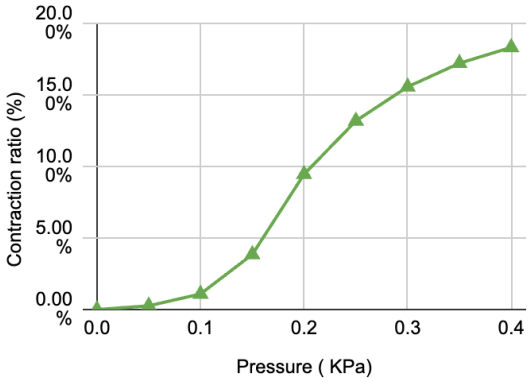

(c) Contraction ratio of contractible module

Figure 5.6: Deformation characteristics of shape-changing modules

5.5.3 Stiffness Control Mechanism

The stiffness variation in locking, malleable, and brake modules is determined by the contraction and radial expansion of the PAMs. Both the contraction and expansion ratios are influenced by the air pressure. Thus, the stiffness of each module could be controlled by adjusting the air pressure.

Stiffness Range of Each Module

Here, we verify the relationship between the stiffness of the modules and the air pressure. Figure 5.7(a)(b) and(c) show the stress-strain curves in a three-point bending flexural test on locking, malleable, and brake module. The applied

pressure was varied in 0.05MPa steps from 0 MPa to 0.4 MPa, and we found that the locking mechanism shows a stiffness change from 0.1 MPa, while malleable and brake modules showed a stiffness change from 0.15 MPa and 0.2 MPa respectively. The dash-dotted line shows the line fit to the approximation formula. All modules show increases in force as the air pressure increases, with the locking module showing the highest force.

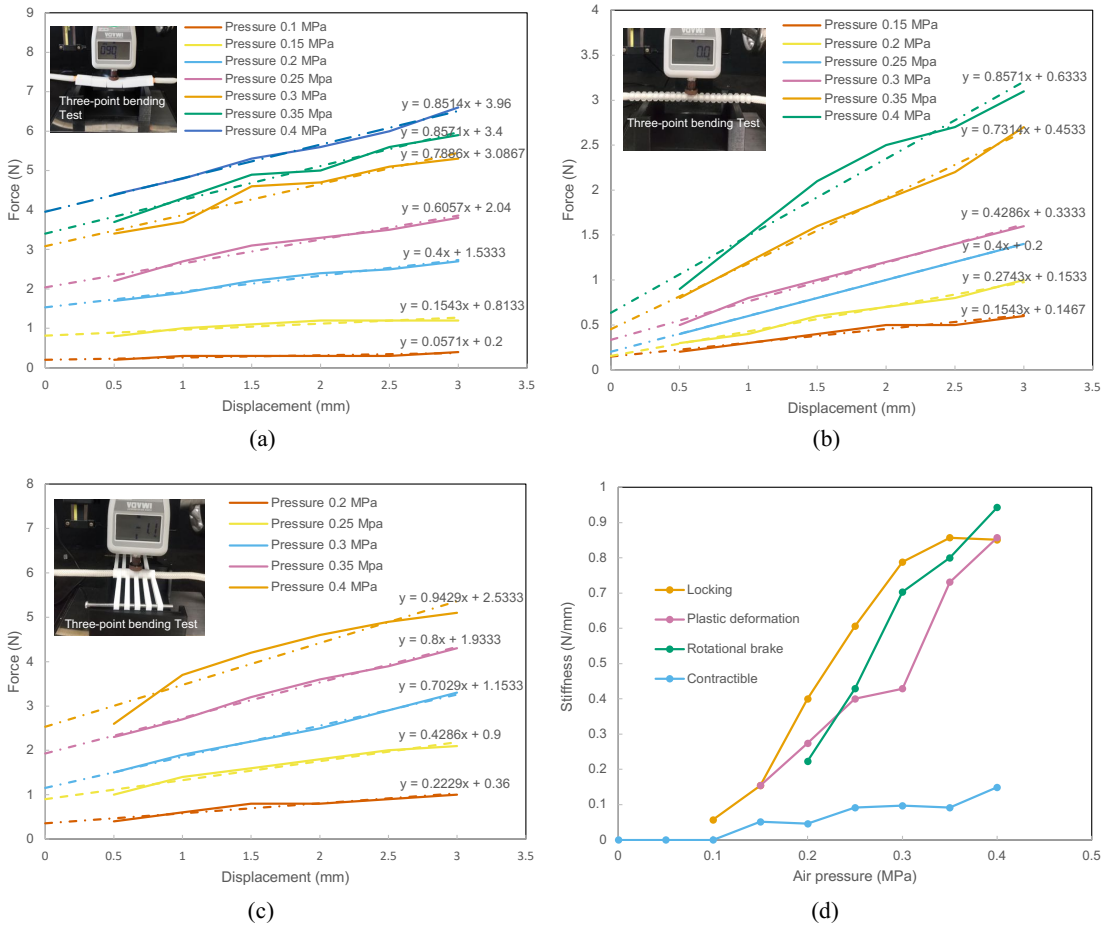

Figure 5.7: Stress-strain graph : (a) Locking module, (b) malleable module, (c) brake module. (d) Relationship between air pressure and module stiffness

Figure 5.7 (d) shows the stiffness change according to the air pressure variation on each module. It shows non-linear increases in stiffness as the air pressure increases. Each module had a different range of stiffness variation, with the rotational brake

module having the highest stiffness of 0.94 N/mm. The locking modules show the widest stiffness range of 0.06 N/mm up to 0.86 N/mm. We also added stiffness measurements of contractible modules to show the stiffness change on the PAMs themselves (0 N/mm to 0.15 N/mm).

Locking and Malleable Characteristics

Both locking and malleable module consist of hollow module arrays, with different hole diameters. In this experiment, we investigate the relationship between hole diameter and stiffness behavior. We measured the three-point bending test of hollow modules with variations in the hole diameter. The pressure was set at 0.4 MPa and we measured the load for every 1 mm displacement. Figure 5.8 shows that forces reduce as the hole diameter increases. However, unloading phase hysteresis (dashed lines) shows each hole diameter exhibited different behavior. The 9 mm and 8 mm holes both exhibited elastic behavior, and the 6 mm and 7 mm holes exhibited plastic behavior. Based on these results, we select the 9 mm hole for locking modules to maximize the elasticity when applied with a load. For plastic deformation modules, we select the 7 mm hole because the properties were similar to the 6 mm hole, while the assembly was easier for threading the PAMs.

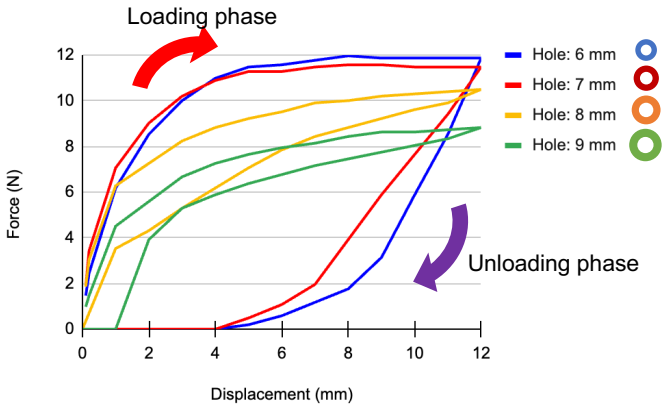

Figure 5.8: Stress-strain graph of locking/maellable modules with variation in diameter

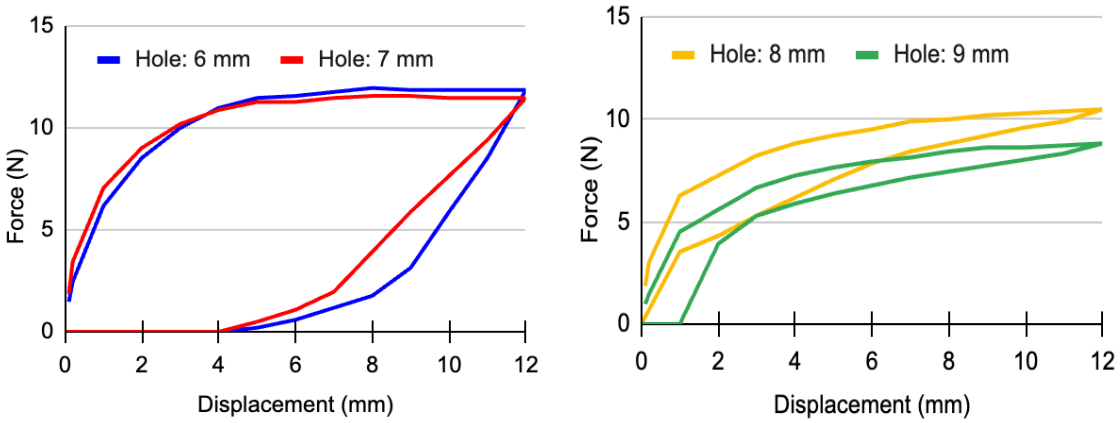

(a) Plastic behavior (b) Elastic behavior

Figure 5.9: Comparison between plastic and elastic behavior

5.6 Fabrication Workflow

The fabrication process of our modules involves the utilization of Pneumatic Artificial Muscles (PAMs) and 3D-printed mechanical constraints. Figure 6.1 illustrates the design space of our modules, which encompasses module design, 3D printing, and module assembly. The modules are attached to a pneumatic control unit.

5.6.1 Module Design

We have developed a user-friendly graphical user interface (GUI) for designing the basic modules, employing the open-source 3D modeling software openSCAD [89]. This GUI facilitates the generation of shape-changing and variable-stiffness modules, while allowing customization of parameters such as length, number of beads, and hole size. Figure 5.10(a) exemplifies the module design process for a bending module. For more complex modules, we employed Fusion 360 software to refine the initial designs [29].

5.6.2 3D Printing

All modules within our toolkit can be fabricated using a standard desktop 3D printer. While we primarily utilized a Fused Deposition Modeling (FDM) printer for our experiments, a Stereolithography Apparatus (SLA) printer can also be employed. In the case of FDM printing, we utilized PLA or ABS materials for the rigid constraints and TPU 95 (Polyflex) for the flexible constraints. Additionally, laser cutting can be used to create beads such as locking beads.

5.6.3 Assembly

The module assembly process bears a resemblance to the threading technique used in bead crafts. While this process may require time and effort, our tests with several individuals demonstrate that most people can easily understand and perform these procedures. To facilitate the threading of soft fibers through the module holes, we incorporate a reinforcement cap at the ends of the PAMs. Figure 5.10(b) showcases the PAMs threading assembly process.

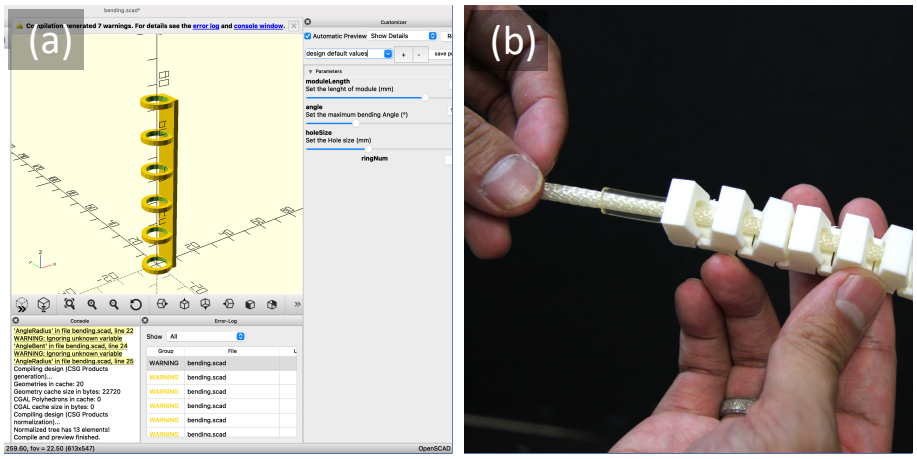

Figure 5.10: Fabrication Workflow. Left: Design tool with GUI to customize 3D printed module, Right: Assembling work of threading PAMs through module

5.6.4 Pneumatic Control

Air pressure is the power resource to actuate PAMs that consequently change the stiffness or deform the module. The air pressure supplied by a pump/compressor can be adjusted using an electro-pneumatic regulator. The regulator can be directly controlled through a command signal from a PC or a potentiometer via a micro-controller. Figure 5.10(c) shows a diagram of the pneumatic control connection.

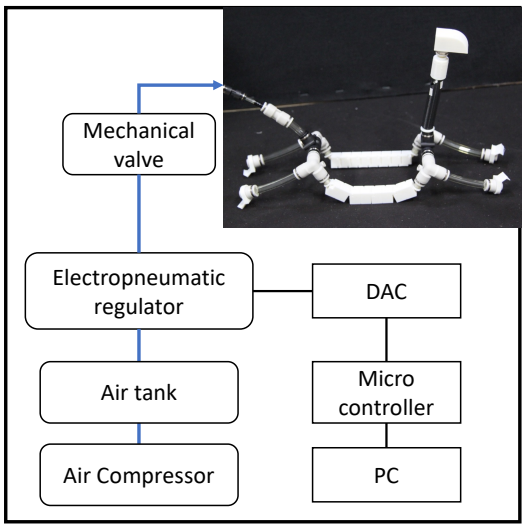

(a) Pneumatic system

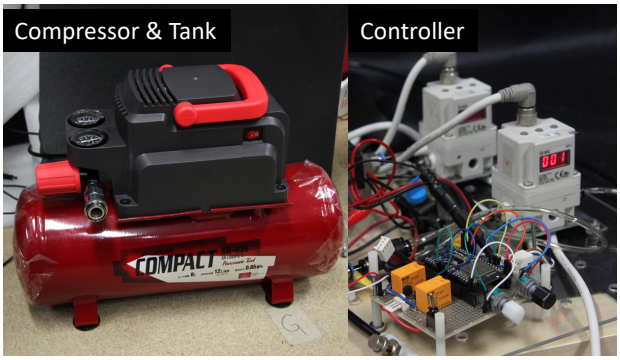

(b) Bulky setup

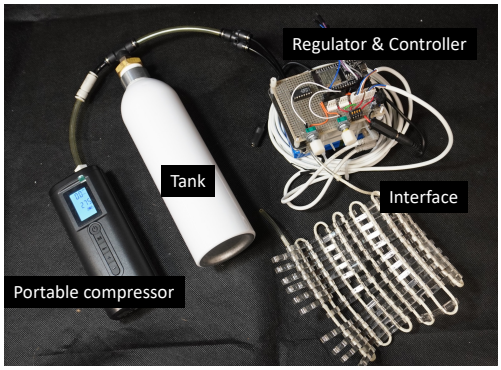

(c) Portable setup

Figure 5.11: Pneumatic control. The system measures and controls the difference between atmospheric and internal volume pressure

We use two types of pneumatic control in this research. First is a bulky setup

using a high-power compressor and medium-size regulator (ITV1050-212BL, SMC Corp.). This unit is able to dynamically change the air pressure with a 300 L/min peak flow rate. In the second setup, we use a battery-powered bicycle compressor and a small-size regulator (ITV0051-2L, SMC Corp.). The total weight of the second setup is 1.2 Kg and the systems can be fitted inside a backpack (Figure 5.11). However, it has low airflow (6 L/min flow rate) and low reservoir volume. Alternatively, a readily available pneumatic controller such as FlowIO and PneuSoRo [177, 230] can also be employed to enhance convenience during the fabrication process, as demonstrated by previous work [2].

5.7 Discussion

5.7.1 Deformation and Stiffness Limitation

This research introduces a novel mechanism for programmable shape change and variable-stiffness. To demonstrate the practical application of our mechanism, we initially address the limitations of the basic module. In Figure 5.1, we illustrate the maximum deformation and stiffness of each module. It is important to note that the maximum angle attainable in the bending and twisting module is dependent on the module's length. Consequently, longer modules allow for a greater maximum angle to be achieved.

5.7.2 Module Assembling Challenge

The prototyping technique employed in this research may not be suitable for large-scale manufacturing due to the drawbacks associated with the manual assembly of PAMs. One approach involves modifying the 3D printing process to allow for easier PAMs placement. This can be achieved by pausing the printing process before closing the threading hole, as depicted in Figure 5.12(a). The PAMs can then be easily laid in place alongside the pre-arranged modules, as shown in Figure 5.12(b).

Table 5.1: Limitation of the ASTRE modules

* Value at 0.4 MPa

		Item	Maximum value *	Unit
Basic PAMs		Contraction ratio	20	%
		Expansion ratio	180	%
		Contraction force	42	N
Shape-changing	Bending	Bending angle	150	°
	Twisting	Twisting angle	410	°
	Contractible	Contractio ratio	18	%
Variable-stiffness	Locking	Stiffness	0.851	N/mm
	Maellable	Stiffness	0.857	N/mm
	Brake	Stiffness	0.940	N/mm

Finally, the printing process can be resumed to close the hole, as illustrated in Figure 5.12(c). In the future, automation can further enhance this procedure by incorporating robotic arms and conveyor belts into the 3D printing process. This would streamline the assembly process and improve efficiency.

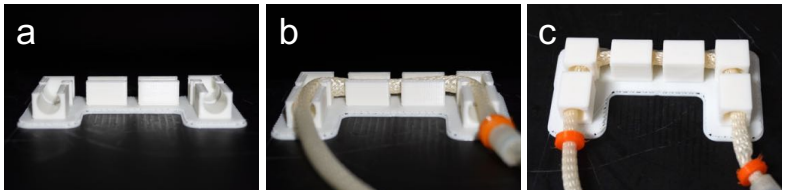

Figure 5.12: Halfway fabrication technique

5.7.3 Implementation to Other Actuators

In the ASTRE mechanism, we designed the mechanical constraint module specifically for PAMs actuators. However, we foresee the potential application of this mechanism to other fiber-shaped actuators such as SMA, tendon-driven actuators, and EAP actuators. While these actuators may not possess the same radial expansion properties as PAMs, they present unique challenges and opportunities for

further technological breakthroughs such as how to make those actuators modular, and how to control the amount of stiffness and deformation.

Chapter 6

AstreToolkit: Constructive Assembly Tools with Shape-changing and Variable-stiffness Capabilities

6.1 Overview

Entry to shape-changing interface research is challenging due to the required knowledge of both complex electronics and mechanical engineering [6]. These complexities increase exponentially when complex structures and physical properties are added to the systems. In shape-changing interface research, truss structures have been widely employed due to several advantages they offer over other types of structures, such as pin arrays [43, 71, 154], continuous tangible surfaces [21, 152, 171], and inflatable bladders [215, 224, 227]. Truss structures are known for their modularity, stability, and excellent volume-weight ratio, which has led to their extensive use in rapid 3D printing tools [66, 125, 198]. In such tools, complex 3D models are simplified into truss-like structures, enabling faster fabrication times. The scalable nature of truss structures also has enabled researchers to construct large-scale kinetic structures [92, 93]. This trait of truss structures allows for the creation of complex configurations that can undergo significant load.

Typical truss structures are composed of linear beams or fibers connected by joints, forming three-dimensional shapes. This construction allows truss structures

to be modular, interchangeable, and reconfigurable. These characteristics have been leveraged by researchers to develop constructive assembly prototyping tools [55, 147, 185]. This research combines Pneumatic Artificial Muscle (PAM) fibers with elongated-shape mechanical constraints to construct truss structures. We also incorporate commercial pneumatic fittings to facilitate quick and easy assembly of the toolkit. This combination provides several benefits, including effortless attachment and detachment of fibers from the joints, as well as interchangeability, allowing for easy maintenance by replacing independent modules. By leveraging this approach, the research aims to improve the usability and versatility of the truss structures toolkit.

We propose ASTRE Toolkit, a constructive assembly tool that combines shape deformation, variable-stiffness capabilities, and pneumatic control. This toolkit enhances the usability of shape-changing interfaces, allowing for the simulation of different physical properties such as softness, malleability, rigidity, and haptic properties like springiness. We utilize our previously proposed ASTRE mechanism for programmable shape-changing and variable-stiffness Pneumatic Artificial Muscle (PAM) modules. Leveraging these advantages, we explore various types of deformation and haptic properties and demonstrate their effectiveness through application examples. Our vision is that this prototyping toolkit will stimulate exploratory work, enabling users to experiment and creatively design novel interfaces while easily constructing proof-of-concept prototypes using constructive assembly methods.

6.2 Related Work

Table 6.1 shows the feature comparison between various shape-changing interface prototyping tools.

Table 6.1: Comparison with related work. ASTRE Toolkit facilitate shape deformation and variable-stiffness with constructive assembly approach

	Toolkit type	Structure	Active Deformation			Variable-stiffness		
			Bending	Twisting	Contraction/ Expansion	Rigidness	Malleability	Springiness
Compressable [38]	Design & Fab. tool	Inflatable			✔			
MorpheesPlug [84]	Design & Fab. tool	Inflatable	✔	✔	✔			
PneuFab [215]	Design & Fab. tool	Inflatable	✔	✔	✔		✔	✔
Magnetform [212]	Modeling	Surface	✔					
Polysurface [39]	Modeling	Surface	✔					
ClaytricSurface (Chapter 4)	Modeling	Surface				✔	✔	
Bosu [147]	Modeling	Truss/Mesh	✔					
Sticky actuator [136]	Constructive Ass.	Baloon	✔		✔			
FaBrickation [126]	Constructive Ass.	Block module						
Topobo [148]	Constructive Ass.	Block module		✔				
Changibles [164]	Constructive Ass.	Block module		✔				
ShapeClip [59]	Constructive Ass.	Block module			✔			
TEX(alive) [22]	Constructive Ass.	Truss/Mesh	✔					
PneuMesh [55]	Constructive Ass.	Truss/Mesh			✔			
MorphIO [134]	Constructive Ass.	Truss/Mesh			✔			
GaussBricks [102]	Constructive Ass.	Truss/Mesh						✔
ASTRE Toolkit (Chapter 6)	Constructive Ass.	Truss/Mesh	✔	✔	✔	✔	✔	✔

6.2.1 Pneumatic Shape-changing Interface

Recent studies have been dedicated to developing fabrication-friendly shape-changing hardware using pneumatic actuators. Pneumatic actuators are advantageous due to their low cost, intuitive nature, and ease of implementation [223]. Previous works have explored various mechanisms to actuate shape-changing interfaces, including inflatable bladders [33, 38, 112, 235], extensible actuator [134, 189, 236], and PAMs [2, 48, 63]. This research mentions low power consumption as the advantage of a pneumatic actuator, as energy is only needed at the phase changes. Among these mechanisms, PAMs, which utilize high pressure for actuation, provide greater force. The Omnifiber [2] stands out as a significant contribution in the field,

as it explores various aspects of PAMs utilization for shape-changing applications, including deformation strategies, modular composition, sleeve materials, and sensor integration.

Although our research shares similarities with Omnifiber [2] in terms of the area of focus, we emphasize the utilization of 3D printed mechanical constraints to achieve both shape-changing and variable-stiffness capabilities. We describe the fundamental mechanism and strategies for adjusting deformations. While Omnifiber also mentions the variable-stiffness properties achieved through the injection of Low Melting Point Polymer (LMPP), our approach relies on mechanical constraints to change the stiffness properties, resulting in a simpler system. Additionally, we place more emphasis on modular structure construction, enabling a wider range of deformations and haptic properties through the use of the six presented modules.

6.2.2 Pneumatic Prototyping Tools

For rapid prototyping purposes, several studies have presented 3D printed pneumatic interfaces as a convenient and readily available method [41, 84, 127]. These works have demonstrated the advantages of 3D printing for fabrication. However, they also require a certain level of understanding of computer-aided design (CAD) tools to operate effectively. An alternative approach to facilitate the design process is the use of modular actuators that can be attached to various media, such as paper, wearable fabric, and shape-changing mesh [22, 38, 136]. This approach offers a user-friendly configuration and assembly process, akin to children's toys like Lego MindStorm [54].

Previous studies have placed significant emphasis on the exploration of modular truss structures in pneumatic interfaces to enable rapid assembly and shape reconfiguration of complex structure [55, 92, 134]. Among these works, PneuMesh [55] is particularly relevant to our research proposal. PneuMesh introduced a truss structure shape-changing system that utilized constructive assembly fabrication. However, it is important to highlight that PneuMesh only provides a linear deformation

module, whereas our framework offers additional deformations such as bending and twisting. Additionally, our research introduces variable-stiffness modules, which have not yet been explored in a modular form in previous studies.

6.2.3 Variable-stiffness Prototyping Tools

Variable-stiffness is an advantageous property for prototyping in the field of HCI. Previous research has successfully utilized variable-stiffness in deformable displays [42, 171], allowing users to mold and iterate 2.5D shapes, resembling the process of sculpting with clay. By incorporating stiffness tuning capabilities, users can easily manipulate a significant portion of the shape in its soft state and then refine the detailed shape in a stiffer state. Variable-stiffness is also beneficial for prototyping interface functions. Researchers have investigated the capabilities of variable-stiffness robotic arms [1] and multi-finger grippers [123]. Stiff robots offer precise control, while softer robots are compliant and adaptable to various objects. While the primary objective of these researches is to create dynamically adaptable robots, they can also be utilized to test the suitability of different stiffness parameters under various conditions. Notably, while the capability to iterate the form or function of an interface has been explored separately in previous studies, the aim of this research is to enable simultaneous iteration of both aspects.

6.3 Design Space

In a previous study by Rasmussen et al., the design traits of shape-changing interfaces were formulated [161]. However, none of the previous work has explored the design potential of shape-changing interfaces with variable-stiffness capabilities. In this research, we build upon their interface classification to showcase the shape-changing capabilities of our toolkit. Additionally, we enhance the scope by incorporating haptic properties derived from the variable-stiffness capabilities. Figure 6.1 provides an illustration of the design space for our toolkit, depicting dimensions

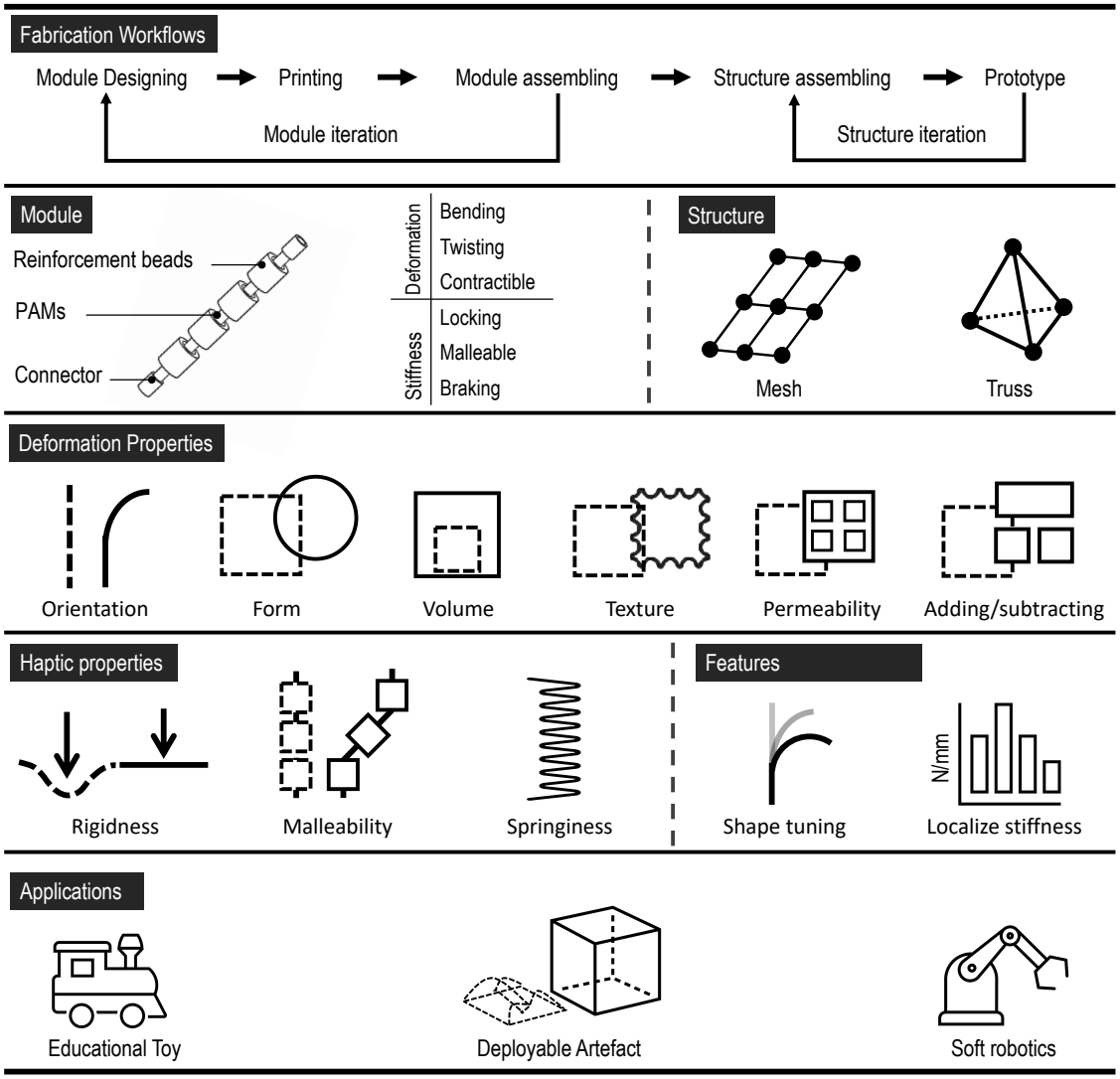

Figure 6.1: Design Space of AstreToolkit

that represent deformations, haptic properties, and application domains.

6.3.1 Constructive Assemblies Approach

The constructive assembly has proven to be an effective and accessible approach for individuals to grasp advanced concepts in a creative and playful manner [229]. This advantage has led to the utilization of constructive assembly systems in various soft robotics [91, 98] and shape-changing [55, 134, 148, 229] research. Our

toolkit is built upon a constructive assembly system with the aim of harnessing its benefits (Figure 6.2. While our toolkit shares similarities in terms of truss structures and deformation capabilities (bending, twisting, and contraction), none of them has presented a comprehensive toolkit that combines both shape-changing and variable-stiffness as one toolkit. Building upon the inspiration from these studies, we introduce a new concept by incorporating the proposed variable-stiffness module, thereby expanding the realm of possibilities for shape-changing interfaces. We identify the contribution of our toolkit as follows:

Rapid prototyping: The modular and reconfigurable toolkit enables convenient testing and on-the-fly adjustments. Both the assembly and disassembly processes are kept simple, allowing for seamless experimentation and modification.

Versatile: The toolkit offers versatile configuration options, allowing for various shape deformations and the manifestation of multiple physical properties. It can be combined to form intricate structures and is flexible in terms of scaling, enabling both upsizing and downsizing as desired.

Accessible: The toolkit is designed with ease of replication in mind, utilizing readily available and affordable equipment and materials. It is user-friendly, allowing novices to operate it intuitively with minimal explanation or guidance.

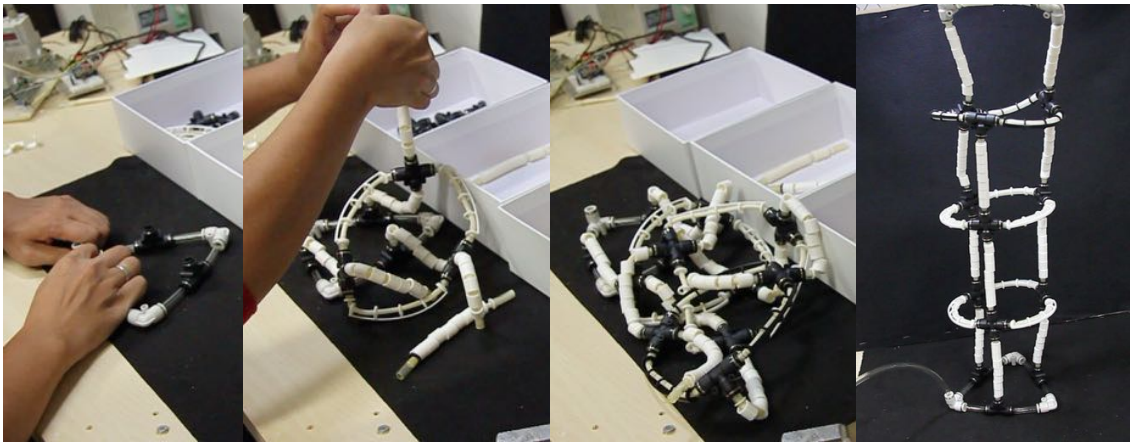

Figure 6.2: The ASTREE Toolkit adopts a constructivist assembling approach to facilitate its functionalities and advantages.

6.4 Deformation Properties

Deformation is the most important property for shape-changing interfaces that determine both the final form and functions of such interfaces. Rasmussen et al. [161] proposed eight categories including orientation, form, volume, texture, viscosity, spatiality, adding/subtracting, and permeability. Our framework successfully achieves six out of the eight deformation categories, demonstrating its versatility and effectiveness in shape transformation.

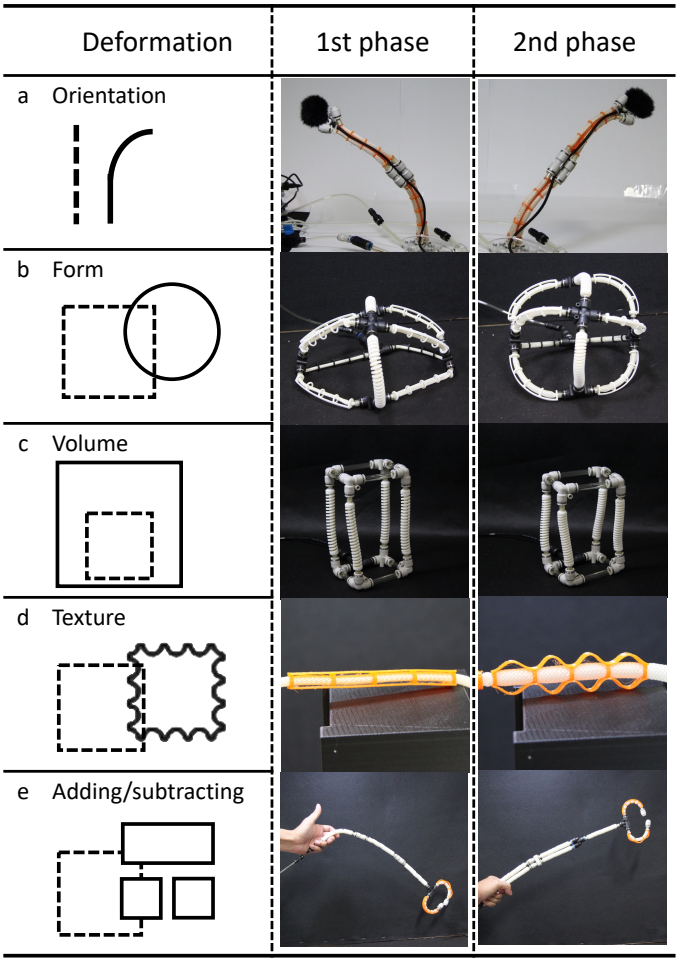

Figure 6.3: Deformation properties

6.4.1 Orientation

Orientation changes in deformation refer to alterations due to bending or twisting. These changes can lead to the object being distorted or warped, but its original form can still be recognized. Figure 6.3a shows how we can control bending orientation in omnidirectional by arranging three bending module parallel (three-chamber actuator). We used three separate pneumatic control for each module to change the bending direction. Although the bending direction control is not precise, this example demonstrates how the framework can conveniently replicate the three-chamber mechanism that has been proposed in previous work [204].

6.4.2 Form

Form changes refer to alterations in the overall shape of an object while preserving the relative volume. Figure 6.3b shows an example, where an octahedron structure constructed from the bending modules can form a ball structure when actuated. All the bending module orientation was aligned to the structural core. Therefore it forms a uniform curved shape on all its surfaces. It can be utilized to create a structure that stands on a flat surface, however, can be rolled like a ball when actuated.

6.4.3 Volume

Volume changes refer to alterations due to the stretching or compressing where the structures maintain the approximate form. Figure 6.3c shows a rectangular cube constructed from contractible modules. When actuated, the cube height is decreasing resulted in a smaller volume. In this particular structure, the maximum volume changes is 15% of the origin.

6.4.4 Textural

Textural changes refer to small deformations on the surface of an object. It alters the contour and tactile properties while maintaining the overall shape. Figure 6.3d shows the exploration of textural changes where PAMs have two layers of mechanical constraint opposite of each other. When actuated, it creates a waving pattern on the module surface.

6.4.5 Adding or Subtracting

Adding and subtracting is shape-change by uniting or dividing the module, while still able to return to the initial shape. In this framework adding or subtracting are passive manipulation by the user. One of the utilization is to scale up the stiffness of modules as shown in figure 6.3e. A single locking module can exert stiffness up to 0.7 N/mm when applied with an air pressure 0.4 MPa. However, the average weight of a module with a connector is about 25 g. Therefore the maximum number of modules that can be supported by a locking module is up to three modules. By adding another locking module in parallel, we can increase the stiffness by almost two times.

6.5 Haptic Properties

Physical property is an important factor that affects interaction. In the primitive module, we provide three types of physical states: soft, malleable, and rigid. In addition to these physical properties, we also introduce a springiness change.

6.5.1 Rigidness

The rigidness of an interface can influence factors such as usability, adaptability, and accessibility. A rigid interface provides consistency and predictability in the interaction. Contrariwise, a flexible interface is more appropriate for customization

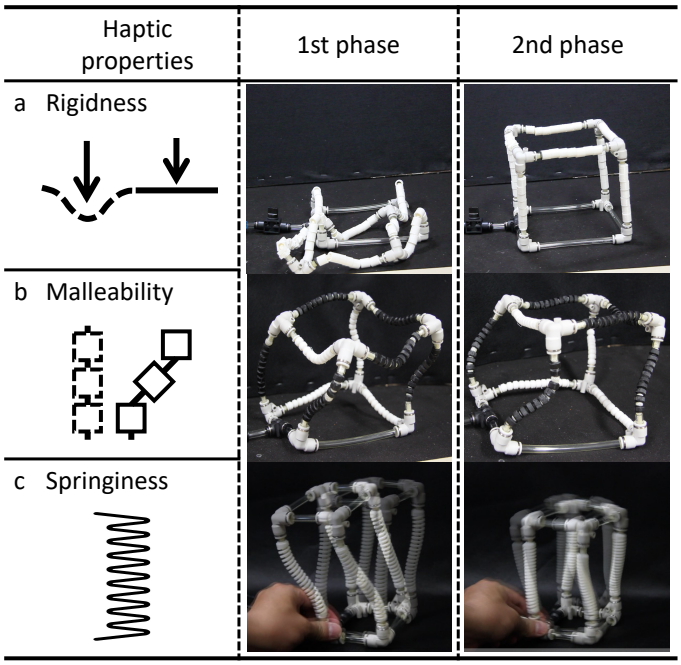

Figure 6.4: Haptic properties

and personalization. Figure 6.4a shows an example of a structure composed of eight locking modules assembled in a cube arrangement. It crumbled in a flexible state and become a rigid cube when actuated. In the flexible state, the structure is adaptable to various environments (e.g. narrow space). In the rigid state, the structure can carry a load of up to 500 gram.

6.5.2 Malleability

Malleable interfaces enable effortless deformation by external forces and retain the shape formed. A malleable interface is suitable for creative and exploratory interaction, where experimentation is valued. Figure 6.4b shows a cube structure composed of eleven malleable modules. When unactuated it crumbled on the ground. When actuated it deployed into a cube shape, however malleable and compliant to the user manipulation.

6.5.3 Springiness

Helical springs offer benefits such as the capability to withstand large-scale deformations and store energy. It can undergo deformation without suffering permanent damage because the applied load is evenly distributed along its length. Therefore it also can absorb shock and convert the energy into an oscillation cycle. Figure 6.4c shows a rectangle structure composed of four contractible modules. When agitated in a normal state, the spring structures will wobble vigorously. However, in an actuated state, the structure wobbles in a more mild manner.

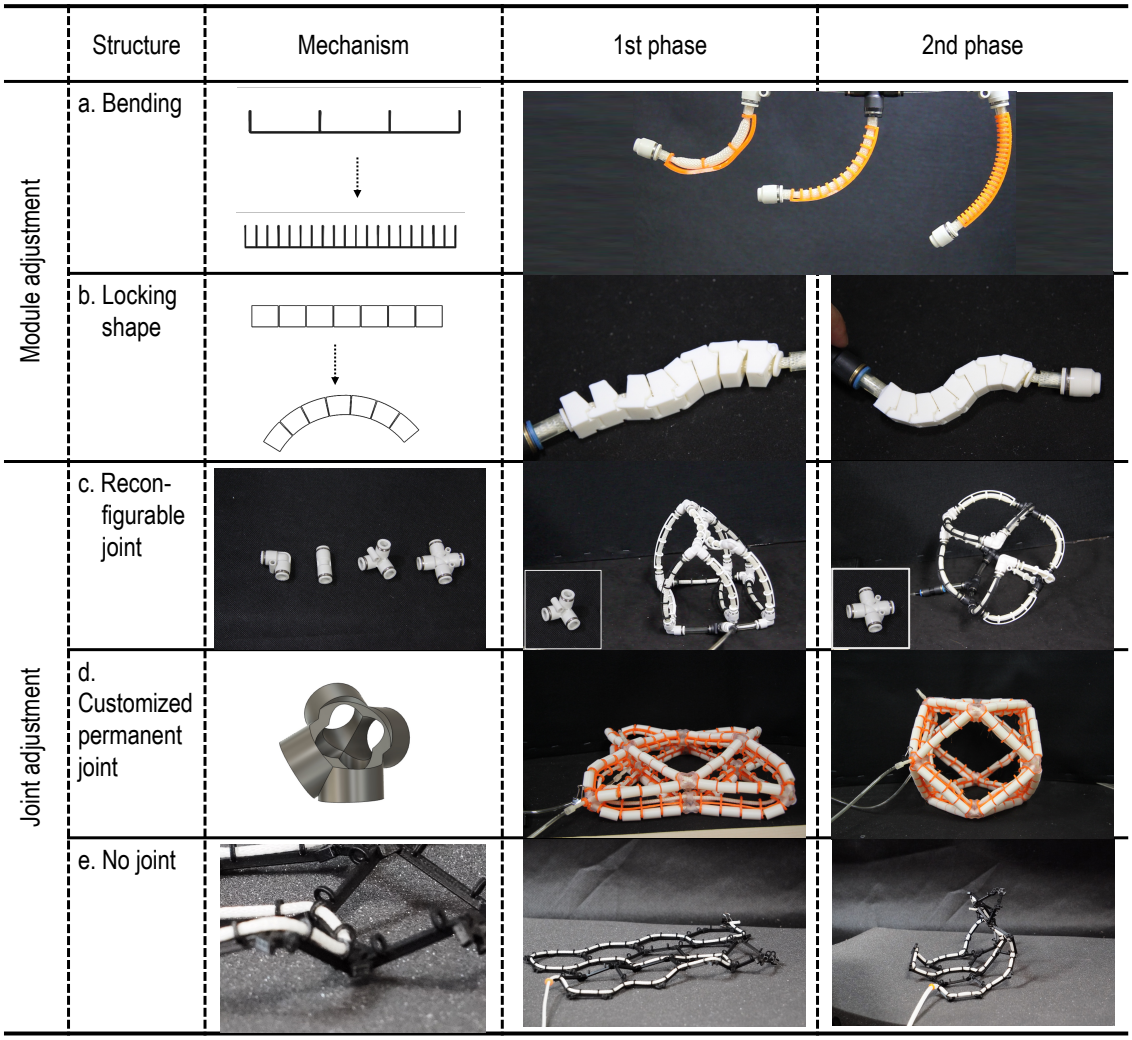

Figure 6.5: Shape tunning

6.6 Shape Tuning

Truss structures do not have specific morphology as they can be assembled into arbitrary shapes [55]. The final shape of truss structures is determined by the length and shape of modules and the types and angles of joints. In this section, we explore the programmability of truss shapes by adjusting either the modules or joints.

6.6.1 Module adjustment

The length parameter of the module can be adjusted in design steps using the provided design algorithm. However, all the primitive's modules have similar elongated shapes. Although the deformation such as bending and contraction can be controlled by air pressure, the deformation rate is evenly distributed on all modules. To personalize the deformation of specific modules, we proposed two types of adjustment which consist of bending module adjustment and locking module adjustment.

Bending Module Adjustment

We 3D printed the bending module with a 6mm diameter guiding ring. This guiding ring functioned as a guide rail, keeping the PAMs along the bending module. However, it also can be functioned to suppress PAMs radial expansion (up to 9 mm in Diameter). Due to this suppression effect, the contraction ratio is also decreased, resulting in a smaller bending angle (Figure 6.5a). Using this phenomenon we can adjust the bending angle according to the number of suppression rings.

Locking Modules Adjustment

The locking module, when composed of beads with aligned edges, forms a straight elongated shape 6.4a. However, if we add an angled chamfer to the bead's edges, we can create a bent shape. Figure 6.5b shows the example of a bent locking module. We also added a hinge structure that connects the beads, to ensure that

the desired shape is formed at each actuation. However, it has a disadvantage that limits flexibility in the soft state.

6.6.2 Joint Angle Adjustment

With the same number of modules, the overall shape of truss structures can be significantly reconfigured by changing the joint's position and types. The number of joints and interior angle of joints also play an important role to determine the truss's final shape. Here we demonstrate the various method to reconfigure or customized the joints.

Reconfigurable Pneumatic Joint

Each of our toolkit modules has an 8 mm pneumatic tube on each end. This tube can be connected with a commercial fitting which incorporates quick-connection fitting. The fittings can be attached and detached quickly with one push, and they can be used repeatedly. Figure 6.5c shows four types of connectors that varied in the number of branches and interior angle between branches. Although this type of joint is convenient to use due to its reconfigurability. The lack of variation in joint types becomes a big limitation for achievable truss shapes.

Customized Permanent Joint

To address the problem of shape limitation in reconfigurable joints, we explored the practicality of 3D-printed customized joints. This joint is able to achieve various truss structures, similar to the system proposed by PneuMesh [55] and FlexTruss [185]. However, as a trade-off for structure versatility, reconfigurability is sacrificed as each module needs to be permanently attached to the joint using adhesives. Figure 6.5d shows an example of the customized joint to create a vector equilibrium structure that can be flattened in a normal state and swell up in the actuated state.

No Joint

To achieve a certain degree of reconfigurability while maintaining shape versatility, a truss structure also can be built using one continuous PAMs filament without any joints. Figure 6.5e shows an example of mesh structures where all the modules are connected by hinges to each other. The fabricator can deliberately adjust the shape deformation by re-routing the PAMs threaded.

6.7 Application

In this section, we demonstrate the variety of applications achieved using our framework.

6.7.1 Educational Toy

Constructive assemblies are designed to be user-friendly and promote creativity. Previous research by Raffle et al. [148] has shown the potential of constructive assembly toys with embedded kinematic memory, which aids children in understanding physical principles and mathematical deformations. In a similar vein, our framework is also intended to be user-friendly, encouraging exploration, and fostering creativity. In this section, we highlight several features that can be beneficial for educational purposes.

Interchangeability

The main inspiration for our toolkit is the LEGO® brick module. We aimed to replicate the simplicity and versatility of LEGO® by designing all the basic modules to have consistent lengths before and after actuation. As a result, each part of the interface can be reconfigured to serve various purposes. Figure 6.6a illustrates how the neck of a giraffe toy can be easily transformed from a locking stiff configuration to twisting, contractible, malleable, and bending configurations. This

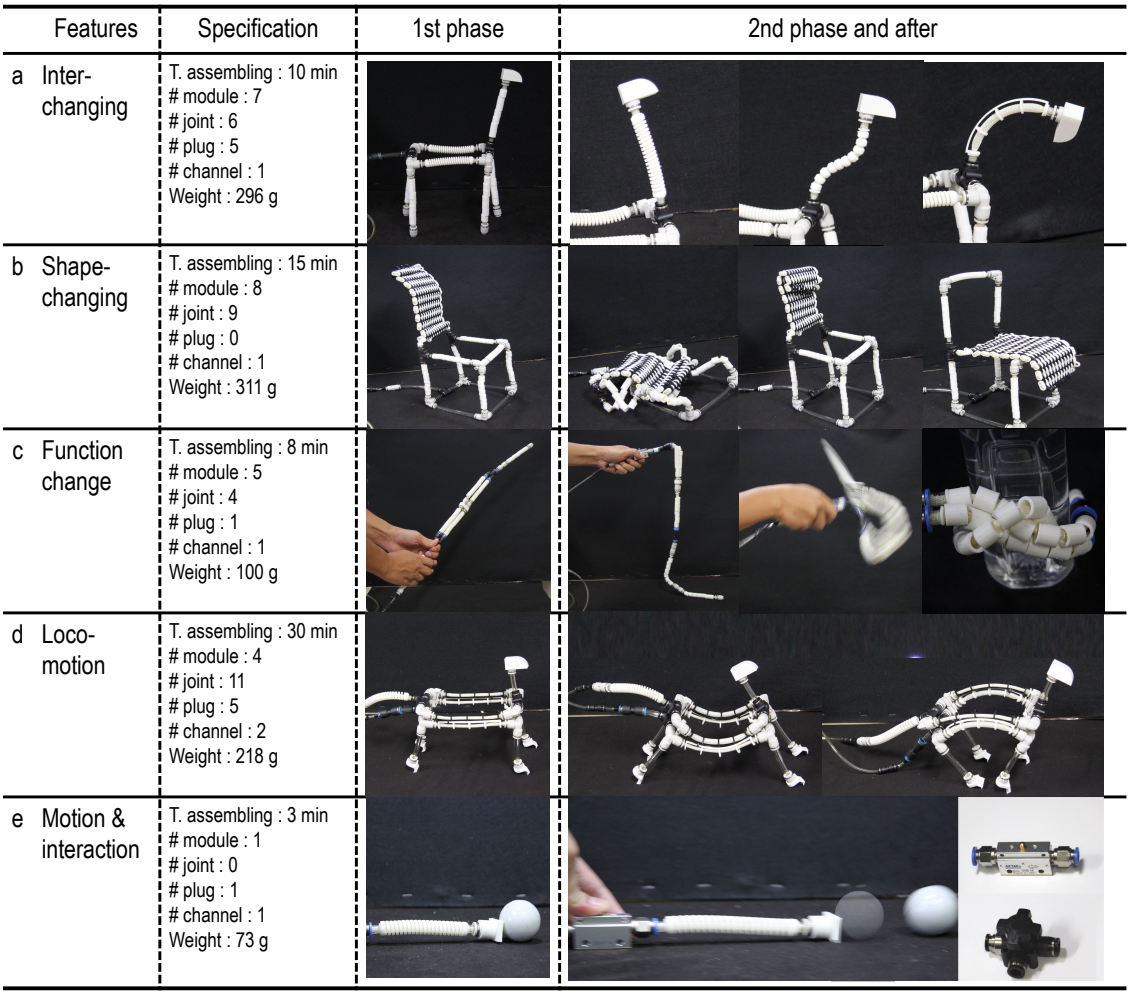

Figure 6.6: Lego application examples

feature allows children to explore and iterate through a prototyping cycle, fostering creativity and supporting their development.

Shape-changing

Figure 6.6b shows a small-scale shape-changing chair. This chair incorporates locking modules for the chair legs, allowing it to be easily deployed and collapsed. Users can conveniently adjust the reclining angles and forms, thanks to the utilization of brake modules. This feature is particularly beneficial for children as it fosters their understanding of programmability. Through experimentation with

different module and joint selections, children can explore the diverse shapes and deformation kinematics that result. This hands-on experience enables them to deepen their comprehension of how design choices influence the chair's functionality and behavior.

Function Repurposing

Figure 6.6c illustrates an example inspired by the works of Katsumoto et al. [80]. It presents a rigid sword that can be transformed into a flexible whip when collapsed. This showcases the versatility of the interface, allowing for different interactions and haptic experiences. The sword consists of a series of locking modules, and its deployment can be controlled by pressing a mechanical valve button. This example provides an opportunity for children to learn about materials physics and the correlation between behavior and function. They can explore the advantages of using soft objects for specific tasks and the suitability of rigid objects for others. Through this hands-on experience, children can develop an understanding of how different materials and their properties contribute to the desired functionality and behavior of an object.

Locomotion

Figure 6.6d exhibits the application of a four-legged robot designed for locomotion. This application draws inspiration from the works of Tang et al. [197], aiming to replicate the movement gait of a cheetah running. By actuating the flexion and extension of the robot's spine alternatively, we achieve a similar motion pattern. Additionally, we incorporate arched claws on each leg to enable forward locomotion. This design feature provides an excellent opportunity for children to learn about kinematic motions and how different movements can result in various forms of locomotion. By observing and experimenting with the robot's motion, children can gain insights into the principles of biomechanics and understand the relationship between specific movements and locomotive behaviors. This hands-on experience

promotes an engaging and educational exploration of robotics and kinematics.

Motion and Interaction

The contractible module in the ASTRE toolkit incorporates a spring structure that can store contraction force and release it rapidly. In Figure 6.6e, we demonstrate how the spring force can be utilized to toss an object using a pneumatic button. Additionally, the twisting module can be employed to simulate a golf swing and hit an object. These interactive features enhance the engagement and playability of the toolkit, encouraging children to remain involved for extended periods. By incorporating elements of physical force and interactive actions, the ASTRE toolkit provides a more immersive and dynamic experience for children. It allows them to explore the concepts of energy storage, release, and transfer of motion in a hands-on and playful manner.

6.7.2 Deployable Artifact

Deployability is a useful feature for advantages such as storing easiness, increased change in durability, and adaptability to various environments. An example of a deployable soft robot demonstrates the adaptibility for rescue purposes [13]. Here we explore the deployable features of our frameworks.

Deployable Tall Structures

Figure 6.7a shows the example of deployable features achieved by arranging 40 locking modules into a 600 mm tall rectangular structure. In its collapsed state, the structure is soft and can be crumbled into a small mass. However, as we actuate the PAMs, the stiffness gradually increased. When the locking module is stiff enough to withhold its own weight, it regains the pre-arranged shape. The structure will retaining its shape even when the air supply is disconnected, as long as there is no air leakage.

	Features	Specification	1st phase	2nd phase
a	Tall structure	T. assembling : 50 min # module : 40 # joint : 30 Weight : 790 g Height : 600 mm Length : 300 mm Width : 150 mm		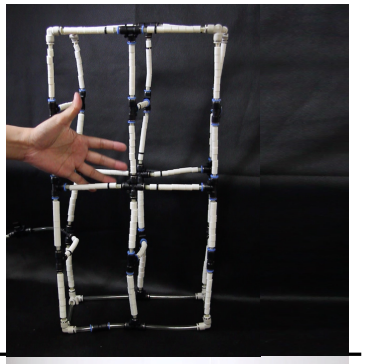
b	Load endurance	T. assembling : 40 min # module : 18 # joint : 18 Weight : 396 g Height : 150 mm Length : 600 mm Width : 150 mm	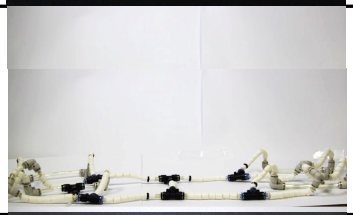	
c	Folding	T. assembling : 12 min # module : 9 # joint : 11 Weight : 228 g Height : 150 mm Length : 150 mm Width : 150 mm	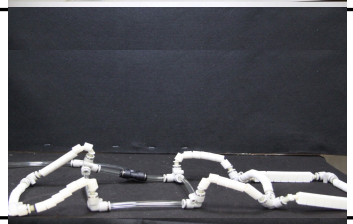	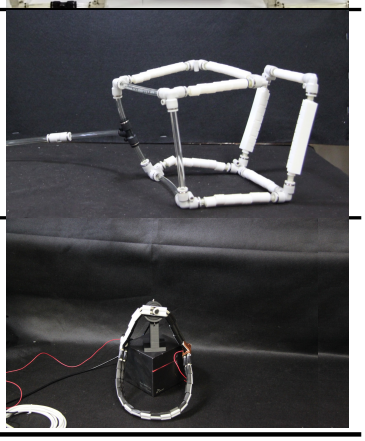
d	Incapaciate	T. assembling : 30 min # module : 6 # joint : 4 Weight : 260 g Height : 280 mm Length : 280 mm Width : 200 mm	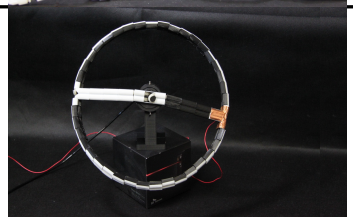	

Figure 6.7: Deployable application

Load Bearing Structures

Figure 6.7b illustrates a compact coffee table that offers instant deployability and collapsibility. This design allows for easy storage in the collapsed state, making it convenient for transportation or space-saving purposes. When deployed into a table, it possesses the strength and stability to support a weight of up to 1.4 kg, making it suitable for holding laptops or other lightweight objects. The collapsible coffee table exemplifies the practical applications of the ASTRE toolkit in furniture design. Its ability to quickly transform between functional and compact states provides users

with a versatile and adaptable furniture solution. This example showcases the toolkit's potential that combines functionality, convenience, and aesthetic appeal.

Folding

Folding is an efficient deformation method that enables the deployment of shapes from a flat surface, drawing inspiration from the principles of origami art. In Figure 6.7c, we present an example of folding deformation with a cube structure. In its flattened state, the cube can pass through narrow spaces, and when deployed, it rapidly transforms into its three-dimensional form. To achieve this folding capability, we designed the cube with four square-shaped locking modules arranged in a specific configuration. Each corner of the cube is connected using a tripod joint, allowing for controlled folding and unfolding motions. This design enables users to easily manipulate the cube's shape, transitioning it between flat and three-dimensional states. By incorporating folding mechanisms into the ASTRE toolkit, we demonstrate how shape-changing structures can be efficiently deployed and reconfigured

Incapacitation

Incapacitation is the opposite concept of deploying, which refers to the capability to render an object useless. In Figure 6.7d, we present a conceptual design of a steering wheel that incorporates incapacitation as a signaling mechanism. This feature communicates important information to the user, such as indicating the car's mode (manual or self-driving). It also ensures safety by detecting and incapacitating itself when small children attempt to operate the vehicle. This example highlights how shape-changing interfaces can adapt to users and their environments, providing enhanced functionality and promoting safety.

6.7.3 Soft robot prototype

Soft robots are a promising area of research that offers great potential for human interaction due to their adaptability and safe operation. However, the complex fabrication process of elastomeric materials with multiple channels poses challenges in soft robot development. In this study, we showcase the capabilities of our framework's modular characteristics in the prototyping of soft robots. Our approach allows for the scaling and rearrangement of robot modules, enabling them to adapt to different environmental conditions.

	Application	Specification	1st phase	2nd phase
a	Customized gripper	T. assembling : 10 min # module : 4 # joint : 5 Weight : 103g	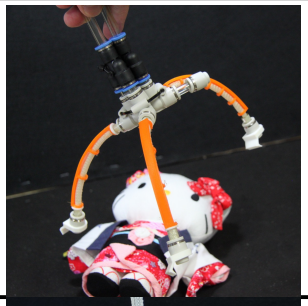	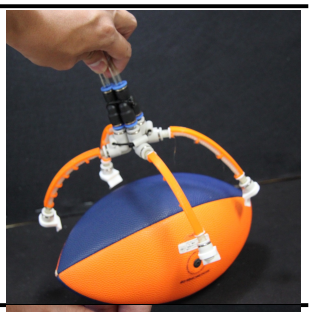
b	Variable stiffness gripper	T. assembling : 20 min Weight : 70g	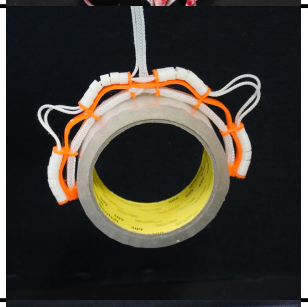	
c	Deployable robot arm	T. assembling : 40 min Weight : 162g	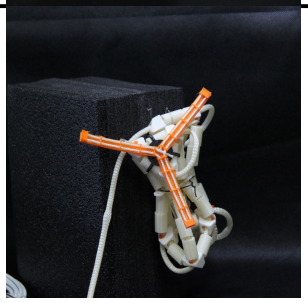	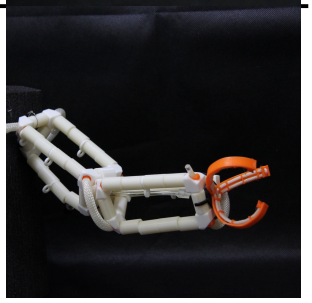

Figure 6.8: Soft robot application

Customized Gripper

In soft robotics, a common application is the development of soft grippers capable of gripping objects of various sizes. Figure 6.8a showcases a prototype of a soft gripper that offers flexibility in adjusting the number of gripper claws. By reconfiguring the structure module and joint, users can freely modify the gripper's configuration. Additionally, the gripper claws can be interchanged between a flexible bending module and a shaped locking module. This versatility enables users to experiment with different gripper sizes and shapes, optimizing their grip for objects based on factors such as size, weight, shape, and softness.

variable-stiffness Gripper

Figure 6.8b presents a soft gripper design composed of bending modules for the claws, which are equipped with embedded locking modules at the claw base and tip. This integration of locking modules introduces controllable stiffness to the claws, resulting in enhanced precision during the grasping of small objects (15 mm diameter). However, it is worth noting that this configuration sacrifices some degree of flexibility. Nevertheless, the gripper remains capable of securely gripping larger objects with diameters of up to 120 mm.

Deployable Robot Arms

Figure 6.8c illustrates the practical application of a deployable robot arm. This arm consists of two truss structures connected by hinges, with a gripper claw attached at the end. In its unactuated state, the arm can be conveniently collapsed into a compact size of 100 mm $\times$ 50 mm $\times$ 50 mm. However, upon deployment, the robot arm expands and doubles its dimensions to approximately 200 mm $\times$ 100 mm $\times$ 100 mm, allowing it to reach and interact with objects over a larger range.

6.8 Technical Evaluation

In the Shape Tuning section, we introduce some methods to control shape deformation based on the alteration in mechanical constraint. Here we conducted an evaluation to validate our proposed method and used the results to provide a rough estimation of our design tools.

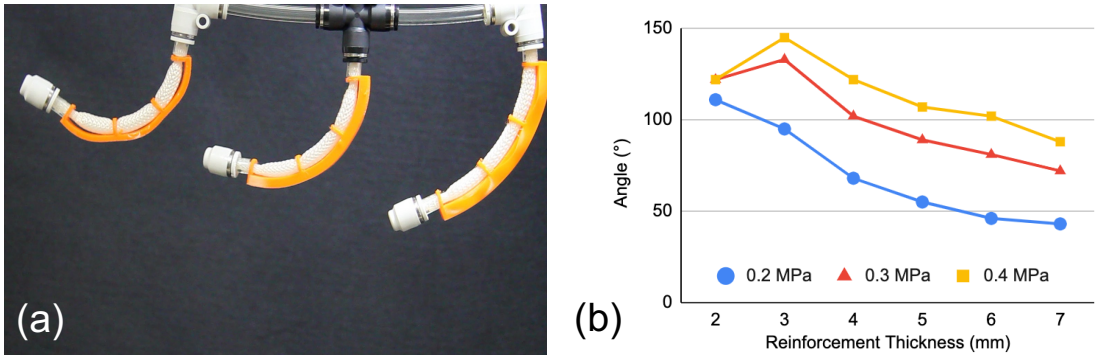

Figure 6.9: (a) Changes in bending angle with respect to the constraint layer thickness. (b) Relation between thickness and bending angle

6.8.1 Bending Angle Adjustment

Here, we introduce two types of bending angle adjustment methods. The first method is by increasing layer thickness to stiffen the mechanical constraint (Figure 6.9(a)). Figure 6.9(b) shows the relation between bending angle, thickness, and air pressure. It shows that (i) the bending angle increases as air pressure increases, (ii) decreasing trend of the bending angle as the thickness increases, (iii) an exception of 2 mm thick constraint. We analyze it behaves strangely, owing to the thin constraint that cannot resist the high compression force. Thus it curves out, converting half of the compression force into bending deformation and another half into shrinking deformation(Figure 6.10(a)). Based on this result, we standardized the minimum TPU thickness for the bending module is 3 mm.

The second method to adjust the bending angle is by varying the number of sup-

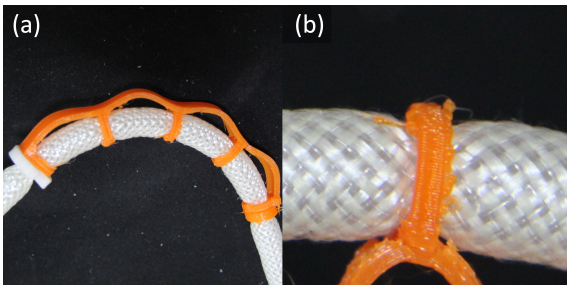

Figure 6.10: (a) Bending buldge (b) suppresing ring

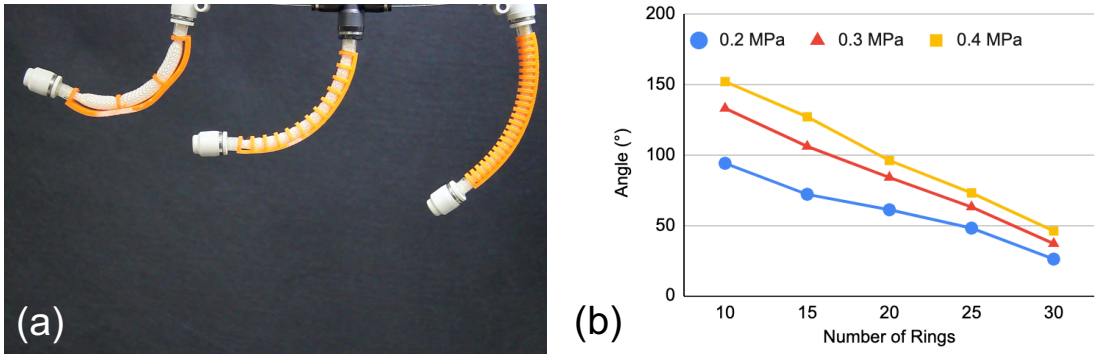

Figure 6.11: (a) Changes in bending angle with respect to the number of suppressing rings (b) Relationship between the number of rings and bending angle

pressing rings. We 3D printed the bending module with a 6mm diameter guiding ring. This guiding ring functioned as a guide rail, keeping the PAMs along the bending module. However, it also can be functioned to suppress PAMs radial expansion (up to 9 mm in Diameter, Figure 6.10(b)). Due to this suppression effect, the contraction ratio is also decreased, resulting in a smaller bending angle. Using this phenomenon we can adjust the bending angle according to the number of suppression rings. Figure 6.11(a) shows how the bending angle decreases as the number of rings increases. Figure 6.11(b) shows the experiment result which is an almost linear change in the bending angle. We conclude this method is easier to control compared to the thickness variation method. It is also more cost and time-effective, as to achieve the same banding angle less material was used in 3D printing (Table 6.10). However, it has a unique characteristic of reducing the difference in bending

angle between different air pressure (0.2, 0.3, and 0.4 MPa).

Table 6.2: Comparison of constraint thickness and suppression rings method

Bending Angle	Material weight	
	Thickness method	Rings method
120° - 130°	3.5 g	2.6 g
70° - 90°	6 g	3.3 g

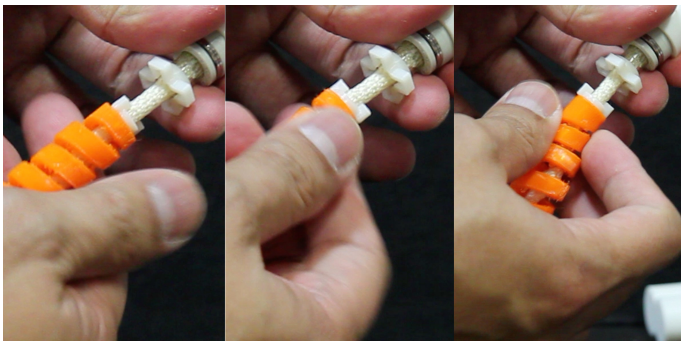

Figure 6.12: Winding method of the twisting module

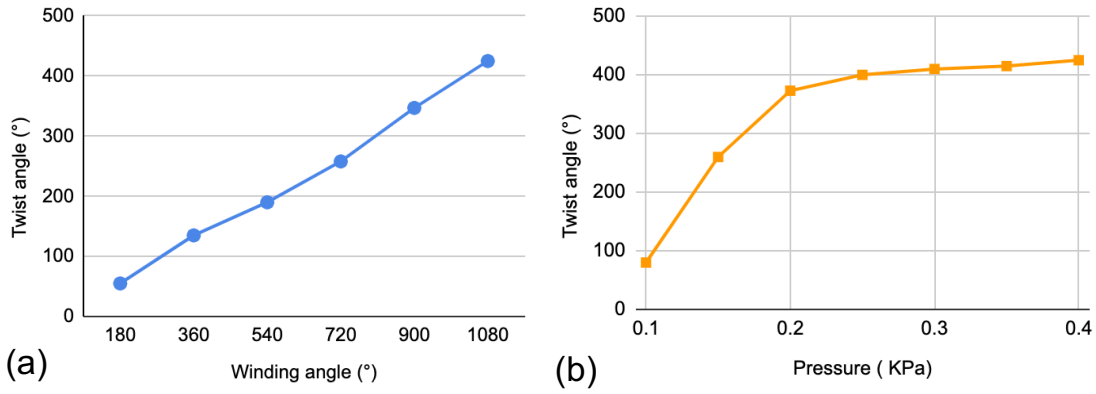

Figure 6.13: (a) Relationship between winding turn and twisting angle at 0.4MPa. (b)Relationship between air pressure and twisting angle at 1080° winding.

6.8.2 Twisting Angle Adjustment

For twisting angle adjustment, we introduce a new method where variation in 3D printed constraint was not needed. However, the user needs to fine-tune the PAMs wind-up or wind down the module manually (Figure 6.12). Figure 6.13(a) shows the results of our experiment where we wind up the module up to 3 turns (1080°) and measure the twisting angle at 0.4MPa. It shows an almost linear increase of twisting angle along with the winding turn.

We also conduct an experiment where we change the air pressure and measure the twisting angle at 1080° winding (Figure 6.13(b)). It shows an asymptotic behavior of bending angle to a constant value as the pressure increases. In this experiment, we limit the winding turn up to 1080° due to the twisting module's maximum spring torsion. Further adjustments to the module can be made to create different twisting behavior.

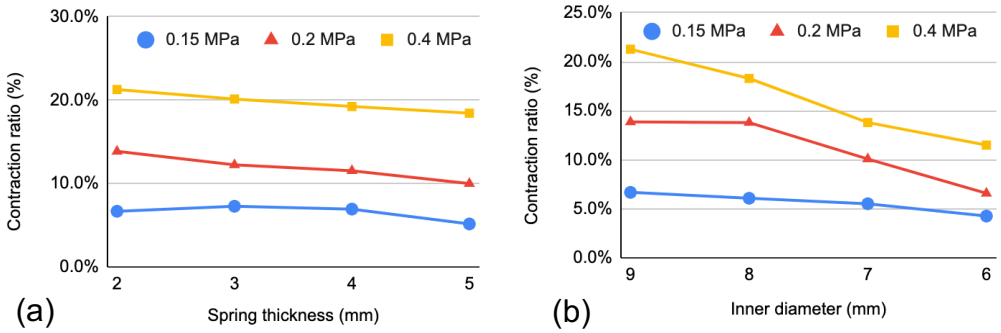

Figure 6.14: (a) Relation between spring thickness and contraction ratio. (b) Relationship between spring diameter and contraction ratio

6.8.3 Contraction Ratio Adjustment

To adjust the contraction ratio, we also introduce two methods that require variation in the module parameter. The first method is to increase the thickness of the spring to increase the spring stiffness, as defined in *Hooke's Law*. As spring

stiffness increases, the force needed to contract also increases, resulting in a shorter contraction ratio. Figure 6.14(a) shows our experimental result of changing spring thickness from 2 mm up to 5 mm. Despite the exponential increase in stiffness, only a slight reduction in the contraction ratio was shown. This result is due to the high contraction force of the PAMs (60 N) that overlook the stiffness.

The second method is relying on the suppression effect, similar to the bending adjustment method. We reduce the spring diameter from 9 mm up to 6 mm and measure the contraction ratio. Figure 6.14(b) shows a drastic change in the contraction ratio compared Figure 6.14(a). This method is also more effective as less material is required for 3D printing.

6.8.4 Summary of the Evaluation

In summary, this experiment shows the feasibility of adjustment in bending angle, twisting angle, and contraction ratio. These results are used as a reference when designing a new module. We also incorporate the suppression-based adjustment into our design tool to give approximate bending angle and contraction ratio.

6.9 Discussion

6.9.1 Structure Limitation

Although truss structures ideally have no morphological limitations, allowing them to be assembled into arbitrary shapes, the truss structures assembled with the ASTRE Toolkit do have certain limitations. These limitations come from factors such as the availability of commercial pneumatic joints and the maximum load-bearing capacity of the structure. To support our assertion regarding the versatility of this framework, as well as to define its boundaries in terms of preliminary design, Figure 6.15 illustrates the range of usage and limitations of the ASTRE Toolkit across dimensions representing shape, deformation, physical properties, and

interaction. This visual representation helps provide a clear understanding of the capabilities and constraints of the ASTRE Toolkit.

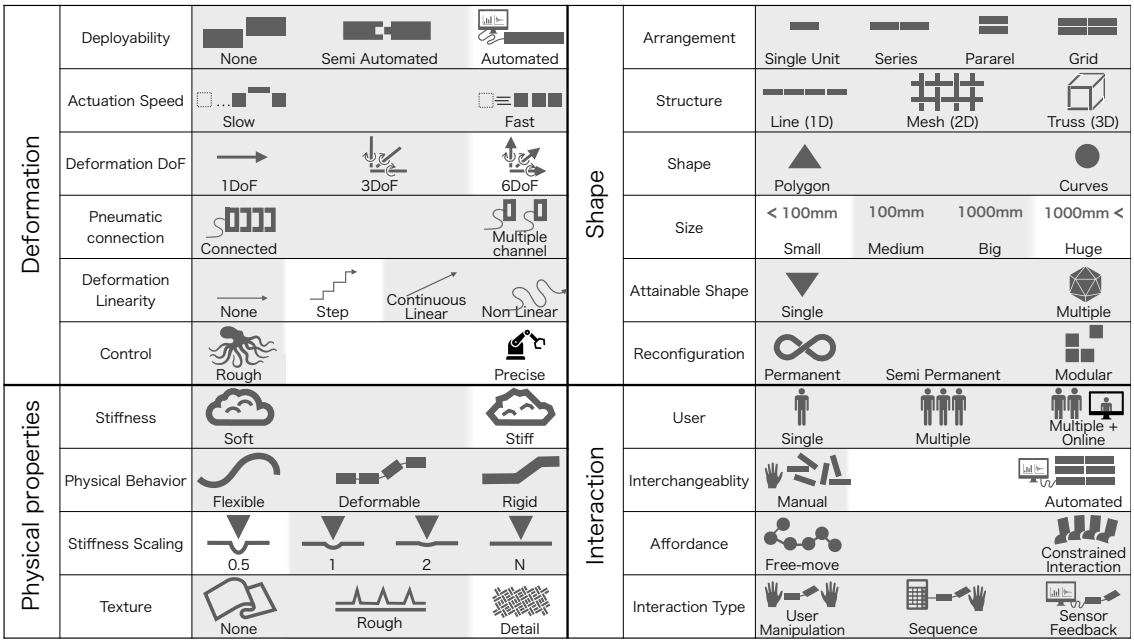

Figure 6.15: Structure limitation

6.9.2 Path for More Complex Structures

As previously mentioned, the ASTRE toolkit currently faces limitations in achieving complex structures due to physical constraints imposed by the modules and joint assemblies. To overcome these spatial limitations, we propose several strategies for future improvement. One approach is to employ optimized truss designs that aim to reduce complexity while maintaining structural integrity. By researching and developing new truss geometries and configurations, we can create more efficient structures that can be assembled within the toolkit's limitations. Additionally, miniaturizing components, such as valves, electronics, and batteries, will help reduce the overall weight and size of the toolkit, enabling the creation of more intricate structures.

In our future work, we intend to incorporate computer-aided design tools to

assist users in generating complex truss structures from 3D objects, building upon previous works in the field [125, 185]. Although this computational approach won't entirely eliminate the manual assembling workload and spatial limitations of the modules, it will provide users with the ability to create inverse design prototypes of structures, reducing the number of iterations needed with physical tools.

Furthermore, we plan to explore the use of virtual reality (VR) and mixed reality (MR) techniques to visualize complex structures in virtual environments alongside simpler models in the physical world. This approach will enable users to interact with virtual ASTRE structures, experiencing various shape deformations and even haptic feedback sensations while touching the virtual objects. Although the actual deformations are simple, the experience will be enhanced through haptic illusions in the virtual environment.

By integrating these future developments into the ASTRE toolkit, we aim to expand its capabilities, allowing users to create more sophisticated structures beyond the current spatial limitations. These advancements will enhance the toolkit's usability and offer new avenues for users to explore and experiment with intricate designs in both virtual and physical realms.

6.9.3 Application for Small Children

The ASTRE Toolkit was designed with LEGO blocks as inspiration, with the intention of enabling young children (starting from 2 years old) to play and experiment with the modules. However, the use of high-pressure and industrial pneumatic fittings poses a safety risk for young children, and the force required to attach and detach the fittings may also be too much for them to handle. Therefore, we recommend a minimum age of 13 years old for children to safely use this toolkit. To address these safety concerns, we propose a two-fold solution. Firstly, we need to create a safer system that operates at a relatively lower pressure (approximately 0.1KPa [38]). To accomplish this, we can increase the diameter of the PAMs to maintain the necessary force. Secondly, we need to create custom attachments that

are both robust enough for children to play with and easy to plug and unplug. In this research, we have experimented with using magnet joints to simplify the assembly process (Figure 6.16. However, we found that while the magnet joints allowed for high-pressure joints, they also increased the weight of the modules and hindered the assembling process. Therefore, we need to further explore alternative attachment solutions that meet both safety and ease-of-use requirements for younger users.

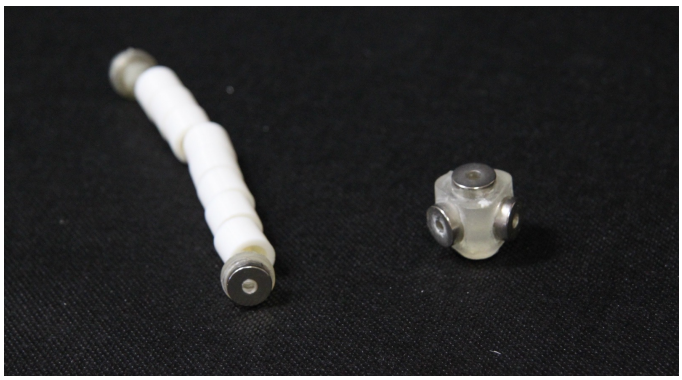

Figure 6.16: Magnetic joint exploration

6.9.4 Localize Deformation Control

The current implementation of the ASTRE Toolkit is designed for a limited number of interconnected truss structure channels, typically up to four channels [55]. This limitation arises from the increasing complexity of the structures, leading to unnecessary bulkiness and complicated joints. To overcome this limitation, one potential solution is to create an untethered valve inspired by the work of Tolley et al. [205]. By implementing such a valve, the structures can undergo complex deformations, allowing for a high degree of freedom and programmable dynamics of multiple structure parts. However, it's worth noting that this approach may introduce challenges related to the weight of the joint, as it would consist of a valve, electronics, and battery.

Alternatively, another approach to address the limitation is by developing a controllable pneumatic source utilizing chemical reactions [218] or liquid-to-gas phase changes mechanism [124]. Such methods could offer a resolution to the issues posed by complex joints, but they would necessitate careful consideration of the design and control of the pneumatic source.

Another avenue to explore is the development of mechanical logic on pneumatic connections, which draws inspiration from various previous works [23, 108, 117, 173]. By incorporating these connectors, it becomes possible to enable simple computation for actuating different parts of the interface independently. Such actuation can be achieved through user interaction [108] or by following predetermined actuation sequences [23]. Although this type of control lacks re-programmability, resulting in fixed and straightforward deformations for specific purposes, it does have its advantages. For example, the physical circuit could be beneficial for novices in robotics programming, as it provides a more tangible understanding of the system due to visible flows. Additionally, this approach might prove valuable in underwater applications and for compliant controls, which can be challenging to achieve using electrical valves.

Chapter 7

VabricBeads: A Design Exploration for Shape-changing and Variable-stiffness Fabric

7.1 Overview

variable-stiffness is an exciting area of research that has the potential to revolutionize many industries including fabric and wearables [222]. It can be used to create an adaptive fabric that can change its stiffness properties in response to changing environmental conditions. This can be useful in applications such as aerospace, underwater and rescue missions where lightweight and adaptable structures are highly desirable [167].

Despite the inherent advantages and potential of variable-stiffness fabric, its exploration has been limited due to various technological challenges, including complex actuator design, heavy weight, and high fabrication costs [116]. In this research, we aim to address these challenges by introducing novel actuation techniques that utilize Pneumatic Artificial Muscle (PAMs) actuators for stiffness control. Building upon the ASTRE mechanism proposed in Chapter 5, we extend this technique to be applied specifically in fabric applications, allowing for the development of new designs with diverse functions and properties.

PAMs such as McKibben actuators have several advantages over other types of

actuators, including their high force-to-weight ratio, low cost, and simplicity. They are also highly adaptable and can be easily scaled to different sizes and shapes to suit a variety of applications. Recent studies in soft PAMs actuators have proposed their application in active fabric [2, 47, 63]. The application of PAMs for variable-stiffness fabric interfaces is still under-explored. Especially the correlation between beads design, weaving pattern, shape deformation, and haptic properties.

We introduce VabricBeads, with twelve novel designs to take advantage of PAMs contraction and expansion force into stiffness variation, shape deformation, or both. We demonstrate the advantage of variable-stiffness fabric with applications such as haptic gloves, shape-changing bags, and shape-changing swords. To support the replication of our designs, we provide evaluations of the stiffness variation on several fabric types. We also introduced a new method to adjust the stiffness locally by varying the beads' hole diameter. Finally, we conclude our design explorations with a discussion.

7.2 Related Work

VabricBeads is focused on demonstrating the programmability of shape-changing and variable-stiffness behavior by varying beads shapes and threading patterns of fabric structures. As such, we based this research based on previous works on shape-changing and variable-stiffness fabric interfaces. Table 7.1 shows the feature comparison between various fabric structured shape-changing interface.

7.2.1 Shape-changing Fabric

Research on shape-changing fabric and garments has been increased due to the availability of flexible and small actuators such as Shape Memory Alloy (SMA) [12, 36, 57, 85, 94, 129, 130, 187], inflatable [86, 112, 150, 209], and tendon actuators [4]. Previous work by Berzowska et. al. [12] is one of the early examples of SMA integration into the fabric for shape deformation. This work demonstrates

the seamless coupling of Nitinol, textiles, and soft electronics for a hedonic and aesthetic garment experience. Further research has explored the integration of SMA wire into clothing, through various fabrication methods such as knitting [85], weaving [94, 187], and stitching [130]. These works have demonstrated the programmability of shape-deformation through various routing patterns of SMA wire. Muthukumarana et al. presented ClothTiles, embedding a 3D printed substrate with SMA actuator to support localized bending deformation on ready-made clothing [129]. This work demonstrates the effectiveness of 3D-printed mechanical constraints to control precise deformation. Inspired by previous works, this research also approaches programmable fabric behavior through PAMs threading patterns. We also combine the variation in 3D printed bead shape to further increase the variation of both shape-changing and variable-stiffness behavior. Our fabrication approach however focuses on the beads threading works and PAMs actuation.

Kim et al. [86] proposed a machine-knitted soft interface that is capable of locomotion through user arms, pipes, or tree branches. Coupled with a linear pneumatic actuator, the knitted sleeve scales can be fine-tuned to adjust the surface friction. VabricBeads use Pneumatic Artificial Muscles (PAMs) to control the brake friction, which exhibits stiffness variation. Compared to pneumatic, SMA actuator has advantages in the small form factor [57] and untethered implementation using the battery. However, the pneumatic actuator is much more responsive especially when releasing the form, as SMA needs to be cooled down to release the actuation force. Therefore, it is more efficient to use on human augmentation [112].

7.2.2 Pneumatic Artificial Muscles (PAMs) for Wearables

Inflatable pneumatic actuator has limitation in expanded size when actuated. To address the limitations of inflatable actuators, researchers have turned their focus towards thin Pneumatic Artificial Muscles (PAMs), which offer both flexibility and high actuation force [95]. Various works have introduced the use of PAMs for haptic feedback [196, 236] and fabric-structure actuator [2, 14, 47, 63, 151]. In this research,

we also investigate the potential of PAMs as actuators, but our primary emphasis lies in exploring the programmability of reinforcement modules to influence the overall shape and stiffness of the interface. Although our focus is variable-stiffness rather than shape-changing capabilities. Conveniently, our actuation technique is also capable of shape deformation. Furthermore, simultaneous stiffness and shape alteration can be beneficial to create a deployable structure that has not been explored on shape-changing fabric.

7.2.3 Variable-stiffness Mechanism

Variable-stiffness mechanism is actively researched in robotics [222], various mechanism has been proposed for stiffness tuning such as vacuum jamming [7, 15, 42, 144, 217], beads jamming [74, 128, 146], Low Melting Point Alloys/Polymers (LMPA/LMPP) [26, 176], gel [78] and SMA actuator [24, 49]. Despite the current technological improvement, variable-stiffness in HCI is under-explored, and most of the research is repetitively using vacuum jamming technique [42, 144], due to easy implementation. Although the vacuum jamming mechanism provides an effective range for stiffness variation, it also has limitations in both bulkiness and the flexibility of the main materials. This characteristic is especially important for fabric types of interfaces, which can limit the utilization of wearable interfaces. Previous studies in robotics actuators have proposed beads jamming [74, 128, 146] to control the stiffness of linked structures using the tension of tendon actuators. This mechanism can improve the flexibility of the robot's body, due to the flexible tendon that works as actuator and joint of the structures. Our research borrows this forefront technique in robotics stiffness controls, however, was able to leverage the structural dimension into 2D dimensional structures.

7.2.4 Variable-stiffness Fabric

Previous works have explored variable-stiffness implementation on fabric-like structures using vacuum jamming mechanism [144, 217], and woven SMA [24, 232]. Jamsheet [144] has proposed applications for vacuum jamming mechanisms to stiffen multi-layer sheets confined inside a membrane. The jammed sheet is capable of enduring high loads up to 55Kg, and pliable enough to be deformed by user manipulation. However, due to the stack of multiple paper sheet structures, it suffers from inflexibility that is not suitable to be used for compliant fabric. Similarly, SMA actuators that are woven into a fabric [24, 232], show stiff characteristics (due to metal wire properties) that are not comfortable for wearability. VabricBeads used PAMs combined with beads structure to change stiffness properties. Although the usage of rigid beads seems counter-intuitive for fabric application. The soft and flexible PAMs that connect the beads can create a soft and flowing drape on the bead's structures. We also introduce new utilization of rapid stiffness change properties that previous work cannot achieve.

7.2.5 Beaded Structures Interface

In this research, our focus was on exploring the potential of beaded structures for fabric interfaces due to their simplicity and ease of fabrication. The beaded structure offers scalability in terms of manufacturing and can be incorporated into various applications such as clothing, accessories, and household items. Previous works in the field have introduced the use of beadwork for input/output (I/O) devices, demonstrating the potential of beads as interactive elements [44, 162]. Some works have specifically explored the integration of beaded electronics into jewelry, showcasing the aesthetic and functional aspects [9, 18, 75]. Taking inspiration from these previous works, our research aims to leverage the capabilities of VabricBeads, combining shape-changing and variable-stiffness features, to introduce novel fabric interfaces. In terms of related work, FlexTruss [185] is closely related to our research.

Table 7.1: Comparison with related work. VabricBeads supports both shape deformation and variable-stiffness with only beads and PAMs mechanism.

	Fabrication	Actuator	Shape-change			Haptic properties			Thick-ness (form factor)	Force /load
			Bending	Twisting	Contraction/ Expansion	Rigidness	Malleablitiy	Elasticity		
Patch-O [94]	Weaving	SMA	✔	✔	✔				0.5 mm	0.17 N
ClothTiles [129]	Surface attachment	SMA	✔						4 mm (Approx.)	1.44 N
Robotics Fabrics [232]	Surface attachment	SMA			✔	✔			2.7 mm	200 g
Springlets [57]	Surface attachment	SMA	✔		✔				3 mm	30 g
SkinMorph [78]	Mold	Gel	✔		✔	✔			4mm	6.8 N
Woven PAMs [151]	Weaving	PAMs	✔		✔		✔	✔	6 mm (expanded)	20 N
Jamsheet [144]	Multilayer sheet	Vacuum Jammming				✔	✔		8.5mm	55 kg
Chain fabric [217]	3D printed chain	Vacuum Jammming				✔	✔		15 mm (Approx)	50 N
OmniFiber [2]	Weaving	PAMs	✔	✔	✔	✔ (LMPA)		✔	4 mm (expanded)	19 N
FlexTruss [185]	3D printed beads	Tendon tension					✔		4 mm	-
VabricBeads	3D printed beads	PAMs	✔	✔	✔	✔	✔	✔	13 mm	60N /2. 2 kg

It presents 3D printed beads that can be assembled into mesh or truss structures using wire as a thread. While the stiffness or malleability of the structure is not actively controlled, users have the ability to manually adjust the tension of the wire, allowing for customization.

7.3 Design Space

We propose VabricBeads: a dynamic variable-stiffness fabric concept by integrating beads shapes and PAMs threading patterns. To summarize VabricBead's capabilities, we characterize the design space into three dimensions as illustrated in

Figure 7.1.

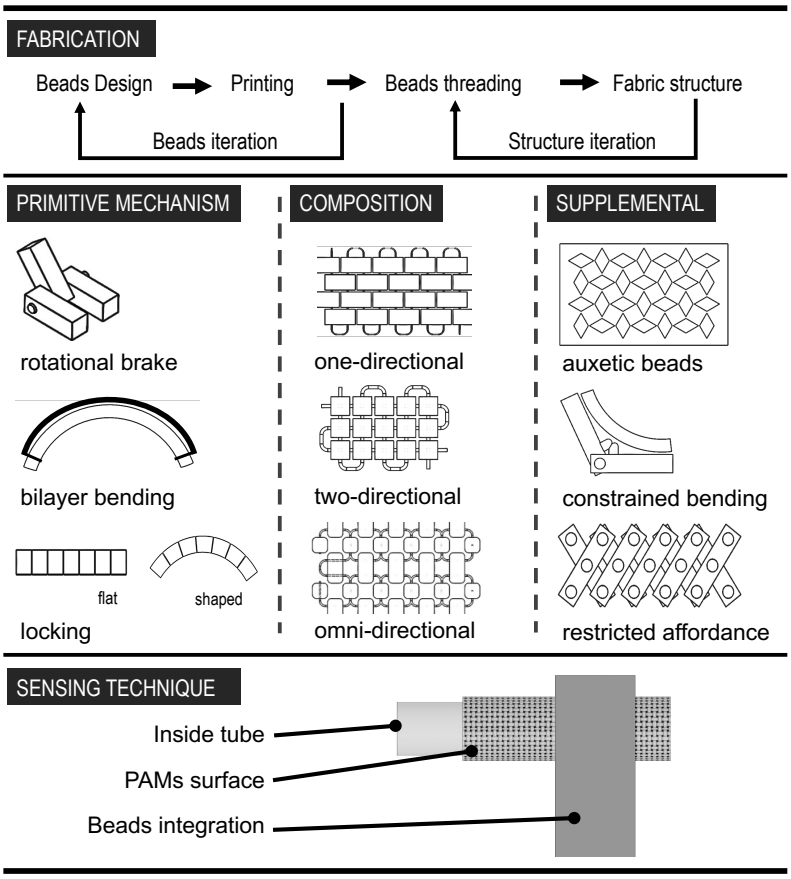

Figure 7.1: Vabricbeads design space

Primitive Mechanism By altering PAMs contraction and expansion forces using beads as mechanical constraints, we are able to create fabrics that exhibit both shape-changing and variable-stiffness properties. We employ three primitive mechanism that previously proposed in ASTRE (chapter 5), and leverage the concept into the fabric structures implementation. "These fabric properties can be categorized into controllable malleability (based on rotational brake mechanism), shape deformation (based on bilayer bending mechanism), and simultaneous shape and stiffness changes (based on locking mechanism)."

Structures Fabric structures and composition determine the deformability of the fabric both by external force or by self-actuation. One-dimensional structures

(1) can only be deformed in one Degree of Freedom (DoF) due to the structural constraint that resulted from beads shape and flat-peyote threading pattern. Similarly, two-directional structures (2), increase the bendability into two DoF because two channels of PAMs that threaded cross each other. Omni-directional structures (3) can be bent or twisted due to the weaving pattern of the fabric that allows vertical, horizontal, and diagonal deformation.

Supplemental Additional features such as auxetic structures, constrained bending angle, and restricted affordance are also explored to enrich the functionality of our proposed fabrics.

7.4 Controllable Malleability

The stiffness variation technique proposed in ASTRE (chapter 5) served as the basis for the primitive mechanism. We utilize both the contraction and expansion forces of the PAMS to create a rotational brake force on the bead's hole surface. The brake stiffness can be changed according to the PAMs air pressure. Additionally, we were able to vary the brake rotation from one-directional to omni-directional resulting in different physical affordances.

7.4.1 One-directional Brake

Figure 7.2a shows the beads design and threading pattern of the One-directional brake fabric. The beads have an oval shape and two holes inside them. Each hole has gear teeth to increase the friction force. Both the hole diameter and gear teeth are important aspects for adjusting brake torsion. (We further discuss these characteristics in the technical evaluation section.) All the beads are arranged in parallel and threaded together using the flat peyote technique[219]. Figure 7.2b shows how the fabric has a flowing drape when unactuated and solidifies its shape when actuated. In its maximum stiffness (0.4MPa) the fabric can withstand loads up to 1.1Kg. Due to the PAMs threaded in straight lines and weaving back in a

zigzag pattern, the fabric is only bendable in one direction.

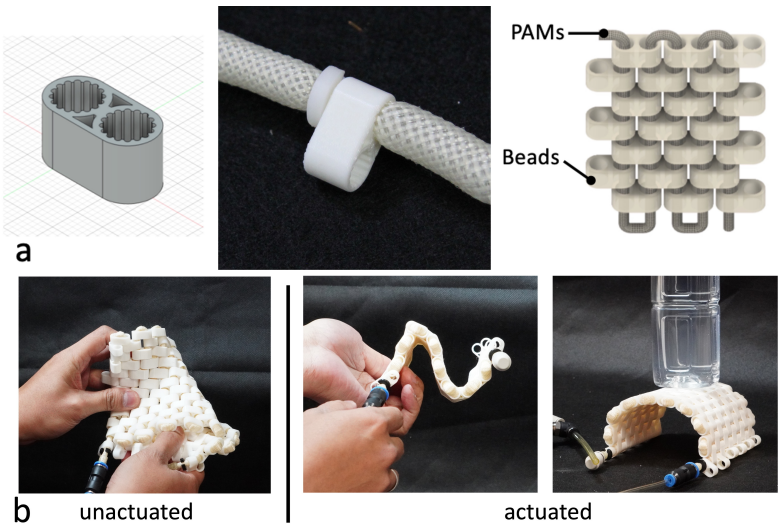

Figure 7.2: One-directional brake: beads design, arrangement, and actuation

7.4.2 Omni-directional Brake

To achieve fabric that is bendable in multiple directions we apply right-angle weave instead of flat peyote stitches. As shown in Figure 7.3 we use a similar beads design with the One-directional brake. Here we try to demonstrate the versatility of our proposed method where one simple beads design can be utilized for several purposes by varying the threading pattern and beads arrangement. As the trade-off for omni-direction bending capabilities, the fabric exhibit a stiffer drape compared with one-direction stiffness fabric in an unactuated state. It also deforms slightly when actuated due to the crossing between the PAMs as shown in Figure 7.3b.

7.4.3 Partial Control Brake

Figure 7.4a shows beads design for fabric that the stiffness can be partially controlled in the vertical and horizontal direction. Two beads are set at a 90-degree angle. We arranged beads in a grid composition and threads two channels of PAMs

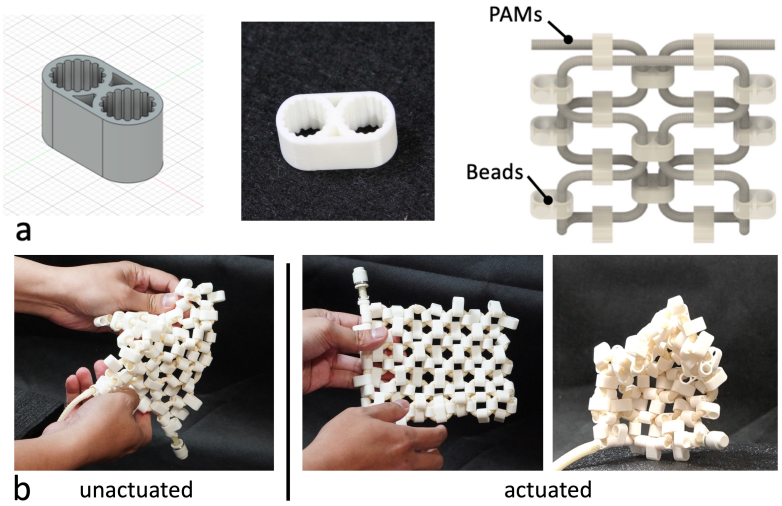

Figure 7.3: Omni-directional brake: beads design, arrangement, and actuation

into the vertical and horizontal directions in a straight line. As shown in figure 7.4b, the fabric falls softly in both directions when unactuated. It becomes stiff partially in one direction or both directions, depending on the channels actuated. It also becomes stiffer than the omni-directional stiffness fabric. However, as a trade-off, it cannot bend in the negative direction.

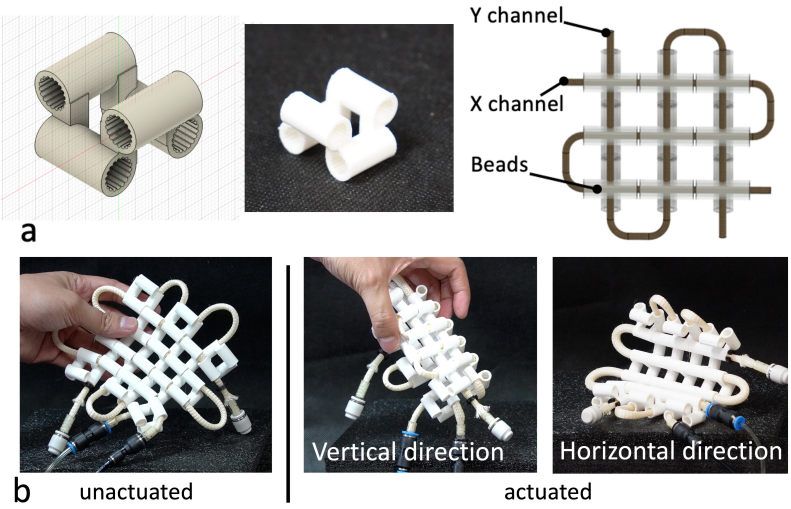

Figure 7.4: Partial control brake: beads design, arrangement, and actuation

7.4.4 Restricted Shape Manipulation

In the VabricBeads system, we use 3D printer or laser cuter to freely customized the beads for special purposes. Here we explore bead shapes where user manipulation is restricted to elongating or shortening the fabric only. Figure 7.5a shows the design where each bead has three holes with gear teeth. We arranged the beads in an articulated scissor structure and threads them in a straight line.

Figure 7.5b shows the fabric properties where it can be freely elongated or contracted in the unactuated state. When actuated it will become stiff and keep the formed length.

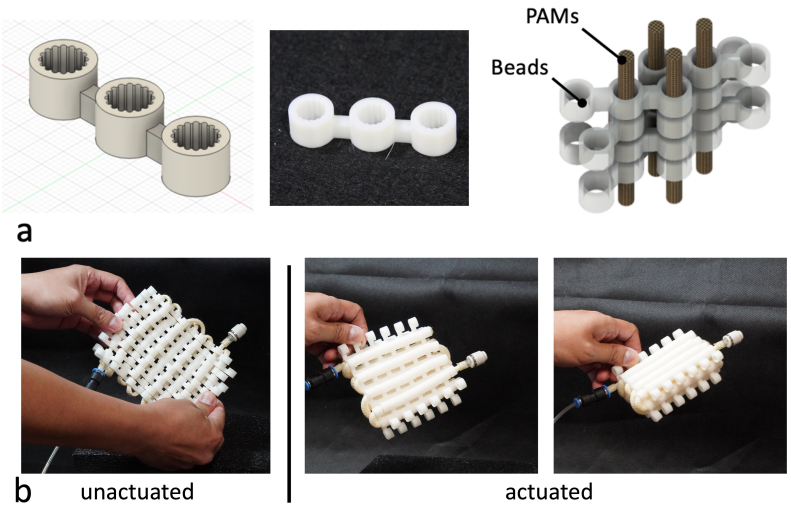

Figure 7.5: Restricted shape manipulation: beads design, arrangement, and actuation

7.5 Deformation Fabric

Although our main contribution in this paper is the variable-stiffness fabric, here we also explore the design of the shape-shifting fabric. We expect these fabrics can be combined to create much more complex behavior.

7.5.1 One-directional Bending

For deformation fabric, we use a mechanical constraint to alter the PAMs contraction force into bending behavior. Figure 7.6a shows the basic deformation beads where a layer of flexible constraint act as a mechanical constraint and four rings act as a guide rail for the PAMs. We then thread the beads using the flat peyote technique.

The fabric is soft and flexible in an unactuated state due to the flexibility of the TPU filament used for the beads material. It bends in one direction when actuated, however, it is still soft enough to be deformed by the user to any other direction (Figure 7.6b)

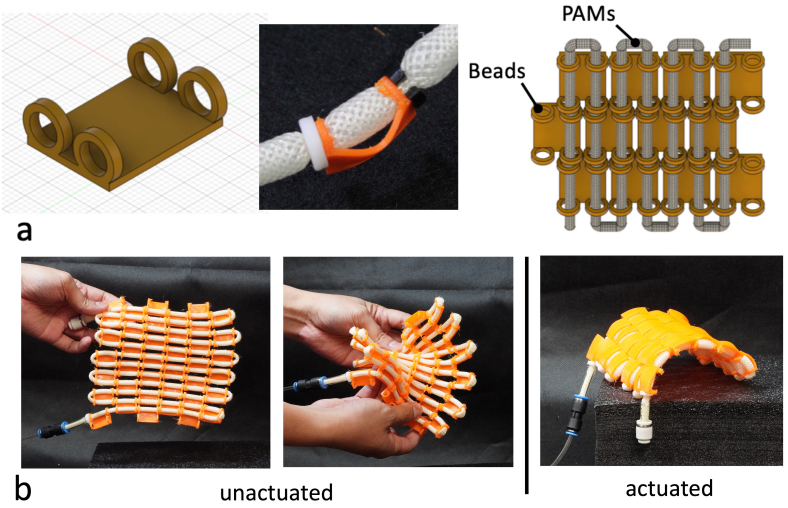

Figure 7.6: One-directional bending: beads design, arrangement, and actuation

7.5.2 Omni-directional Bending

We can further extend the bending deformation capabilities into omniple directions by modifying the beads into a cross shape(Figure 7.7a). Hence, it can bend in both horizontal and vertical directions. It also can be partially actuated by separating the PAMs channel between the horizontal and vertical axis. We also can

adjust the bending in the same direction or in reverse by adjusting the 3D model in the inward or outward course. Figure 7.7b shows the fabric both in unactuated and actuated states. Other than cross-shape beads, we also can increase the bending direction into three or more by shaping the beads into triangles or other polygonal shapes.

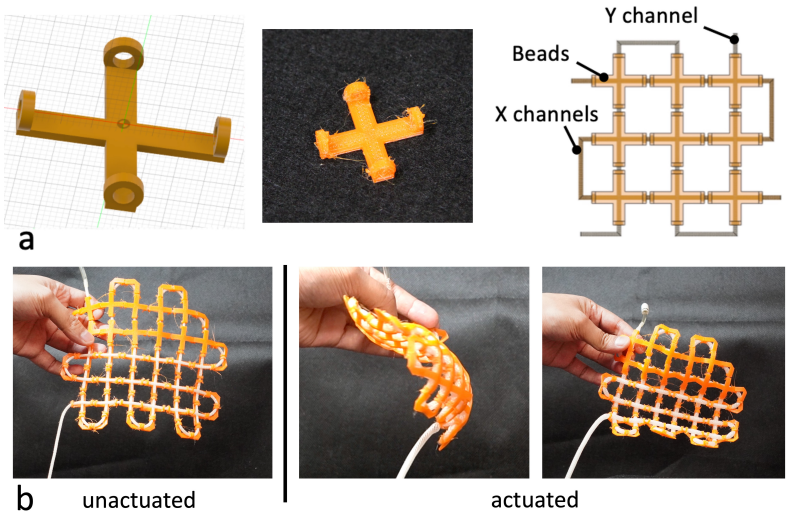

Figure 7.7: Omni-directional bending: beads design, arrangement, and actuation

7.5.3 Permeability Changes

Permeability is an important property of fabric that determines the capability of air, water, or other fluids to pass through the fabric. We design beads with auxetic structures that open up width-wise when compressed by PAMs. As a result, it expands the hole area and thus increases its permeability (Figure 7.8a). For fabrication convenience, we thread the beads using the flat peyote technique. However, it results in some overlap between the bead's petals when actuated.

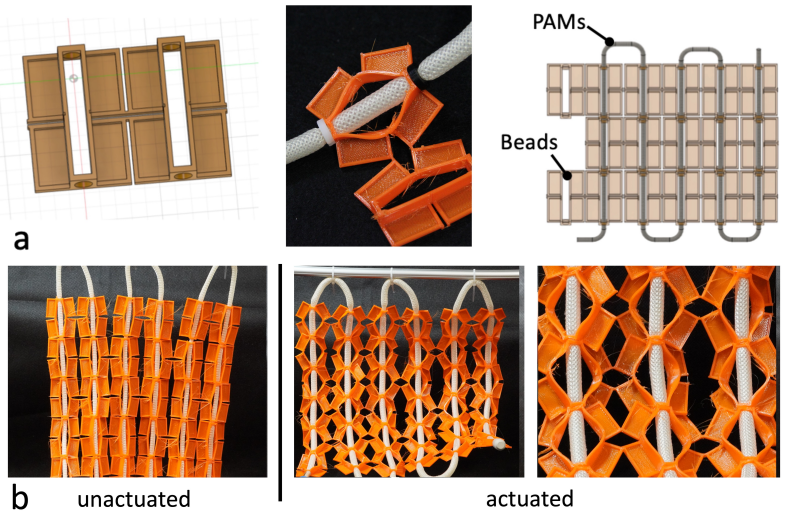

Figure 7.8: Permeability changes: beads design, arrangement, and actuation

7.5.4 Constrained Bending

To have a more sophisticated shape, we assume the bending angle of each bead needs to be controlled separately. We designed two-part beads that connected with a hinge structure and add a stopper to control the maximum bending angle of each bead. The beads are threaded using the flat peyote technique as shown in figure 7.9a.

Compared with the TPU beads fabric, in unactuated stated, this constrained fabric is less flexible. And in actuated state, it has a pointy edge rather than a curvy surface, as shown in figure 7.9b. Other types of hinges or joints similar to previous work by He et. al. [60] can be implemented to create a more complex shape and affordance.

7.6 Simultaneous Shape and Stiffness Changes

To achieve a shape deformation and stiffness change simultaneously, we use a locking mechanism proposed in ASTRE mechanism. This locking mechanism is based on the beads jamming technique [32, 74] where the contraction force of PAMs

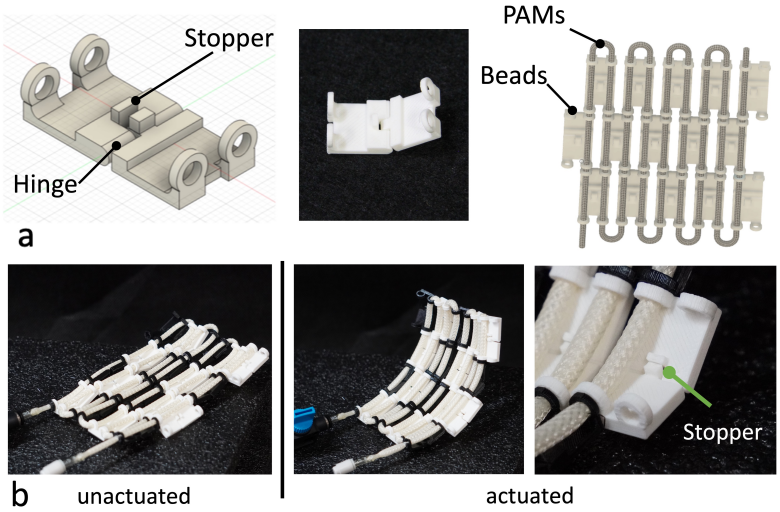

Figure 7.9: Constrained bending: beads design, arrangement, and actuation

compresses the beads to create one interlocked structure.

7.6.1 One-directional Locking into Flat Surface

Figure 7.10a shows the most basic beads for the locking mechanism. It has four holes without gear teeth with the hole diameter equal to or less than the expanded PAMs maximum diameter. It is important as it will remove the leeway for beads to move in an actuated state. Figure 7.10b shows in an unactuated state, the fabric is fully bendable on the y-axis but has some restrictions on the x-axis. When actuated, it turns completely flat and stiff at the same time.

7.6.2 One-directional Locking into Shaped Surface

We can create a surface that has shape, by adjusting the contour of the bead. Figure 7.11a shows the beads with bent contours and the threading pattern. As shown in figure 7.11b, even when unactuated the fabric already has a certain shape formed. Albeit it is still flexible and bendable in multiple directions. When actuated it instantaneously shifts into the stiff predetermined shapes.

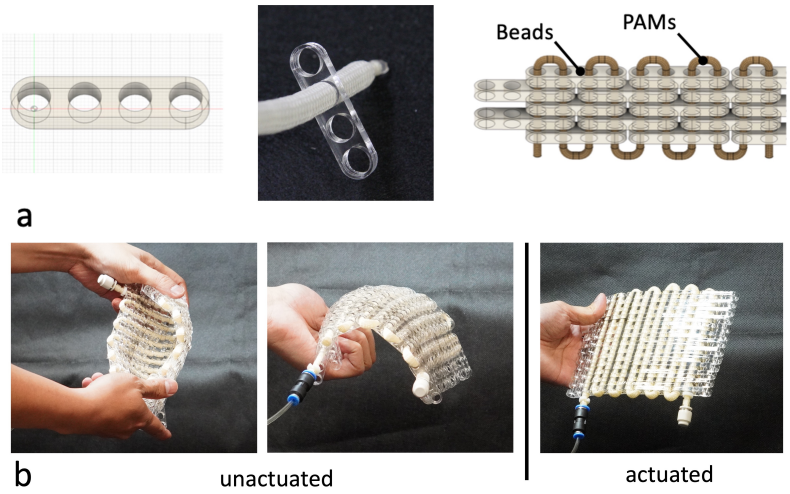

Figure 7.10: One-directional locking into flat surface: beads design, arrangement, and actuation

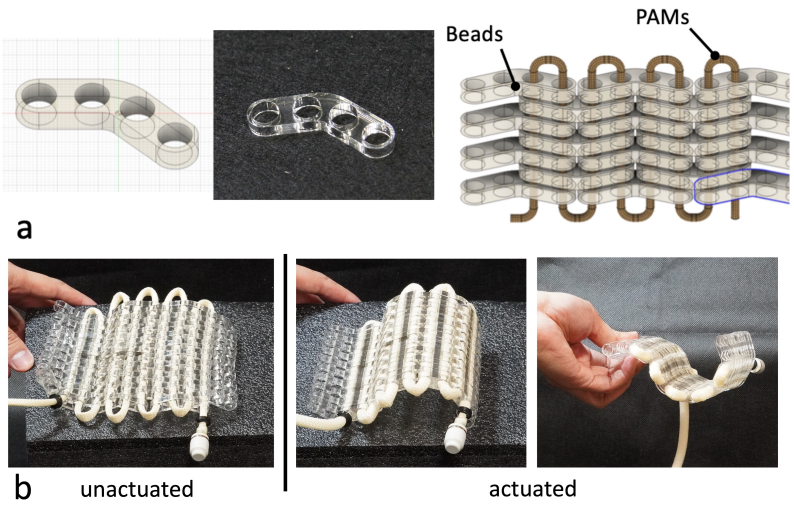

Figure 7.11: One-directional locking into shaped surface: beads design, arrangement, and actuation

7.6.3 Omni-directional Locking into Flat Surface

To create a fabric whose movement is not restricted in any direction, we designed a locking structure that threaded both from the vertical and horizontal directions.

Figure 7.12a shows the design of the beads which is an octagon with four holes. The beads are arranged in a grid with both the x and y channel of PAMs threaded in straight lines. Figure 7.12b shows the fabric is bendable to multiple directions in an unactuated state. It can be actuated partially into a flat-stiff in one direction and bendable in another direction. It also can be actuated into a completely flat and rigid surface.

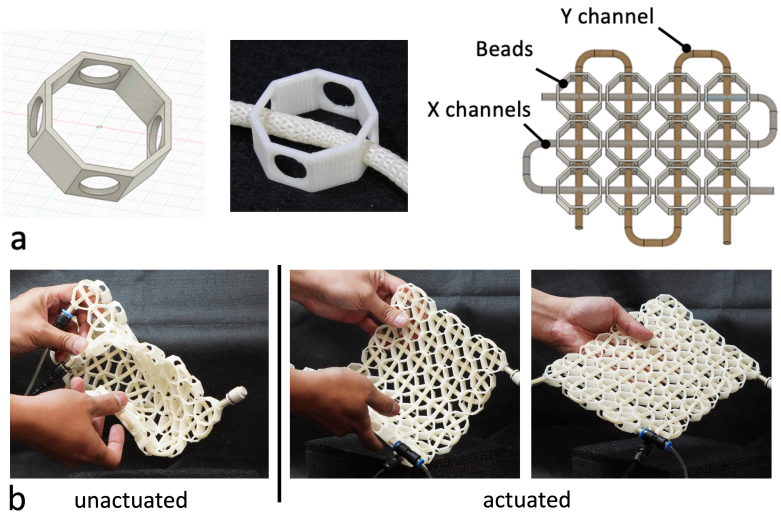

Figure 7.12: Omni-directional locking into flat surface: beads design, arrangement, and actuation

7.6.4 Omni-directional Locking into Shaped Surface

Finally, to create a fabric that can deform into a stiff-shaped surface, we designed beads similar to the flat surface ones, however with a slanted surface on each side. Figure 7.13a shows the design and arrangement of the beads. When actuated, the slanted face closely adheres to another bead face, resulting in locked bending deformation. Figure 7.13b shows the fabric can shape-changes from a flexible surface into a rigid hemisphere.

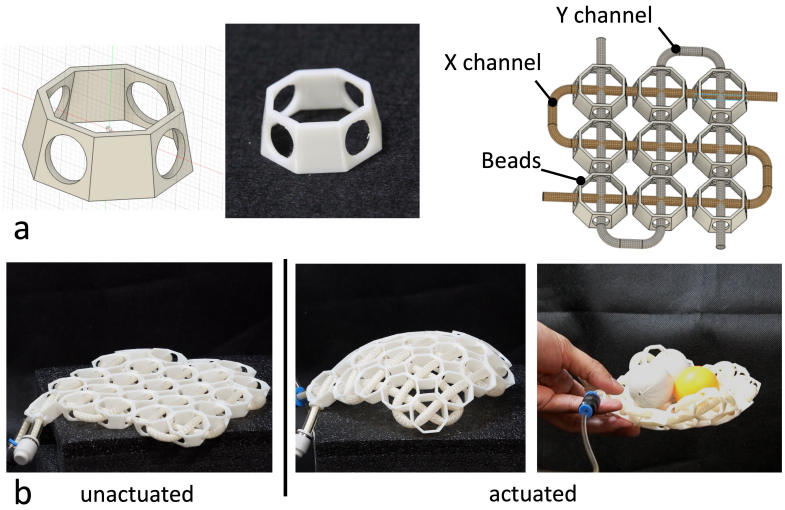

Figure 7.13: Omni-directional locking into shaped surface: beads design, arrangement, and actuation

7.7 Sensing Techniques

To enhance VabricBeads with interaction, we consider three types of sensing techniques.

7.7.1 Pressure-based Sensing

When the PAMs are in the actuated state, the pressure inside can be substantially changed by an external force. The pressure change can then be detected using the pressure sensor inside the electro-pneumatic regulator. Figure 7.14a shows how the pressure inside the locking fabric changes when the module is forcefully bent by an external force. We then can use the sensed fluctuation for interaction purposes such as unactuated the fabric.

7.7.2 At PAMs Surface

PAMs surface is covered by breaded fabric that expands radially while contracted in length. The breaded fabric on PAMs we use is not conducting electricity, however,

we can add an additional layer of breaded shielding that conduct electricity (Figure 7.14b). Capacitive touch detection on PAMs surface can be achieved using this setup. It also can be used to conduct electricity for electronics I/O purposes.

7.7.3 On Beads

We mainly use 3D-printed PLA or laser-cut acrylic for beads material for convenience purposes. However, conductive materials and other special materials e.g. conductive, carbon-filled, and triboelectric materials can be used to enhance the bead's utilization. Figure 7.14c shows our experimental setup where acrylic beads are incorporated with LED and conductive tape arranged in parallel. When unactuated, the beads barely touch each other and didn't conduct electricity. However, when actuated the beads are interlocked making a complete electrical circuit to light up the LED. Flexible and stretchable sensors such as those previously proposed by Gholke et. al can be utilized for touch detection on beads surface [51].

7.8 Application

In previous studies, Alexander et. al. [6] have proposed five purposes of shape-changing interfaces. It includes adaptive affordance, communicating information, augmenting users, hedonic and symbolic, and simulating objects. In this section, we devised applications based on these ideas and demonstrate the versatility of our proposed frameworks for variable-stiffness and shape-changing fabric interfaces.

7.8.1 Input Wristband

Figure 7.15a shows another application on a wearable device which is a shape-changing wristband. In a normal state, it is actuated to be constantly bent to cover the user's arm. When actuated it instantly becomes a flat and rigid slab that can be used for an input device. We incorporated two types of VabricBeads which are

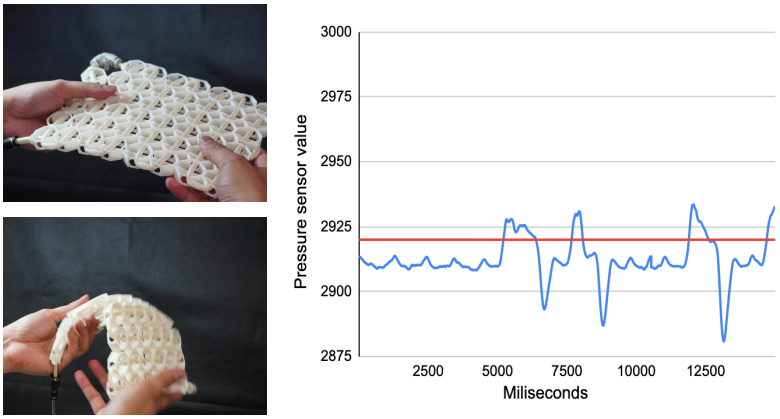

(a) Pressure based sensing

(b) PAMs surface touch detection

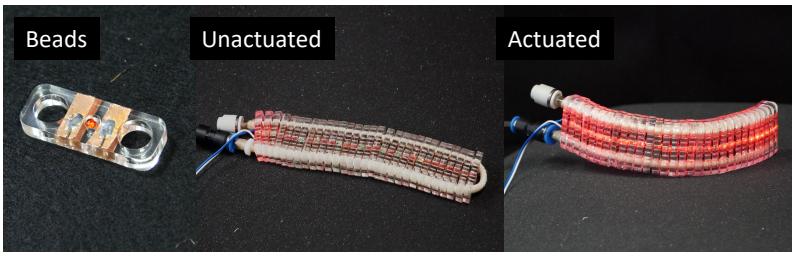

(c) Beads sensing

Figure 7.14: Interaction technique: a. Inside PAMs tube, b. At PAMs surface, c. On beads

locking into flat, and locking into shaped (curved) beads. We also add a conductive shield on the PAMs surface to provide touch interactions. This application also demonstrates the benefit of pneumatic actuators where it doesn't need the energy to keep the pressurized state (therefore will keep the shape).

7.8.2 Haptic Glove

Figure 7.15b shows an application on Haptic VR Glove where one-directional brake fabric is incorporated into a glove. We attach flex sensors to the glove palm-side to detect user gripping motion. It can be used to simulate various stiffness on VR objects. It can generate strange sensations such as ice melting spontaneously due to the rapid changes in stiffness. It also can be used to augment the user when grabbing an object as it can be stiffened to reduce muscle fatigue.

7.8.3 Shape Changing Hat

Figure 7.15c shows the shape-changing hat as a wearable device application. The fit around the head can be adjusted by varying the contractible length and bending angle. It also featured a variable-stiffness visor that can become hard like plastic or flexible like a fabric. The shape can be adjusted depending on the sunlight and can be used for the protection of the head like a helmet.

7.8.4 Variable-stiffness Bag

Figure 7.15d shows a handbag created with VabricBeads. We use one-directional locking beads that will stiffen into a box shape when actuated. In an unactuated state, the bag can be crumbled without breaking and easily deformed to be stored in tight spaces. When actuated it will become a stiff box that has a big opening on the top, making it easy to put in or take out objects from inside. It also stabilizes in the stiffened state, making it not easy to tumble on a reclined surface.

7.8.5 Lamp Shade

Figure 7.15e shows a robotic lampshade inspired by flower petals movement. We threaded triangle-shaped beads with a Omni-directional bending function. It can dynamically flex to adjust light distribution in the rooms. The movement can also be utilized to notify information such as incoming calls or emails to users.

	Application	Specification	1st phase	2nd phase
a	Input wrist band	T. assembling : 40 min # beads : 15 Pams length : 2.7m Weight : 102 g		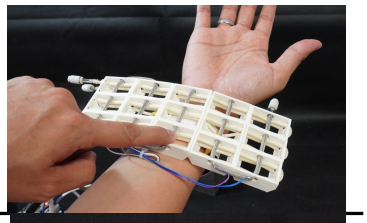
b	Haptic glove	T. assembling : 50 min # beads : 96 Pams length : 1.4 m Weight : 162 g	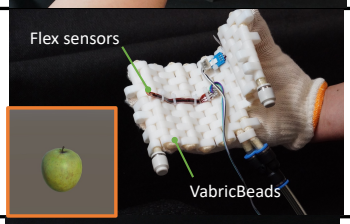	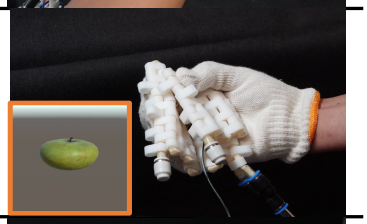
c	Shape changing hat	T. assembling : 1.2 H # beads : 228 Pams length : 1.23 m Weight : 207 g		
d	Variable-stiffness bag	T. assembling : 3H # beads : 1050 Pams length : 2.9 m Weight : 506 g	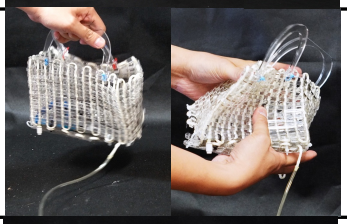	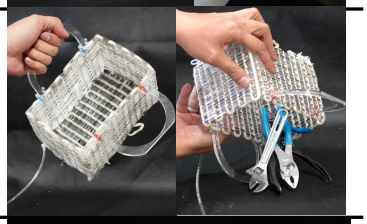
e	Decorative lamp shade	T. assembling : 3H # beads : 1050 Pams length : 2.9 m Weight : 506 g	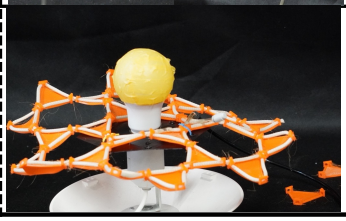	

Figure 7.15: Wearable application

7.9 Technical Evaluation

7.9.1 Stiffness Range Comparison

To help other researchers replicate and utilize Vabricbeads, here we show the correlation between pressure change and stiffness. We selected one-directional brake, omni-directional brake, one-directional bend, one-directional locking, and omni-

directional locking as representative beads design. Although the bending beads are not designed for stiffness changes, we acknowledge that there are slight stiffness differences due to the PAMs swelling.

Figure 7.16shows our experimental setup. We conducted three-point bending flexural tests on each fabric type and plot the stress-strain curve. We calculated the stiffness(N/mm) based on the line fit approximation on each strain-stress curve. Figure 7.17, shows how the stiffness increases almost linearly along with the pressure changes. It shows that one-directional locking has the highest stiffness range and that the bending shows a minimal variation in stiffness.

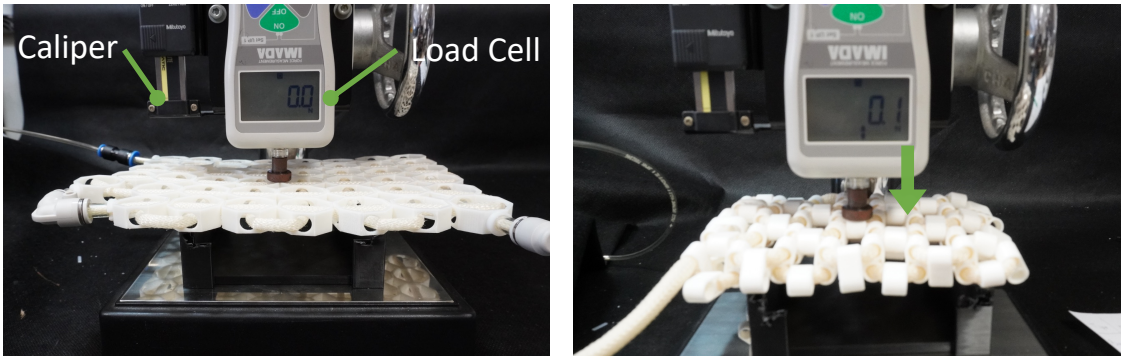

Figure 7.16: Experimental setup

7.9.2 Localize Stiffness Adjustment

In a practical use case, we expect the capability to locally adjust the stiffness on one piece of fabric will be beneficial. Although we can create an additional pneumatic channel to control the area we wish to modify. It will cost an additional pneumatic controller and need separated air tubes that will reduce the aesthetic. Here we introduce a novel approach to adjusting the stiffness by varying the hole diameter. We created four types of beads, each with different hole diameters (6 mm,7 mm,8 mm, and 9 mm). Then conducted three-point bending flexural tests and calculate the stiffness of each beads type. We conducted this experiment both on the brake mechanism and locking beads only in one PAMs fiber.

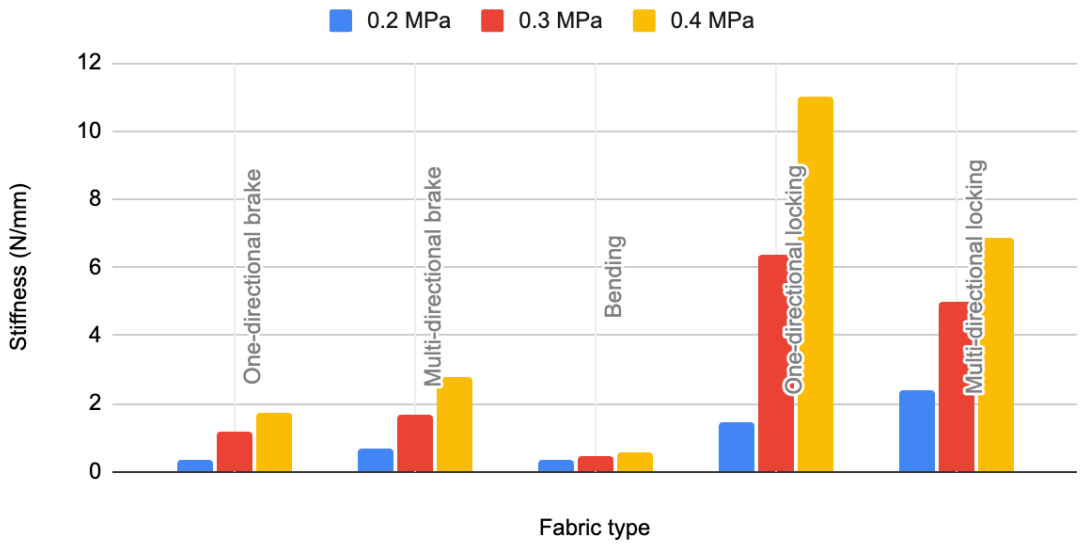

Figure 7.17: Comparison between the fabrics stiffness range

Figure 7.18 shows the stiffness difference attained by varying brake mechanism bead hole sizes. All the hole sizes did not show stiffness up to 0.2 MPa, whereas the 9 mm hole only show stiffness at 0.4 MPa. Both 6 mm and 7 mm hole sizes show similar stiffness change, with maximum stiffness being 1.85 N/mm at 0.4 MPa.

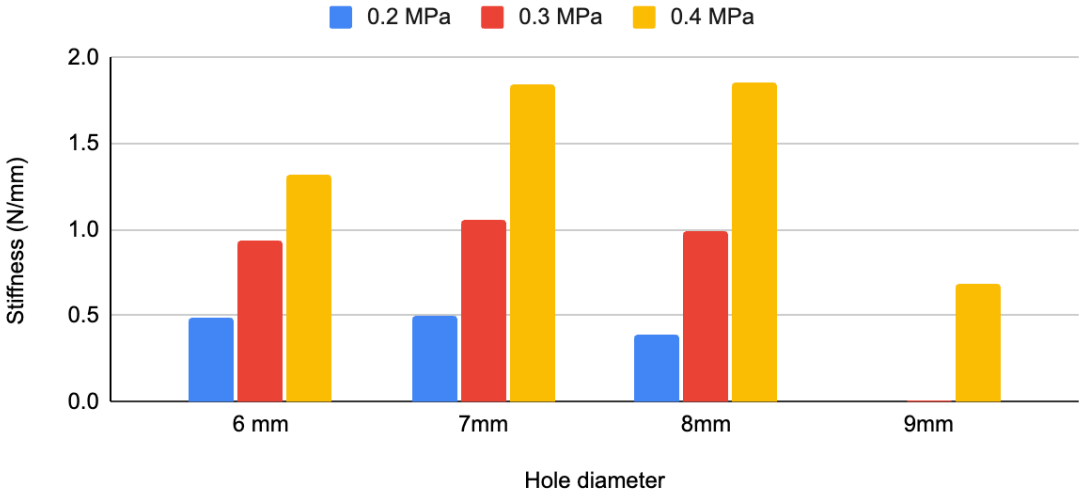

Figure 7.18: Relationship of brake mechanism beads hole size and stiffness

Figure 7.19 shows the stiffness change in the locking beads according to the

variation in the hole size. It shows that all hole sizes exhibit similar stiffness up to 0.2 MPa; however, they widely vary on 0.4 MPa. The highest stiffness of 1.57 N/mm can be attained with a 7 mm hole size, however, it will exhibit a plastic deformation behavior where it retains its shape after being bent.

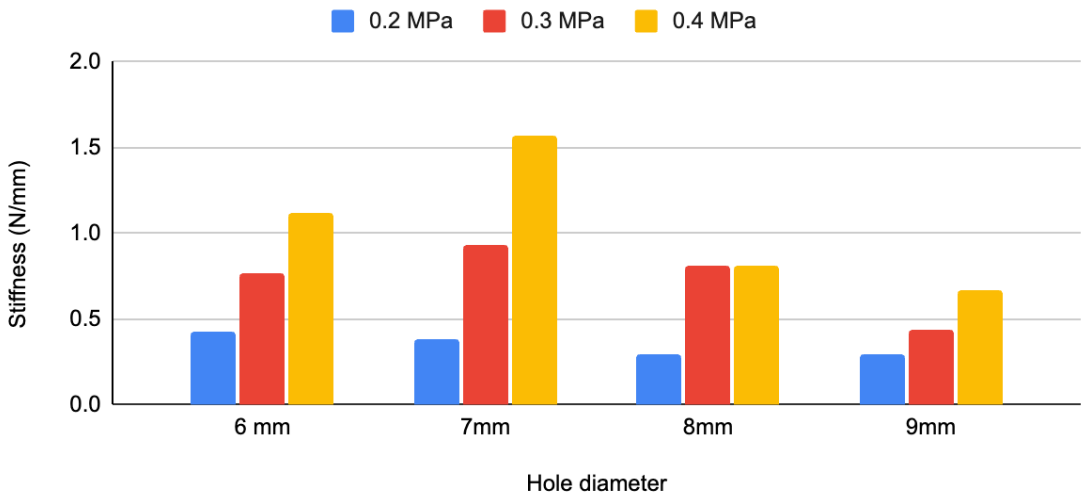

Figure 7.19: Relationship of locking mechanism beads hole size and stiffness

7.9.3 Scaling Evaluation

This research employs the flat peyote pattern, where PAMs filaments are threaded into the beads in a zigzag loop. This technique allows for convenient scaling implementation, where the fabric can be extended by adding a greater number of loops. By scaling the fabric, not only does the spatial dimension increase, but the accumulated strength of the PAMs also increases. Consequently, this leads to an increase in bending force or locking stiffness. In this study, we aim to verify the effectiveness of this scaling technique.

Bending Force scaling

Figure 7.20(a) shows the relationship between the applied air pressure and the bending force on a parallel bending arrangement. The contraction force increased

with the number of PAMs filaments, but not proportionally. The maximum bending force of the five filaments was 10.9 N at an applied pressure of 0.4 MPa.

Figure 7.20(b) shows the three-point bending test of the bending module in an arched state. It shows a trend of increase in the bending force, similar to that shown in Figure 7.20(a). The hysteresis loop in the dotted line shows a reduction in elastic behavior as the number of filaments increases.

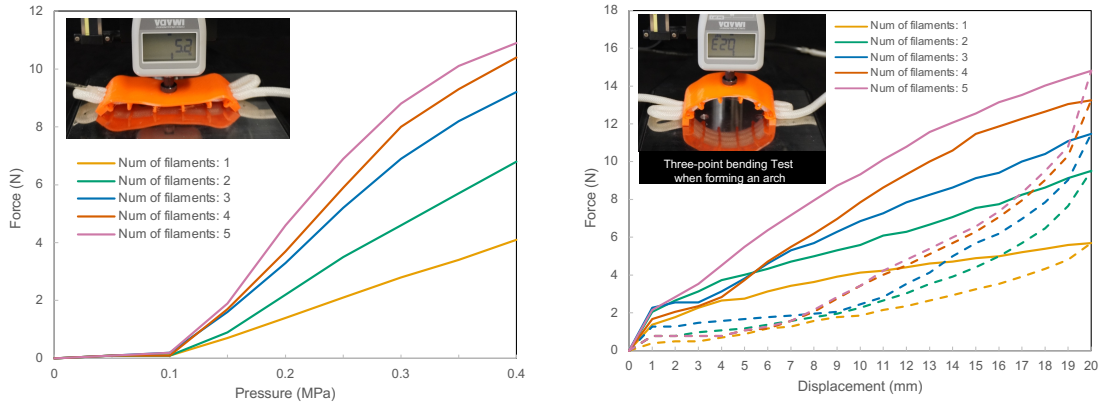

(a) Relationship between applied pressure and bending force.

(b) Three-point bending test on arched state, with 0.4 MPa applied pressure.

Figure 7.20: Bending scalability

Locking Stiffness Scaling

A stiffer locking mechanism is advantageous for increasing structural strength when withstanding heavy load. Figure 7.21 shows a three-point bending test of the locking module with a variation in the number of PAMs filaments. This figure shows that the strength of the locking module was nearly proportional to the number of PAMs filaments. The hysteresis loop also shows that the module always exhibits elastic behavior even when scaled up to five filaments.

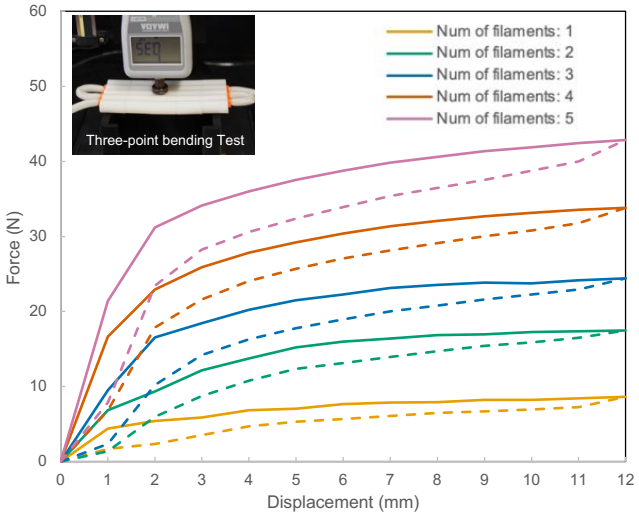

Figure 7.21: Locking scalability: Three-point bending test, with 0.4 MPa applied pressure.

7.10 Discussion

7.10.1 Bulky Form Factor

We define the term "bulky" in relation to the thickness of the beads used in the fabric. The range of bead thicknesses varies from 11 mm for applications such as bags to 25 mm for wristbands, with an average thickness of 13 mm. The bead thickness is dependent on the diameter of the Pneumatic Artificial Muscles (PAMs) holes and the bead walls. For instance, a 5 mm PAM expands radially to 9 mm, and with the addition of a 2 mm bead wall, the resulting bead thickness is 13 mm. Comparing our fabric to related works in Table 7.1, the thickness of other fabrics ranges from 0.5 mm to 15 mm, with thickness directly linked to force. Although our fabric is on the thicker side, with an average thickness of 6 mm, we are able to demonstrate unique properties such as rigidity, malleability, elasticity, high force, and fast response that were not achievable by previous works.

There are two strategies for miniaturizing the beads: using smaller Pneumatic Artificial Muscles (PAMs) and reducing the wall thickness of the beads. However,

these methods have their limitations. Using smaller PAMs can result in reduced force, and reducing the wall thickness of the beads may impact the durability of the fabric. To address these limitations, tougher materials like nylon or metal can be employed to enhance fabric durability. Additionally, smaller PAMs can be utilized to create a denser arrangement, which may help compensate for the lower force. Despite the existing limitations in terms of thickness, our fabric's stiffness range is sufficient for applications in human augmentation, particularly in restricting movement.

7.10.2 Assembling Challenge

In the fabrication workflow of VabricBeads, threading plays a critical role as it directly impacts the properties of the fabric. There are several factors to consider during the threading process. Firstly, the selection of Pneumatic Artificial Muscles (PAMs) is crucial in determining the form-factor and the force exerted during actuation. In our study, we incorporate three types of PAMs with different diameters: 2mm, 3mm, and 5mm. The 5mm PAMs provide a larger contraction force of 40 N, while the force decreases as the diameter is reduced.

Another crucial element is the contraction of the PAMs, as it affects the fabric behavior in both unactuated and actuated states. We use PAMs, which have a maximum contraction ratio of 20%. This factor is important for calculating the excess length required for each threading turn. Insufficient excess length can result in the fabric being too stiff in an unactuated state, while excessive length can lead to inadequate stiffness in an actuated state. In our study, the threading process is performed manually by hand. However, an augmented reality (AR) application similar to the tools proposed by Tao et al.[199] can be beneficial in guiding the process.

7.10.3 Mobility Challenge

In the application section, we highlight the utilization of VabricBeads as a wearable and portable device, showcasing the fabric advantages such as flexibility, lightweight, and adaptability. However, we acknowledge that practical implementation as a wearable device currently poses challenges due to the heavy and bulky pneumatic source that is connected to the fabric. We believe that these technological hurdles will be overcome in the near future with the development of small-sized compressors or alternative power sources.

In future work, we intend to explore alternative pumping methods, such as chemical reactions, that have been investigated in Auto-Inflatables [218] for pneumatic inflation. However, it is important to note that these options may result in irreversible shape changes and slower response times. Consequently, they may be suitable for specific use cases, such as emergency medical casts. Another approach we plan to explore is the use of liquid-to-gas phase change, as demonstrated in InflatableMod [124]. However, there are several technological challenges associated with this approach, including operating within a low-pressure range and achieving faster deflation speeds.

Considering the current stage of development, we find the most practical usage of VabricBeads to be in the realm of furniture and decoration. Many existing furniture pieces incorporate beads as primary or cover materials. We envision a future home where pneumatic sources are piped inside the walls, similar to industrial setups. Individuals would be able to connect the VabricBeads tube, akin to plugging in electrical devices, enabling easy integration into the living space.

7.10.4 Design Challenge

Currently, the design process for VabricBeads involves the manual creation of patterns and beads using CAD software. However, in the future, we aim to develop a computer-aided design tool that will streamline this process and empower users to

easily adjust the beads and patterns according to their specific requirements. This design tool will provide intuitive customization of VabricBeads designs.

One of the key features of the design tool will be its ability to accommodate the combination of various types of VabricBeads beads. By offering a wide range of bead options, users will have greater flexibility in creating complex fabric properties and achieving desired performance characteristics. The design tool will provide parameters and controls that allow users to experiment with different combinations of beads, enabling the generation of unique and customized fabric designs. The development of such a design tool will not only simplify the design process but also promote creativity and exploration in the field of VabricBeads. It will empower users, including designers and researchers, to easily iterate and refine their fabric designs.

Chapter 8

Discussion

In this chapter, the insights and findings of the frameworks and applications described in Chapters four, five, six, and seven will be summarized, analyzed and discussed.

8.1 Insights and Findings

8.1.1 Pneumatic Actuation Presents a Suitable Choice for Prototyping Shape-changing Interfaces

In this thesis, Chapter 4 focuses on the utilization of a vacuum to control stiffness using a vacuum jamming mechanism. The chapter explores the effectiveness of this approach and its implications for shape-changing interfaces. In Chapter 5, the utilization of compressed air is presented as a means to control both shape deformation and stiffness through the ASTRE mechanism. The implementation experience in both systems highlights the advantages of pneumatic actuation, which simplifies the prototyping process and facilitates ease of use.

1. **Simplicity**. Unlike electrical connections, pneumatic connections do not have polarity. This means that the same pneumatic tube can be used for both positive and negative pressure without the need for a specific orientation or connection. This simplifies the connection process and reduces the potential for mistakes during assembly, making it a convenient and user-friendly choice

for various applications.

2. **Soft**. Softness is a special property of human-computer interactions where it can enhance the approachability and visual appeal of an interface. Compared to rigid interfaces, soft interfaces are more comfortable to engage with. It also can create emotional connections that are difficult to achieve with rigid interfaces.

3. **Intuitive**. When using motor and shape memory alloy (SMA) actuators, energy is converted from electric or heat forms into motion, which is not commonly observed in our daily lives. On the other hand, pneumatic actuation relies on air compression force, which is a natural phenomenon that we encounter in various daily activities, such as inflating a balloon or pulling a string. This familiarity with physical concepts makes pneumatic actuation more relatable and easier to understand for users

4. **Lightweight**. When working with prototypes, it's often desirable to test the product under practical conditions. One advantage of using lighter actuators, such as pneumatic systems, is that the weight of the prototype can be easily adjusted by adding or removing peripheral materials. In contrast, when using heavier actuators, such as electric or hydraulic systems, reducing the weight of the actuator itself may not be feasible without changing the actuator technology or components.

5. **Scalable**. Scalability is indeed a significant advantage of pneumatic actuators. Both vacuum jamming actuators and PAMs actuators exhibit consistent behavior and functionality across different scales, whether it's in a small-scale prototype (50 x 50 mm) or a large-scale prototype (600 x 600 mm). This consistency simplifies the prediction and design of prototype functions, as the same principles and control mechanisms can be applied regardless of size. Furthermore, pneumatic control can be easily adapted to actuate prototypes

of various sizes. While there might be a decrease in actuation time for larger prototypes due to the increased volume of air to be compressed or evacuated, the fundamental principles and control methods remain the same. This allows for a seamless transition in applying pneumatic actuation to prototypes of different scales, providing flexibility and convenience in the design and testing process.

6. **Low-Cost**.The vacuum jamming actuator in the ClaytricSurface system primarily consists of polystyrene beads and stretchable inflatables, while the ASTRE mechanisms utilize materials such as silicone tubes, aramid sleeves, and 3D printed constraints. These materials are readily available in the market and are relatively inexpensive, with costs typically under $10 for actuators up to 100 mm in size. The affordability of these materials is particularly advantageous for the prototyping process. Prototyping involves creating multiple iterations and conducting extensive testing to refine and improve the design. With low-cost materials, researchers and designers can easily produce and experiment with various prototypes without incurring substantial expenses.

8.1.2 Novelties

The contributions of this research also come from the novelties of the systems, which are shown as follows:

1. ClaytricSurface is a pioneering system that introduces the concept of utilizing stiffness control to enhance modeling processes. The controllable stiffness range offered by the vacuum jamming actuator proves to be a perfect fit for traditional sculpting work, as it allows for adjusting the stiffness to match the desired level of shape deformability.

2. The ASTRE locking module is the first to introduce a mechanism by using PAMs actuators for simultaneous shape-changing and variable stiffness. Un-

like previous wire-based concepts [74], the even distribution of contraction force along the PAMs enables superior performance.

3. The ASTRE malleable module introduces a pioneering use of PAMs for shape malleability. While previous research has explored the malleability behavior in single PAMs arrangement based on locking mechanism [32, 74], this study is the first to leverage hole diameter variation to induce malleability behavior.

4. The ASTRE brake module introduces a pioneering concept of rotational brake mechanism utilizing the radial expansion of PAMs. While a similar concept was demonstrated by Hiramitsu et al. [63], the detailed mechanism was not described. This research is the first to provide a comprehensive description of the mechanism and leverage the use of gear-tooth mechanical constraints to expand the stiffness range.

5. The ASTRE twisting module is a new mechanism that utilizes twisted PAMs to generate twisting deformation and use spring reinforcement to revert the twisting. None of the previous works have presented a similar mechanism.

6. The ASTRE contractible module introduces a pioneering mechanism that utilizes PAMs to compress an outer reinforcement spring, creating a spring loading and unloading cycle using pneumatic.

7. The ASTRE Toolkit is the first shape-changing interface prototyping tool that empowers constructive assembly frameworks with variable stiffness capabilities.

8. VabricBeads is the first fabric implementation of both beads jamming and rotational brake mechanism into a two-dimensional structures using PAMs as the actuators.

8.2 Limitations

8.2.1 Reproduceable Shape

Both the ClaytricSurface and ASTRE Toolkit offer distinct capabilities for generating various types of shapes. The ClaytricSurface excels in creating intricate 2.5D shapes, enabling precise sculpting and rapid modeling. In contrast, the ASTRE Toolkit enables the construction of 3D truss-like structures, offering greater versatility in modules albeit with a coarser overall shape. The utilization of VabricBeads allows for detailed surface prototyping, but it involves a significant amount of manual threading.

In general, the three prototyping systems we have introduced can be compared as depicted in Table 8.1.

Table 8.1: General comparison of the three proposed prototyping systems

	ClaytricSurface	Astre Toolkit	VabricBeads
Actuation source	Vacuum	Compressed air	ompressed air
Active deformation	✖	◯	◯
Stiffness control	◯	◯	◯
Structure	2.5 D surface	Truss	Sheet/ layer
Modularity	Integrated	Modular	Woven
Scalability	✖	◯	Δ
Shape creation	Sculpturing	Constructive assembly	Beads threading
Max shape height	150 mm	600 mm	600 mm
Actuation response	slow	fast	fast
Localize stiffness	✖	◯	◯

1. ClaytricSurface relies on user manipulation for deformation, while ASTRE Toolkit and VabricBeads enable active shape-change.

2. ClaytricSurface excels at creating detailed models, while ASTRE Toolkit is

more suited for simplified versions of 3D objects. The VabricBeads serve as an intermediate option, providing a balance between rough and detailed shapes.

3. ClaytricSurface has volume limitations determined by granule volume and spandex stretchability, while ASTRE Toolkit can be easily scaled up by adding modules to the peak connector. VabricBeads can be scaled up by joining PAMs and threading additional beads into the fabric.

4. ClaytricSurface utilizes vacuum molding tools for shape replication, while ASTRE Toolkit and VabricBeads do not have a comparable feature.

5. In the ClaytricSurface system, the programmability of stiffness is achieved by controlling the amount of vacuum pressure applied. On the other hand, ASTRE Toolkit and VabricBeads enable variable stiffness through the selection of the modules in addition to the adjustable stiffness by air pressure.

6. The ClaytricSurface offers a unique sensation of softness that can be likened to the tactile experience of touching liquid or foam. The ASTRE Toolkit and VabricBeads, with PAMs as the main structure, offer a different sensation that is more akin to the drape of a fabric.

8.2.2 Portability

Portability is a significant advantage for interfaces, but the incorporation of bulky compressors or vacuum pumps in systems like ClaytricSurface and ASTRE mechanisms presents a challenge to achieving portability. To address this issue, several approaches have been explored. The first approach involves using a small pump with a portable battery. Although this approach has been attempted (Chapter 5), the smallest form factor achieved thus far is a backpack weighing 1.2 kg. While we anticipate that technological advancements will lead to a breakthrough in this area in the future, the current demand for such pumps is limited, which may slow down progress.

The second approach explores alternative methods of generating air pressure, such as chemical reactions. Some researchers have investigated techniques like liquid-to-gas phase changes[124] and chemical reactions to produce CO2 [218]. However, these approaches still face challenges, such as finding ways to reverse the reactions and controlling the amount of reaction.

8.2.3 Manual Fabrication

While the ClaytricSurface and ASTRE mechanisms were designed with convenience as a primary goal, the current fabrication process still involves manual labor, such as filling granular materials, threading PAMs, and adhesive sealing. It's worth noting that similar limitations exist in many other fabrication techniques, as mentioned in previous studies [55, 185]. To further enhance the practical application of these mechanisms, the development of automated and mass-production techniques would be a valuable contribution to future projects.

8.2.4 Utilization of Dynamic Stiffness Changes

In both the ASTRE Toolkit and VabricBeads application, we primarily focused on showcasing shape-changing capabilities to highlight the variable stiffness properties. In these systems, we effectively demonstrated how stiffness tuning can be utilized to fix a malleable object or create deployable structures. However, our demonstrations only showcased the extreme soft and stiff states to illustrate the state changes in a straightforward manner. As a result, we did not fully exploit the potential of gradual changes in stiffness, which can be achieved through pneumatic pressures and mechanical constraint parameters.

In future work, we plan to expand the application to include more refined stiffness control, showcasing various utilizations of mid-stiffness levels. For instance, a fully soft robot is collapsible and easy to store but cannot function as a robot. On the other hand, a fully stiff robot can function as a normal robot with significant force,

but might be dangerous for human interaction. By tuning the robot to a medium stiffness level, we can create a safer human-robot interaction while sacrificing some applicable load capacity.

Another approach to leverage the in-between stiffness levels is to implement haptic devices that can simulate various tactile and haptic feedback of physical objects. By dynamically changing the stiffness of the haptic device, we can present new haptic sensations that are not typically achievable in everyday objects. This can greatly enhance the user experience and immersion in virtual environments or haptic interactions.

8.3 Vision for the Futures

8.3.1 From Prototype to Final Product

In their book "Product Design and Development," Ulrich et al. [233] propose four dimensions of prototyping, which include physical, analytical, focused, and comprehensive axes. Based on these dimensions, we position our prototyping tools' main focus in the physical space, incorporating both the focused and comprehensive aspects (see Figure 8.1).

The prototypes developed in ClaytricSurface enable us to demonstrate products through a visual, tactile, and three-dimensional representation. This form of representation is easier for users to understand compared to verbal descriptions or even 2D and 3D sketches of the products. The prototypes created in VabricBeads serve as valuable learning tools for discovering how the interface will function and how well it will serve the users, as determined through user testing. Additionally, these prototypes facilitate communication about the product through physical presentations, allowing stakeholders to better comprehend the product's features and functionalities.

Furthermore, the modularity of the ASTRE Toolkit proves to be highly beneficial

for testing the integration between various parts of the product. By utilizing the toolkit, we can assess the overall function of the product in the minimum viable ways and detect any potential issues before moving on to creating preproduction prototypes. Through this multi-faceted approach to prototyping, we aim to facilitate a one-stop solutions for various prototyping challenges.

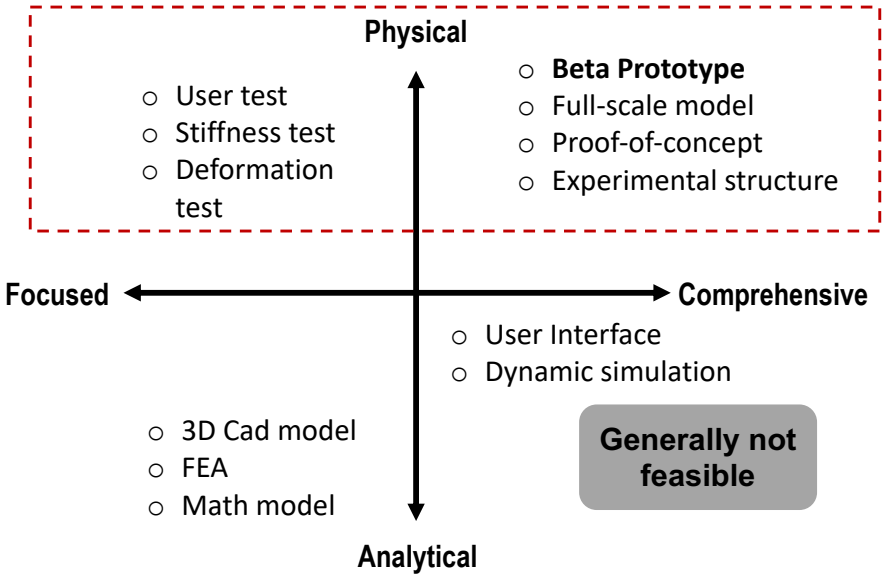

Figure 8.1: Prototyping dimensions

8.3.2 Interconnected System

In this research, we introduce three distinct prototyping systems: ClaytricSurface, ASTRE Toolkit, and VabricBeads, each exhibiting different form factors (2.5D surface, truss structure, and fabric). Despite sharing common characteristics such as pneumatic actuation, mechanical constraint mechanisms, and variable-stiffness capabilities, these systems serve different functions within the prototyping workflow. ClaytricSurface, functions as a modeling tool, enabling designers to shape the overall form and incorporate intricate details through hands-on manipulation. The ASTRE Toolkit, is designed for the rapid prototyping of truss shapes and supports iterative deformation of individual modules or changes in stiffness. Lastly,

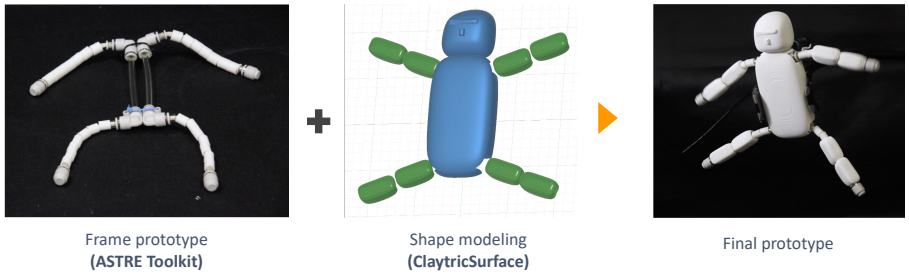

(a) First case: Truss prototype and shape modeling

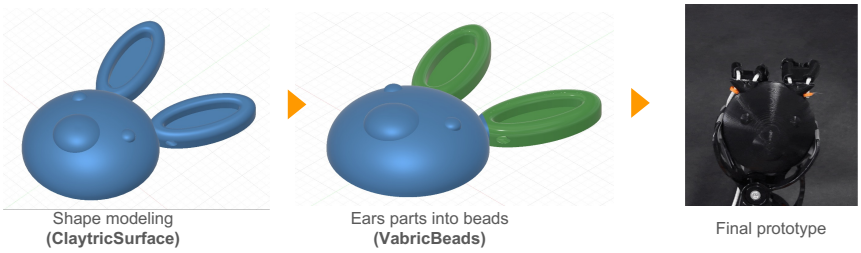

(b) Second case : Shape modeling and parts conversion into beads structures

Figure 8.2: Future works: Interconnected systems

VabricBeads, serves the purpose of creating surface prototypes using beads, allowing various fabric features such as restrained affordance and permeability changes.

In our future plans, we aim to create an interconnected system where each component can complement and enhance the functionality of the others. This interconnected system will facilitate seamless connections and streamline the functions of each individual system through the use of computer-aided design tools. In the first case, users will be able to create a truss prototype using the ASTRE Toolkit. Subsequently, they can iterate on the body of the truss using the ClaytricSurface shape modeling application (see Figure 8.2a). The final product will involve 3D printing and assembling the designed body to cover the truss structures, resulting in a complete and functional product.

In the second case, users will augment an already made shape model in ClaytricSurface with VabricBeads fabric properties (see Figure 8.2b). They can select specific parts of the model to be converted into bead structures, and the system will

generate 3D printed files for both the main model and the bead parts, which can then be assembled into the final product. This interconnected system will significantly streamline the design and prototyping process, facilitating rapid and convenient iterations between the three proposed systems. Users will be able to seamlessly transition from creating truss prototypes to shaping the body and incorporating fabric properties, resulting in a more efficient and effective product development workflow.

8.3.3 Horizontal Expansion

We propose the ASTRE mechanism as a means of actuating shape-changing interfaces primarily in the context. However, we believe that this mechanism has the potential for broader applications in fields such as soft robotics, deployable architecture, and biomedical engineering. For example, in the field of minimally invasive surgery (MIS), a fiber jamming mechanism has been proposed to enhance the stiffness of soft manipulators when motion stability is required[234]. Similarly, the ASTRE mechanism utilizes elongated shape actuators, and the PAMs used in their unactuated state exhibit high flexibility. The ASTRE mechanism also offers the advantage of utilizing compressed air to enable both shape deformation and stiffness tuning. However, it is worth noting that the current size of the ASTRE module is 6 mm in diameter, which may require further development to test its practicality in millimeter-sized robots. Nonetheless, with the current version, researchers can rapidly prototype conceptual models to understand the basic requirements for the eventual product.

8.3.4 Large-size Deployable

Deployability is indeed a unique property of the ASTRE mechanism that holds great potential for various applications. One such application is the creation of large-scale kinematic structures, similar to the previous work by Kovacs et.al. in

their studies [92, 93]. However, there are still several technological challenges that need to be addressed to further develop the ASTRE framework. For instance, ensuring that the modules do not become entangled when deployed from a compact state is crucial. Additionally, simulating truss structures that can bear significant weight and maintain stability at considerable heights poses another challenge. Addressing these challenges will require further research and development, but the potential benefits of deploying large-size kinematic structures using ASTRE make it an exciting area for exploration and innovation.

8.3.5 VR Application

Haptic feedback in VR is an actively researched area, and both the ClaytricSurface and ASTRE Toolkit have the potential to be employed as haptic controllers in VR systems. While there are still challenges related to mobility and untethered operation, previous works have explored the use of tethered pumps to adjust the weight of VR controllers using a liquid, as seen in the example of PumpVR [77].

Taking inspiration from such works, we envision using the shape-changing and variable-stiffness capabilities of ClaytricSurface and ASTRE Toolkit in VR devices. For instance, a glove controller could simulate various levels of stiffness, allowing users to experience sensations like ice melting spontaneously due to rapid changes in stiffness (see Figure 8.3a). Another example could be a shape-changing sword that behaves like a rope when colliding with an object, providing a realistic feeling of cutting through the object (see Figure 8.3b). Moreover, the adjustable stiffness feature can be leveraged to create handicap effects in Mixed Reality (MR) ping-pong, where the paddle's stiffness can be adjusted to create more challenging gameplay. These examples demonstrate the potential for using ClaytricSurface and ASTRE Toolkit to enhance haptic experiences in VR and MR applications.

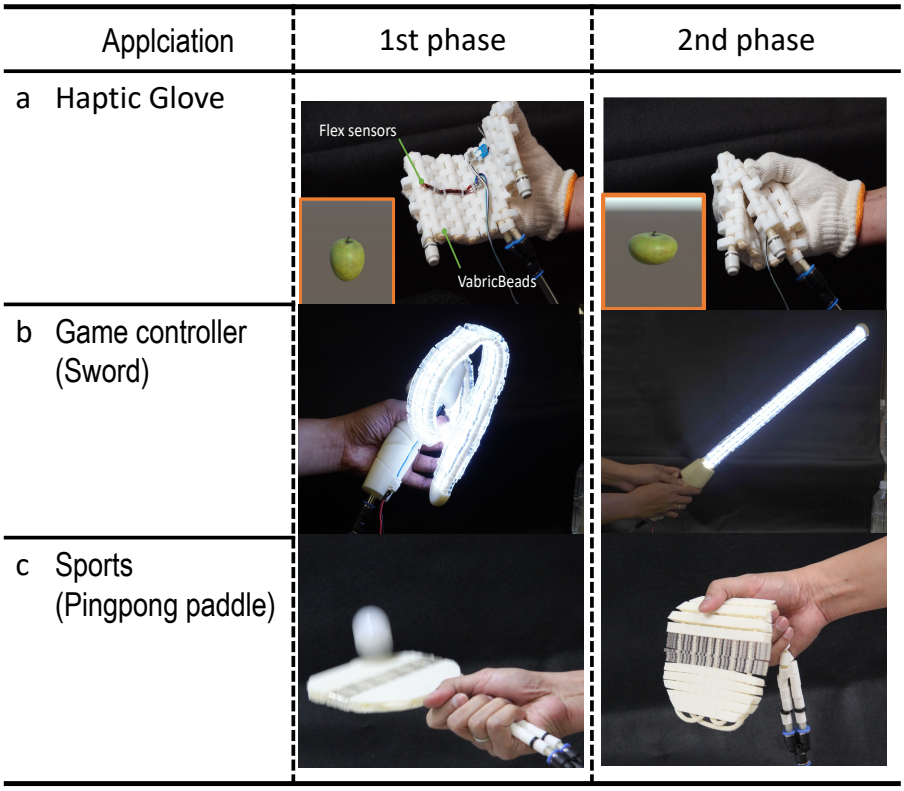

Figure 8.3: Future works: Haptic VR controller

Chapter 9

Conclusion

This thesis introduced a framework for prototyping shape-changing and variable-stiffness interfaces using pneumatic actuation.

Chapter One provides an introduction to the research, including an overview of the existing issues in shape-changing interfaces and the motivation behind developing prototyping tools for such interfaces.

Chapter Two reviews related works in shape-changing and variable-stiffness mechanisms, as well as existing prototyping tools for shape-changing interfaces. The positioning of the proposed research is also discussed in relation to previous works.

Chapter Three explains the common framework underlying the research, highlighting the benefits of pneumatic actuation and how it connects the ClaytricSurface and ASTRE mechanisms.

Chapter Four introduces the ClaytricSurface system, which focuses on exploring the use of variable-stiffness displays for 2.5D modeling. The basic mechanism of Vacuum Jamming is investigated, and its application in an interactive display with graphical input-output is demonstrated. Various use cases and features to support shape modeling and painting applications are showcased.

Chapter Five addresses the limitations of ClaytricSurface, particularly its active deformation capabilities, and presents the ASTRE mechanism as a solution. ASTRE is a programmable shape-changing and variable stiffness mechanical constraint for PAMs actuators. The characteristics of each module are examined, and the design space, fabrication workflow, and hardware control system are described.

Chapter Six introduces the ASTRE Toolkit, a prototyping tool that utilizes the ASTRE mechanism and employs a constructive assembly system. The chapter discusses a constructivist approach to shape-changing interfaces and presents design guidelines for deformation properties, haptic properties, and shape-tuning capabilities. The toolkit is demonstrated through various applications, including educational toys, deployable artifacts, and soft robots. The chapter also includes a technical evaluation of shape tuning.

Chapter Seven focuses on VabricBeads, a design exploration for shape-changing and variable-stiffness fabric. The application of the ASTRE mechanism in fabric structures is explored, resulting in the synthesis of 12 types of fabrics. The chapter presents three sensing techniques to enhance the fabric with interactive capabilities and showcases the usability of such fabrics in wearables and decorative applications.

Chapter Eight provides insights, findings, and discussions on the systems and applications described in Chapters Four, Five, Six, and Seven (ClaytricSurface, ASTRE mechanism, ASTRE Toolkit, and VabricBeads). The advantages and limitations of each system are summarized and analyzed. The chapter also discusses the overall findings and contributions of the research framework and presents potential future applications.

Bibliography

[1] *Design and Prototype of a Tunable Stiffness Arm for Safe Human-Robot Interaction*, volume Volume 5B: 40th Mechanisms and Robotics Conference of *International Design Engineering Technical Conferences and Computers and Information in Engineering Conference*, 08 2016.

[2] Ozgun Kilic Afsar, Ali Shtarbanov, Hila Mor, Ken Nakagaki, Jack Forman, Karen Modrei, Seung Hee Jeong, Klas Hjort, Kristina Höök, and Hiroshi Ishii. Omnifiber: Integrated fluidic fiber actuators for weaving movement based interactions into the 'fabric of everyday life'. pages 1010–1026. ACM, 10 2021.

[3] Buse Aktas, Yashraj Narang, Nick Vasios, Katia Bertoldi, and Robert Howe. A modeling framework for jamming structures. *Advanced Functional Materials*, 31:2007554, 04 2021.

[4] Lea Albaugh, Scott Hudson, and Lining Yao. Digital fabrication of soft actuated objects by machine knitting. In *Proceedings of the 2019 CHI Conference on Human Factors in Computing Systems*, CHI '19, page 1–13, New York, NY, USA, 2019. Association for Computing Machinery.

[5] Jason Alexander, Andrés Lucero, and Sriram Subramanian. Tilt displays: designing display surfaces with multi-axis tilting and actuation. In Elizabeth F. Churchill, Sriram Subramanian, Patrick Baudisch, and Kenton O'Hara, editors, *Mobile HCI*, pages 161–170. ACM, 2012.

[6] Jason Alexander, Anne Roudaut, Jürgen Steimle, Kasper Hornbæk, Miguel Bruns Alonso, Sean Follmer, and Timothy Merritt. Grand challenges in shape-changing interface research. In *Proceedings of the 2018 CHI Conference on*

Human Factors in Computing Systems, volume 2018-April of *CHI '18*, page 1–14, New York, NY, USA, 4 2018. Association for Computing Machinery.

[7] John R. Amend, Eric Brown, Nicholas Rodenberg, Heinrich M. Jaeger, and Hod Lipson. A positive pressure universal gripper based on the jamming of granular material. *IEEE Transactions on Robotics*, 28:341–350, 4 2012.

[8] Morteza Amjadi and Metin Sitti. High-performance multiresponsive paper actuators. *ACS Nano*, 10(11):10202–10210, 2016. PMID: 27744680.

[9] Jatin Arora, Kartik Mathur, Aryan Saini, and Aman Parnami. Gehna: Exploring the design space of jewelry as an input modality. In *Proceedings of the 2019 CHI Conference on Human Factors in Computing Systems*, CHI '19, page 1–12, New York, NY, USA, 2019. Association for Computing Machinery.

[10] Daniel M. Aukes, Barrett Heyneman, John Ulmen, Hannah Stuart, Mark R. Cutkosky, Susan Kim, Pablo Garcia, and Aaron Edsinger. Design and testing of a selectively compliant underactuated hand. *The International Journal of Robotics Research*, 33(5):721–735, February 2014.

[11] Hamzah M. Beakawi Al-Hashemi and Omar S. Baghabra Al-Amoudi. A review on the angle of repose of granular materials. *Powder Technology*, 330:397–417, 2018.

[12] J. Berzowska and M. Coelho. Kukkia and vilkas: kinetic electronic garments. In *Ninth IEEE International Symposium on Wearable Computers (ISWC'05)*, pages 82–85, 2005.

[13] Laura H. Blumenschein, Margaret M. Coad, David A. Haggerty, Allison M. Okamura, and Elliot W. Hawkes. Design, modeling, control, and application of everting vine robots. *Frontiers in Robotics and AI*, 7, November 2020.

[14] Joran W. Booth, Dylan Shah, Jennifer C. Case, Edward L. White, Michelle C. Yuen, Olivier Cyr-Choiniere, and Rebecca Kramer-Bottiglio. Omniskins:

Robotic skins that turn inanimate objects into multifunctional robots. *Science Robotics*, 3(22), September 2018.

[15] James Brett, Katrina Lo Surdo, Lauren Hanson, Joshua Pinskier, and David Howard. Jammkle: Fibre jamming 3d printed multi-material tendons and their application in a robotic ankle, 2021.

[16] Anke Brocker, Jakob Strüver, Simon Voelker, and Jan Borchers. Sorocad: A design tool for the building blocks of pneumatic soft robotics. In *Extended Abstracts of the 2022 CHI Conference on Human Factors in Computing Systems*, CHI EA '22, New York, NY, USA, 2022. Association for Computing Machinery.

[17] Eric Brown, Nicholas Rodenberg, John Amend, Annan Mozeika, Erik Steltz, Mitchell R. Zakin, Hod Lipson, and Heinrich M. Jaeger. Universal robotic gripper based on the jamming of granular material. *Proceedings of the National Academy of Sciences*, 107(44):18809–18814, 2010.

[18] Oğuz 'Oz' Buruk, Çağlar Genç, undefinedhsan Ozan Yıldırım, Mehmet Cengiz Onbaşlı, and Oğuzhan Özcan. Snowflakes: A prototyping tool for computational jewelry. In *Proceedings of the 2021 CHI Conference on Human Factors in Computing Systems*, CHI '21, New York, NY, USA, 2021. Association for Computing Machinery.

[19] Changyong Cao and Xuanhe Zhao. Tunable stiffness of electrorheological elastomers by designing mesostructures. *Applied Physics Letters*, 103(4):041901, July 2013.

[20] Federico Carpi, Gabriele Frediani, Carlo Gerboni, Jessica Gemignani, and Danilo De Rossi. Enabling variable-stiffness hand rehabilitation orthoses with dielectric elastomer transducers. *Medical Engineering and Physics*, 36(2):205–211, February 2013.

[21] Alvaro Cassinelli and Masatoshi Ishikawa. Khronos projector. In *ACM SIGGRAPH 2005 Emerging Technologies*, SIGGRAPH '05, page 10–es, New York, NY, USA, 2005. Association for Computing Machinery.

[22] Jose Francisco Martinez Castro, Alice Buso, Jun Wu, and Elvin Karana. Tex(alive): A toolkit to explore temporal expressions in shape-changing textile interfaces. pages 1162–1176. Association for Computing Machinery, Inc, 6 2022.

[23] Yu-Wen Chen, Wei-Ju Lin, Yi Chen, and Lung-Pan Cheng. Pneuseries: 3d shape forming with modularized serial-connected inflatables. In *The 34th Annual ACM Symposium on User Interface Software and Technology*, UIST '21, page 431–440, New York, NY, USA, 2021. Association for Computing Machinery.

[24] Thomas P. Chenal, Jennifer C. Case, Jamie Paik, and Rebecca K. Kramer. Variable stiffness fabrics with embedded shape memory materials for wearable applications. In *2014 IEEE/RSJ International Conference on Intelligent Robots and Systems*, pages 2827–2831, 2014.

[25] Bernard Cheng, Antonio Gomes, Paul Strohmeier, and Roel Vertegaal. Mood fern: Exploring shape transformations in reactive environments. In *Proceedings of the 11th Conference on Advances in Computer Entertainment Technology*, ACE '14, New York, NY, USA, 2014. Association for Computing Machinery.

[26] Nadia G. Cheng, Arvind Gopinath, Lifeng Wang, Karl Iagnemma, and Anette E. Hosoi. Thermally tunable, self-healing composites for soft robotic applications. *Macromolecular Materials and Engineering*, 299:1279–1284, 11 2014.

[27] Marcelo Coelho, Hiroshi Ishii, and Pattie Maes. Surflex: a programmable surface for the design of tangible interfaces. In Mary Czerwinski, Arnold M.

Lund, and Desney S. Tan, editors, *CHI Extended Abstracts*, pages 3429–3434. ACM, 2008.

[28] Stelian Coros, Bernhard Thomaszewski, Gioacchino Noris, Shinjiro Sueda, Moira Forberg, Robert W. Sumner, Wojciech Matusik, and Bernd Bickel. Computational design of mechanical characters. *ACM Trans. Graph.*, 32(4), jul 2013.

[29] Autodesk Corporation. Fusion360. `https://www.autodesk.com/`. Accessed: 2020-09-3.

[30] Haitao Cui, Shida Miao, Timothy Esworthy, Se jun Lee, Xuan Zhou, Sung Yun Hann, Thomas J. Webster, Brent T. Harris, and Lijie Grace Zhang. A novel near-infrared light responsive 4d printed nanoarchitecture with dynamically and remotely controllable transformation. *Nano Research*, 12(6):1381–1388, May 2019.

[31] Alexandru Dancu, Catherine Hedler, Stig Anton Nielsen, Hanna Frank, Zhu Kening, Axel Pelling, Adviye Ayça Ünlüer, Christian Carlsson, Max Witt, and Morten Fjeld. Emergent interfaces: Constructive assembly of identical units. In *Proceedings of the 33rd Annual ACM Conference Extended Abstracts on Human Factors in Computing Systems*, CHI EA '15, page 451–460, New York, NY, USA, 2015. Association for Computing Machinery.

[32] A. Degani, H. Choset, A. Wolf, and M.A. Zenati. Highly articulated robotic probe for minimally invasive surgery. In *Proceedings IEEE International Conference on Robotics and Automation. ICRA 2006.*, pages 4167–4172, 2006.

[33] Alexandra Delazio, Ken Nakagaki, Roberta L. Klatzky, Scott E. Hudson, Jill Fain Lehman, and Alanson P. Sample. Force jacket: Pneumatically-actuated jacket for embodied haptic experiences. In *Proceedings of the 2018 CHI Conference on Human Factors in Computing Systems*, CHI '18, page 1–12, New York, NY, USA, 2018. Association for Computing Machinery.

[34] Himani Deshpande, Haruki Takahashi, and Jeeeun Kim. Escapeloom: Fabricating new affordances for hand weaving. In *Proceedings of the 2021 CHI Conference on Human Factors in Computing Systems*, CHI '21, New York, NY, USA, 2021. Association for Computing Machinery.

[35] Stuart B Diller, Steven H Collins, and Carmel Majidi. The effects of electroadhesive clutch design parameters on performance characteristics. *Journal of Intelligent Material Systems and Structures*, 29(19):3804–3828, 2018.

[36] Julia C. Duvall, Lucy E. Dunne, Nicholas Schleif, and Brad Holschuh. Active "hugging" vest for deep touch pressure therapy. In *Proceedings of the 2016 ACM International Joint Conference on Pervasive and Ubiquitous Computing: Adjunct*, UbiComp '16, page 458–463, New York, NY, USA, 2016. Association for Computing Machinery.

[37] Soya Eguchi, Claire Okabe, Mai Ohira, and Hiroya Tanaka. Pneumatic auxetics: Inverse design and 3d printing of auxetic pattern for pneumatic morphing. In *Extended Abstracts of the 2022 CHI Conference on Human Factors in Computing Systems*, CHI EA '22, New York, NY, USA, 4 2022. Association for Computing Machinery.

[38] Shreyosi Endow, Hedieh Moradi, Anvay Srivastava, Esau G Noya, and Cesar Torres. Compressables: A haptic prototyping toolkit for wearable compression-based interfaces. In *Designing Interactive Systems Conference 2021*, DIS '21, page 1101–1114, New York, NY, USA, 2021. Association for Computing Machinery.

[39] Aluna Everitt and Jason Alexander. Polysurface: A design approach for rapid prototyping of shape-changing displays using semi-solid surfaces. In *Proceedings of the 2017 Conference on Designing Interactive Systems*, DIS '17, page 1283–1294, New York, NY, USA, 6 2017. Association for Computing Machinery.

[40] Mohammad Fatahillah, Namsoo Oh, and Hugo Rodrigue. A novel soft bending actuator using combined positive and negative pressures. *Frontiers in Bioengineering and Biotechnology*, 8, May 2020.

[41] Yuan-Ling Feng, Charith Lasantha Fernando, Jan Rod, and Kouta Minamizawa. Submerged haptics: A 3-dof fingertip haptic display using miniature 3d printed airbags. In *ACM SIGGRAPH 2017 Posters*, SIGGRAPH '17, New York, NY, USA, 2017. Association for Computing Machinery.

[42] Sean Follmer, Daniel Leithinger, Alex Olwal, Nadia Cheng, and Hiroshi Ishii. Jamming user interfaces: Programmable particle stiffness and sensing for malleable and shape-changing devices. In *Proceedings of the 25th Annual ACM Symposium on User Interface Software and Technology*, UIST '12, page 519–528, New York, NY, USA, 2012. Association for Computing Machinery.

[43] Sean Follmer, Daniel Leithinger, Alex Olwal, Akimitsu Hogge, and Hiroshi Ishii. Inform: Dynamic physical affordances and constraints through shape and object actuation. In *Proceedings of the 26th Annual ACM Symposium on User Interface Software and Technology*, UIST '13, page 417–426, New York, NY, USA, 2013. Association for Computing Machinery.

[44] Jutta Fortmann, Heiko Müller, Susanne Boll, and Wilko Heuten. Illumee: Aesthetic light bracelet as a wearable information display for everyday life. In *Proceedings of the 2013 ACM Conference on Pervasive and Ubiquitous Computing Adjunct Publication*, UbiComp '13 Adjunct, page 393–396, New York, NY, USA, 2013. Association for Computing Machinery.

[45] Karmen Franinović and Luke Franzke. Shape changing surfaces and structures: Design tools and methods for electroactive polymers. In *Proceedings of the 2019 CHI Conference on Human Factors in Computing Systems*, CHI '19, page 1–12, New York, NY, USA, 2019. Association for Computing Machinery.

[46] Mikhaila Friske, Shanel Wu, and Laura Devendorf. Adacad: Crafting software for smart textiles design. In *Proceedings of the 2019 CHI Conference on Human Factors in Computing Systems*, CHI '19, page 1–13, New York, NY, USA, 2019. Association for Computing Machinery.

[47] Yuki Funabora. Flexible fabric actuator realizing 3d movements like human body surface for wearable devices. In *2018 IEEE/RSJ International Conference on Intelligent Robots and Systems (IROS)*, pages 6992–6997, 2018.

[48] Yuki Funabora. Prototype of a fabric actuator with multiple thin artificial muscles for wearable assistive devices. *SII 2017 - 2017 IEEE/SICE International Symposium on System Integration*, 2018-January:356–361, 2 2018.

[49] Farhan Gandhi and Sang-Guk Kang. Beams with controllable flexural stiffness. *Smart Materials and Structures*, 16(4):1179–1184, June 2007.

[50] Qi Ge, Amir Hosein Sakhaei, Howon Lee, Conner K. Dunn, Nicholas X. Fang, and Martin L. Dunn. Multimaterial 4d printing with tailorable shape memory polymers. *Scientific Reports*, 6(1), August 2016.

[51] Kristian Gohlke and Eva Hornecker. A stretch-flexible textile multitouch sensor for user input on inflatable membrane structures and non-planar surfaces. In *Adjunct Proceedings of the 31st Annual ACM Symposium on User Interface Software and Technology*, UIST '18 Adjunct, page 191–193, New York, NY, USA, 2018. Association for Computing Machinery.

[52] Matthew G. Gorbet, Maggie Orth, and Hiroshi Ishii. Triangles: Tangible interface for manipulation and exploration of digital information topography. In *Proceedings of the SIGCHI Conference on Human Factors in Computing Systems*, CHI '98, page 49–56, USA, 1998. ACM Press/Addison-Wesley Publishing Co.

[53] Mark Goulthorpe, Mark C. Burry, and Grant Dunlop. Aegis hyposurface©: The bordering of university and practice. 2001.

[54] LEGO Group. Lego mindstorms. `http://www.lego.com/`. Accessed: 2020-09-3.

[55] Jianzhe Gu, Yuyu Lin, Qiang Cui, Xiaoqian Li, Jiaji Li, Lingyun Sun, Fangtian Ying, Guanyun Wang, and Lining Yao. Pneumesh: Pneumatic-driven truss-based shape changing system; pneumesh: Pneumatic-driven truss-based shape changing system. 2022.

[56] Carter S. Haines, Na Li, Geoffrey M. Spinks, Ali E. Aliev, Jiangtao Di, and Ray H. Baughman. New twist on artificial muscles. *Proceedings of the National Academy of Sciences*, 113(42):11709–11716, 2016.

[57] Nur Al-huda Hamdan, Adrian Wagner, Simon Voelker, Jürgen Steimle, and Jan Borchers. Springlets: Expressive, flexible and silent on-skin tactile interfaces. In *Proceedings of the 2019 CHI Conference on Human Factors in Computing Systems*, CHI '19, page 1–14, New York, NY, USA, 2019. Association for Computing Machinery.

[58] Teng Han, Shubhi Bansal, Xiaochen Shi, Yanjun Chen, Baogang Quan, Feng Tian, Hongan Wang, and Sriram Subramanian. Hapbead: On-skin microfluidic haptic interface using tunable bead. In *Proceedings of the 2020 CHI Conference on Human Factors in Computing Systems*, CHI '20, page 1–10, New York, NY, USA, 2020. Association for Computing Machinery.

[59] John Hardy, Christian Weichel, Faisal Taher, John Vidler, and Jason Alexander. Shapeclip: Towards rapid prototyping with shape-changing displays for designers. In *Proceedings of the 33rd Annual ACM Conference on Human Factors in Computing Systems*, CHI '15, page 19–28, New York, NY, USA, 2015. Association for Computing Machinery.

[60] Liang He, Huaishu Peng, Michelle Lin, Ravikanth Konjeti, François Guimbretière, and Jon E. Froehlich. Ondulé: Designing and controlling 3d printable springs. In *Proceedings of the 32nd Annual ACM Symposium on User Interface Software and Technology*, UIST '19, page 739–750, New York, NY, USA, 10 2019. Association for Computing Machinery.

[61] Takayuki Hirai, Satoshi Nakamaru, Yoshihiro Kawahara, and Yasuaki Kakehi. Xslate: A stiffness-controlled surface for shape-changing interfaces. In *Extended Abstracts of the 2018 CHI Conference on Human Factors in Computing Systems*, CHI EA '18, page 1–4, New York, NY, USA, 2018. Association for Computing Machinery.

[62] Tatsuhiro Hiramitsu, Koichi Suzumori, Hiroyuki Nabae, and Gen Endo. *Experimental Evaluation of Textile Mechanisms Made of Artificial Muscles.* 2019.

[63] Tatsuhiro Hiramitsu, Koichi Suzumori, Hiroyuki Nabae, and Gen Endo. Experimental evaluation of textile mechanisms made of artificial muscles. In *2019 2nd IEEE International Conference on Soft Robotics (RoboSoft)*, pages 1–6, 2019.

[64] Jana Hoffard, Shio Miyafuji, Jefferson Pardomuan, Toshiki Sato, and Hideki Koike. OmniTiles - A User-Customizable Display Using An Omni-Directional Camera Projector System. In Hideaki Uchiyama and Jean-Marie Normand, editors, *ICAT-EGVE 2022 - International Conference on Artificial Reality and Telexistence and Eurographics Symposium on Virtual Environments*. The Eurographics Association, 2022.

[65] David Holman and Roel Vertegaal. Organic user interfaces: Designing computers in any way, shape, or form. *Commun. ACM*, 51(6):48–55, jun 2008.

[66] Yijiang Huang, Juyong Zhang, Xin Hu, Guoxian Song, Zhongyuan Liu, Lei

Yu, and Ligang Liu. Framefab: Robotic fabrication of frame shapes. *ACM Trans. Graph.*, 35(6), dec 2016.

[67] Takeo Igarashi, Satoshi Matsuoka, and Hidehiko Tanaka. Teddy: A sketching interface for 3d freeform design. In *ACM SIGGRAPH 2006 Courses*, SIGGRAPH '06, page 11–es, New York, NY, USA, 2006. Association for Computing Machinery.

[68] Alexandra Ion, Johannes Frohnhofen, Ludwig Wall, Robert Kovacs, Mirela Alistar, Jack Lindsay, Pedro Lopes, Hsiang-Ting Chen, and Patrick Baudisch. Metamaterial mechanisms. In *Proceedings of the 29th Annual Symposium on User Interface Software and Technology*, UIST '16, page 529–539, New York, NY, USA, 2016. Association for Computing Machinery.

[69] H Ishii, C Ratti, B Piper, Y Wang, A Biderman, and E Ben-Joseph. Bringing clay and sand into digital design — continuous tangible user interfaces. *BT Technology Journal*, 22(4):287–299, October 2004.

[70] Hiroshi Ishii and Brygg Ullmer. Tangible bits: Towards seamless interfaces between people, bits and atoms. In Steven Pemberton, editor, *CHI*, pages 234–241. ACM/Addison-Wesley, 1997.

[71] Hiroo Iwata, Hiroaki Yano, Fumitaka Nakaizumi, and Ryo Kawamura. Project feelex: adding haptic surface to graphics. In Lynn Pocock, editor, *SIGGRAPH*, pages 469–476. ACM, 2001.

[72] S. Jain, T. Stalin, V. Subramaniam, J. Agarwal, and P. Valdivia y Alvarado. pages 6928–6934, 2020.

[73] Yvonne Jansen, Thorsten Karrer, and Jan Borchers. Mudpad: Localized tactile feedback on touch surfaces. In *Adjunct Proceedings of the 23nd Annual ACM Symposium on User Interface Software and Technology*, UIST '10, page 385–386, New York, NY, USA, 2010. Association for Computing Machinery.

[74] Yongkang Jiang, Diansheng Chen, Che Liu, and Jian Li. Chain-like granular jamming: A novel stiffness-programmable mechanism for soft robotics. *Soft Robotics*, 6(1):118–132, February 2019.

[75] Jeyeon Jo, Doyeon Kong, and Huiju Park. Bling: Beads-laden interactive garment. In *Proceedings of the 2021 ACM International Symposium on Wearable Computers*, ISWC '21, page 189–193, New York, NY, USA, 2021. Association for Computing Machinery.

[76] Hiroki Kaimoto, Junichi Yamaoka, Satoshi Nakamaru, Yoshihiro Kawahara, and Yasuaki Kakehi. Expandfab: Fabricating objects expanding and changing shape with heat. In *Proceedings of the Fourteenth International Conference on Tangible, Embedded, and Embodied Interaction*, TEI '20, page 153–164, New York, NY, USA, 2020. Association for Computing Machinery.

[77] Alexander Kalus, Martin Kocur, Johannes Klein, Manuel Mayer, and Niels Henze. Pumpvr: Rendering the weight of objects and avatars through liquid mass transfer in virtual reality. In *Proceedings of the 2023 CHI Conference on Human Factors in Computing Systems*, CHI '23, New York, NY, USA, 2023. Association for Computing Machinery.

[78] Hsin-Liu (Cindy) Kao, Miren Bamforth, David Kim, and Chris Schmandt. Skinmorph: Texture-tunable on-skin interface through thin, programmable gel. In *Proceedings of the 2018 ACM International Symposium on Wearable Computers*, ISWC '18, page 196–203, New York, NY, USA, 2018. Association for Computing Machinery.

[79] Shohei Katakura and Keita Watanabe. Protohole: Prototyping interactive 3d printed objects using holes and acoustic sensing. In *Extended Abstracts of the 2018 CHI Conference on Human Factors in Computing Systems*, CHI EA '18, page 1–6, New York, NY, USA, 2018. Association for Computing Machinery.

[80] Yuichiro Katsumoto, Satoru Tokuhisa, and Masa Inakage. Ninja track: Design of electronic toy variable in shape and flexibility. In *Proceedings of the 7th International Conference on Tangible, Embedded and Embodied Interaction*, TEI '13, page 17–24, New York, NY, USA, 2013. Association for Computing Machinery.

[81] Sajeewa D. Katugampala, Kasun M. S. Arachchi, Suresh Asanka, Rancimal B. Arumathanthri, Asitha L. Kulasekera, and Nirosh D. Jayaweera. Design and characterization of a novel vacuum bending actuator and a bimorph: for preliminary use in a continuum robot arm. In *2019 IEEE International Conference on Cybernetics and Intelligent Systems (CIS) and IEEE Conference on Robotics, Automation and Mechatronics (RAM)*, pages 263–268, 2019.

[82] Yoshihiro Kawahara, Steve Hodges, Benjamin S. Cook, Cheng Zhang, and Gregory D. Abowd. Instant inkjet circuits: Lab-based inkjet printing to support rapid prototyping of ubicomp devices. In *Proceedings of the 2013 ACM International Joint Conference on Pervasive and Ubiquitous Computing*, UbiComp '13, page 363–372, New York, NY, USA, 2013. Association for Computing Machinery.

[83] Mohammadreza Khalilbeigi, Roman Lissermann, Wolfgang Kleine, and Jürgen Steimle. Foldme: Interacting with double-sided foldable displays. In *Proceedings of the Sixth International Conference on Tangible, Embedded and Embodied Interaction*, TEI '12, page 33–40, New York, NY, USA, 2012. Association for Computing Machinery.

[84] Hyunyoung Kim, Aluna Everitt, Carlos Tejada, Mengyu Zhong, and Daniel Ashbrook. Morpheesplug: A toolkit for prototyping shape-changing interfaces. pages 1–13. ACM, 5 2021.

[85] Jin Hee (Heather) Kim, Kunpeng Huang, Simone White, Melissa Conroy, and Cindy Hsin-Liu Kao. Knitdermis: Fabricating tactile on-body interfaces

through machine knitting. In *Designing Interactive Systems Conference 2021*, DIS '21, page 1183–1200, New York, NY, USA, 2021. Association for Computing Machinery.

[86] Jin Hee (Heather) Kim, Shreyas Dilip Patil, Sarina Matson, Melissa Conroy, and Cindy Hsin-Liu Kao. Knitskin: Machine-knitted scaled skin for locomotion. In *Proceedings of the 2022 CHI Conference on Human Factors in Computing Systems*, CHI '22, New York, NY, USA, 2022. Association for Computing Machinery.

[87] Seoktae Kim, Hyunjung Kim, Boram Lee, Tek-Jin Nam, and Woohun Lee. Inflatable mouse. In *Proceedings of the SIGCHI Conference on Human Factors in Computing Systems*. ACM, April 2008.

[88] Yong-Jae Kim, Shanbao Cheng, Sangbae Kim, and Karl Iagnemma. Design of a tubular snake-like manipulator with stiffening capability by layer jamming. *2012 IEEE/RSJ International Conference on Intelligent Robots and Systems*, pages 4251–4256, 10 2012.

[89] Marius Kintel. Openscad. `https://openscad.org/`. Accessed: 2020-09-3.

[90] Donghyeon Ko, Yoonji Kim, Junyi Zhu, Michael Wessely, and Stefanie Mueller. Flexboard: A flexible breadboard for interaction prototyping on curved and deformable surfaces. In *Proceedings of the 2023 CHI Conference on Human Factors in Computing Systems*, CHI '23, New York, NY, USA, 2023. Association for Computing Machinery.

[91] Christopher Kopic and Kristian Gohlke. Inflatibits: A modular soft robotic construction kit for children. In *Proceedings of the TEI '16: Tenth International Conference on Tangible, Embedded, and Embodied Interaction*, TEI '16, page 723–728, New York, NY, USA, 2016. Association for Computing Machinery.

[92] Robert Kovacs, Alexandra Ion, Pedro Lopes, Tim Oesterreich, Johannes Filter, Philipp Otto, Tobias Arndt, Nico Ring, Melvin Witte, Anton Synytsia, and Patrick Baudisch. Trussformer: 3d printing large kinetic structures. In *Extended Abstracts of the 2019 CHI Conference on Human Factors in Computing Systems*, CHI EA '19, page 1, New York, NY, USA, 2019. Association for Computing Machinery.

[93] Robert Kovacs, Lukas Rambold, Lukas Fritzsche, Dominik Meier, Jotaro Shigeyama, Shohei Katakura, Ran Zhang, and Patrick Baudisch. Trusscillator: A system for fabricating human-scale human-powered oscillating devices. In *The 34th Annual ACM Symposium on User Interface Software and Technology*, UIST '21, page 1074–1088, New York, NY, USA, 10 2021. Association for Computing Machinery.

[94] Pin-Sung Ku, Kunpeng Huang, and Cindy Hsin-Liu Kao. Patch-o: Deformable woven patches for on-body actuation. In *Proceedings of the 2022 CHI Conference on Human Factors in Computing Systems*, CHI '22, New York, NY, USA, 2022. Association for Computing Machinery.

[95] Shunichi Kurumaya, Hiroyuki Nabae, Gen Endo, and Koichi Suzumori. Design of thin mckibben muscle and multifilament structure. *Sensors and Actuators, A: Physical*, 261:66–74, 7 2017.

[96] Mannu Lambrichts, Jose Maria Tijerina, and Raf Ramakers. Softmod: A soft modular plug-and-play kit for prototyping electronic systems. In *Proceedings of the Fourteenth International Conference on Tangible, Embedded, and Embodied Interaction*, TEI '20, page 287–298, New York, NY, USA, 2020. Association for Computing Machinery.

[97] Gierad Laput, Eric Brockmeyer, Scott E. Hudson, and Chris Harrison. Acoustruments: Passive, acoustically-driven, interactive controls for handheld devices. In *Proceedings of the 33rd Annual ACM Conference on Human Factors*

in Computing Systems, CHI '15, page 2161–2170, New York, NY, USA, 2015. Association for Computing Machinery.

[98] Jun-Young Lee, Jaemin Eom, Woo-Young Choi, and Kyu-Jin Cho. Soft lego: Bottom-up design platform for soft robotics. In *2018 IEEE/RSJ International Conference on Intelligent Robots and Systems (IROS)*, pages 7513–7520, 2018.

[99] Joanne Leong, Florian Perteneder, Hans-Christian Jetter, and Michael Haller. What a life! building a framework for constructive assemblies. In *Proceedings of the Eleventh International Conference on Tangible, Embedded, and Embodied Interaction*, TEI '17, page 57–66, New York, NY, USA, 2017. Association for Computing Machinery.

[100] Jiaji Li, Mingming Li, Junzhe Ji, Deying Pan, Yitao Fan, Kuangqi Zhu, Yue Yang, Zihan Yan, Lingyun Sun, Ye Tao, and Guanyun Wang. All-in-one print: Designing and 3d printing dynamic objects using kinematic mechanism without assembly. In *Proceedings of the 2023 CHI Conference on Human Factors in Computing Systems*, CHI '23, New York, NY, USA, 2023. Association for Computing Machinery.

[101] Nianlong Li, Han-Jong Kim, LuYao Shen, Feng Tian, Teng Han, Xing-Dong Yang, and Tek-Jin Nam. Haplinkage: Prototyping haptic proxies for virtual hand tools using linkage mechanism. In *Proceedings of the 33rd Annual ACM Symposium on User Interface Software and Technology*, UIST '20, page 1261–1274, New York, NY, USA, 2020. Association for Computing Machinery.

[102] Rong-Hao Liang, Liwei Chan, Hung-Yu Tseng, Han-Chih Kuo, Da-Yuan Huang, De-Nian Yang, and Bing-Yu Chen. Gaussbricks: Magnetic building blocks for constructive tangible interactions on portable displays. In *CHI '14 Extended Abstracts on Human Factors in Computing Systems*, CHI EA '14, page 181–182, New York, NY, USA, 2014. Association for Computing Machinery.

[103] Jason Lin, Jasmine Zhou, and Helen Koo. Enfold: Clothing for people with cerebral palsy. In *Adjunct Proceedings of the 2015 ACM International Joint Conference on Pervasive and Ubiquitous Computing and Proceedings of the 2015 ACM International Symposium on Wearable Computers*, UbiComp/ISWC'15 Adjunct, page 563–566, New York, NY, USA, 2015. Association for Computing Machinery.

[104] David Lindlbauer, Jens Emil Grønbæk, Morten Birk, Kim Halskov, Marc Alexa, and Jörg Müller. Combining shape-changing interfaces and spatial augmented reality enables extended object appearance. In *Proceedings of the 2016 CHI Conference on Human Factors in Computing Systems*, CHI '16, page 791–802, New York, NY, USA, 5 2016. Association for Computing Machinery.

[105] Andrea J. Liu and Sidney R. Nagel. Jamming is not just cool any more. *Nature*, 396(6706):21–22, November 1998.

[106] Arjo J. Loeve, Oscar S. van de Ven, Johan G. Vogel, Paul Breedveld, and Jenny Dankelman. Vacuum packed particles as flexible endoscope guides with controllable rigidity. *Granular Matter*, 12(6):543–554, June 2010.

[107] Qiuyu Lu, Jifei Ou, João Wilbert, André Haben, Haipeng Mi, and Hiroshi Ishii. Millimorph – fluid-driven thin film shape-change materials for interaction design. In *Proceedings of the 32nd Annual ACM Symposium on User Interface Software and Technology*, UIST '19, page 663–672, New York, NY, USA, 2019. Association for Computing Machinery.

[108] Qiuyu Lu, Haiqing Xu, Yijie Guo, Joey Yu Wang, and Lining Yao. Fluidic computation kit: Towards electronic-free shape-changing interfaces. In *Proceedings of the 2023 CHI Conference on Human Factors in Computing Systems*, CHI '23, New York, NY, USA, 2023. Association for Computing Machinery.

[109] Caroline Lundqvist, Daniel Klinkhammer, Kim Halskov, Stefan Paul Feyer, Jeanette Falk Olesen, Nanna Inie, Harald Reiterer, and Peter Dalsgaard. Physical, digital, and hybrid setups supporting card-based collaborative design ideation. In *Proceedings of the 10th Nordic Conference on Human-Computer Interaction*, NordiCHI '18, page 260–272, New York, NY, USA, 2018. Association for Computing Machinery.

[110] Danli Luo, Aditi Maheshwari, Andreea Danielescu, Jiaji Li, Yue Yang, Ye Tao, Lingyun Sun, Dinesh K. Patel, Guanyun Wang, Shu Yang, Teng Zhang, and Lining Yao. Autonomous self-burying seed carriers for aerial seeding. *Nature*, 614(7948):463–470, February 2023.

[111] Meng Luo, Lei Liu, Chen Liu, Bo Li, Chongjing Cao, Xing Gao, and Dichen Li. A single-chamber pneumatic soft bending actuator with increased stroke-range by local electric guidance. *IEEE Transactions on Industrial Electronics*, 68(9):8455–8463, 2021.

[112] Yiyue Luo, Kui Wu, Andrew Spielberg, Michael Foshey, Daniela Rus, Tomás Palacios, and Wojciech Matusik. Digital fabrication of pneumatic actuators with integrated sensing by machine knitting. In *Proceedings of the 2022 CHI Conference on Human Factors in Computing Systems*, CHI '22, New York, NY, USA, 2022. Association for Computing Machinery.

[113] Robert MacCurdy, Robert Katzschmann, Youbin Kim, and Daniela Rus. Printable hydraulics: A method for fabricating robots by 3d co-printing solids and liquids. In *2016 IEEE International Conference on Robotics and Automation (ICRA)*, page 3878–3885. IEEE Press, 2016.

[114] Carmel Majidi and Robert J. Wood. Tunable elastic stiffness with micro-confined magnetorheological domains at low magnetic field. *Applied Physics Letters*, 97(16):164104, October 2010.

[115] Guirec Maloisel, Espen Knoop, Christian Schumacher, and Moritz Bächer. Automated routing of muscle fibers for soft robots.

[116] Mariangela Manti, Vito Cacucciolo, and Matteo Cianchetti. Stiffening in soft robotics: A review of the state of the art. *IEEE Robotics and Automation Magazine*, 23:93–106, 9 2016.

[117] Yoichi Masuda, Kazuhiro Miyashita, Kaisei Yamagishi, Masato Ishikawa, and Koh Hosoda. Brainless running: A quasi-quadruped robot with decentralized spinal reflexes by solely mechanical devices. In *2020 IEEE/RSJ International Conference on Intelligent Robots and Systems (IROS)*, pages 4020–4025, 2020.

[118] Yasushi Matoba, Toshiki Sato, Nobuhiro Takahashi, and Hideki Koike. Claytricsurface: An interactive surface with dynamic softness control capability. In *ACM SIGGRAPH 2012 Emerging Technologies*, SIGGRAPH '12, New York, NY, USA, 2012. Association for Computing Machinery.

[119] Mikihito Matsuura, Koya Narumi, Toshiki Aoki, Yuta Noma, Kazutaka Nakashima, Yoshihiro Kawahara, and Takeo Igarashi. Blow-up print: Rapidly 3d printing inflatable objects in the compressed state. In *ACM SIGGRAPH 2022 Posters*, SIGGRAPH '22, New York, NY, USA, 2022. Association for Computing Machinery.

[120] Andrea Mazzone, Christian Spagno, and Andreas Kunz. The hovermesh: A deformable structure based on vacuum cells: New advances in the research of tangible user interfaces. In *Proceedings of the 2004 ACM SIGCHI International Conference on Advances in Computer Entertainment Technology*, ACE '04, page 187–193, New York, NY, USA, 2004. Association for Computing Machinery.

[121] Seyed M. Mirvakili and Ian W. Hunter. Artificial muscles: Mechanisms, applications, and challenges. *Advanced Materials*, 30:1704407, 2 2018.

[122] T. Mitsuda, S. Kuge, M. Wakabayashi, and S. Kawamura. Wearable haptic display by the use of a particle mechanical constraint. In *Proceedings 10th Symposium on Haptic Interfaces for Virtual Environment and Teleoperator Systems. HAPTICS 2002*, pages 153–158, 2002.

[123] Kaori Mizushima, Takumi Oku, Yosuke Suzuki, Tokuo Tsuji, and Tetsuyou Watanabe. Multi-fingered robotic hand based on hybrid mechanism of tendon-driven and jamming transition. In *2018 IEEE International Conference on Soft Robotics (RoboSoft)*, pages 376–381, 2018.

[124] Takafumi Morita, Ziyuan Jiang, Kanon Aoyama, Ayato Minaminosono, Yu Kuwajima, Naoki Hosoya, Shingo Maeda, and Yasuaki Kakehi. Demonstrating inflatablemod: Untethered and reconfigurable inflatable modules for tabletop-sized pneumatic physical interfaces. In *Extended Abstracts of the 2023 CHI Conference on Human Factors in Computing Systems*, CHI EA '23, New York, NY, USA, 2023. Association for Computing Machinery.

[125] Stefanie Mueller, Sangha Im, Serafima Gurevich, Alexander Teibrich, Lisa Pfisterer, François Guimbretière, and Patrick Baudisch. Wireprint: 3d printed previews for fast prototyping. In *Proceedings of the 27th Annual ACM Symposium on User Interface Software and Technology*, UIST '14, page 273–280, New York, NY, USA, 10 2014. Association for Computing Machinery.

[126] Stefanie Mueller, Tobias Mohr, Kerstin Guenther, Johannes Frohnhofen, and Patrick Baudisch. Fabrickation: Fast 3d printing of functional objects by integrating construction kit building blocks. In *CHI '14 Extended Abstracts on Human Factors in Computing Systems*, CHI EA '14, page 187–188, New York, NY, USA, 2014. Association for Computing Machinery.

[127] Stefanie Mueller, Anna Seufert, Huaishu Peng, Robert Kovacs, Kevin Reuss, François Guimbretière, and Patrick Baudisch. Formfab: Continuous interactive fabrication. In *Proceedings of the Thirteenth International Conference on*

Tangible, Embedded, and Embodied Interaction, TEI '19, page 315–323, New York, NY, USA, 2019. Association for Computing Machinery.

[128] Rio Mukaide, Masahiro Watanabe, Kenjiro Tadakuma, Yu Ozawa, Tomoya Takahashi, Masashi Konyo, and Satoshi Tadokoro. Radial-layer jamming mechanism for string configuration. *IEEE Robotics and Automation Letters*, 5:5221–5228, 10 2020.

[129] Sachith Muthukumarana and Moritz A. Messerschmidt. Clothtiles: A prototyping platform to fabricate customized actuators on clothing using 3d printing and shape-memory alloys. Association for Computing Machinery, 5 2021.

[130] Sara Nabil, Jan Kučera, Nikoletta Karastathi, David S. Kirk, and Peter Wright. Seamless seams: Crafting techniques for embedding fabrics with interactive actuation. In *Proceedings of the 2019 on Designing Interactive Systems Conference*, DIS '19, page 987–999, New York, NY, USA, 2019. Association for Computing Machinery.

[131] Ken Nakagaki, Sean Follmer, and Hiroshi Ishii. Lineform: Actuated curve interfaces for display, interaction, and constraint. In Celine Latulipe, Bjoern Hartmann, and Tovi Grossman, editors, *UIST*, pages 333–339. ACM, 2015.

[132] Ken Nakagaki, Luke Vink, Jared Counts, Daniel Windham, Daniel Leithinger, Sean Follmer, and Hiroshi Ishii. Materiable: Rendering dynamic material properties in response to direct physical touch with shape changing interfaces. *Proceedings of the 2016 CHI Conference on Human Factors in Computing Systems*, 2016.

[133] Yutaka Nakanishi and Akihiro Matsuura. An interactive haptic display system with changeable hardness using magneto-rheological fluid. In *Proceedings of the 28th ACM Symposium on Virtual Reality Software and Technology*, VRST '22, New York, NY, USA, 2022. Association for Computing Machinery.

[134] Ryosuke Nakayama, Ryo Suzuki, Satoshi Nakamaru, Ryuma Niiyama, Yoshihiro Kawahara, and Yasuaki Kakehi. Morphio: Entirely soft sensing and actuation modules for programming shape changes through tangible interaction. pages 975–986. Association for Computing Machinery, Inc, 6 2019.

[135] Ryuma Niiyama, Hiroki Sato, Kazzmasa Tsujimura, Koya Narumi, Young ah Seong, Ryosuke Yamamura, Yasuaki Kakehi, and Yoshihiro Kawahara. Poimo: Portable and inflatable mobility devices customizable for personal physical characteristics. In *Proceedings of the 33rd Annual ACM Symposium on User Interface Software and Technology*, UIST '20, page 912–923, New York, NY, USA, 2020. Association for Computing Machinery.

[136] Ryuma Niiyama, Xu Sun, Lining Yao, Hiroshi Ishii, Daniela Rus, and Sangbae Kim. Sticky actuator: Free-form planar actuators for animated objects. In *Proceedings of the Ninth International Conference on Tangible, Embedded, and Embodied Interaction*, TEI '15, page 77–84, New York, NY, USA, 2015. Association for Computing Machinery.

[137] Jun Ogawa, Tomoharu Mori, Yosuke Watanabe, Masaru Kawakami, MD Nahin Islam Shiblee, and Hidemitsu Furukawa. Mori-a: Soft vacuum-actuated module with 3d-printable deformation structure. *IEEE Robotics and Automation Letters*, 7:2495–2502, 4 2022.

[138] Luke Olsen, Faramarz F. Samavati, Mario Costa Sousa, and Joaquim A. Jorge. Sketch-based modeling: A survey. *Computers and Graphics*, 33(1):85–103, 2009.

[139] Cagdas D. Onal and Daniela Rus. A modular approach to soft robots. In *2012 4th IEEE RAS EMBS International Conference on Biomedical Robotics and Biomechatronics (BioRob)*, pages 1038–1045, 2012.

[140] Issei Onda, Kenjiro Tadakuma, Masahiro Watanabe, Kazuki Abe, Tetsuyou Watanabe, Masashi Konyo, and Satoshi Tadokoro. Highly articulated tube

mechanism with variable stiffness and shape restoration using a pneumatic actuator. *IEEE Robotics and Automation Letters*, 7(2):3664–3671, 2022.

[141] Anke Van Oosterhout and Eve Hoggan. Deformation techniques for shape changing interfaces. Association for Computing Machinery, 5 2021.

[142] Jifei Ou, Zhao Ma, Jannik Peters, Sen Dai, Nikolaos Vlavianos, and Hiroshi Ishii. Kinetix - designing auxetic-inspired deformable material structures. *Computers and Graphics (Pergamon)*, 75:72–81, 10 2018.

[143] Jifei Ou, Mélina Skouras, Nikolaos Vlavianos, Felix Heibeck, Chin-Yi Cheng, Jannik Peters, and Hiroshi Ishii. Aeromorph - heat-sealing inflatable shape-change materials for interaction design. In *Proceedings of the 29th Annual Symposium on User Interface Software and Technology*, UIST '16, page 121–132, New York, NY, USA, 10 2016. Association for Computing Machinery.

[144] Jifei Ou, Lining Yao, Daniel Tauber, Jürgen Steimle, Ryuma Niiyama, and Hiroshi Ishii. jamsheets. pages 65–72. ACM Press, 2013.

[145] Julian Panetta, Florin Isvoranu, Tian Chen, Emmanuel Siéfert, Benoît Roman, and Mark Pauly. Computational inverse design of surface-based inflatables. *ACM Trans. Graph.*, 40(4), jul 2021.

[146] Jefferson Pardomuan, Nobuhiro Takahashi, and Hideki Koike. Astre: Prototyping technique for modular soft robots with variable stiffness. *IEEE Access*, 10:80495–80504, 2022.

[147] Amanda Parkes and Hiroshi Ishii. Bosu: A physical programmable design tool for transformability with soft mechanics. In *Proceedings of the 8th ACM Conference on Designing Interactive Systems*, DIS '10, page 189–198, New York, NY, USA, 2010. Association for Computing Machinery.

[148] Amanda J. Parkes, Hayes Solos Raffle, and Hiroshi Ishii. Topobo in the wild: Longitudinal evaluations of educators appropriating a tangible interface. In *Proceedings of the SIGCHI Conference on Human Factors in Computing Systems*, CHI '08, page 1129–1138, New York, NY, USA, 2008. Association for Computing Machinery.

[149] Bryan N. Peele, Thomas J. Wallin, Huichan Zhao, and Robert F. Shepherd. 3d printing antagonistic systems of artificial muscle using projection stereolithography. *Bioinspiration and Biomimetics*, 10, 9 2015.

[150] Laura Perovich, Philippa Mothersill, and Jennifer Broutin Farah. Awakened apparel: Embedded soft actuators for expressive fashion and functional garments. In *Proceedings of the 8th International Conference on Tangible, Embedded and Embodied Interaction*, TEI '14, page 77–80, New York, NY, USA, 2014. Association for Computing Machinery.

[151] Phuoc Thien Phan, Mai Thanh Thai, Trung Thien Hoang, James Davies, Chi Cong Nguyen, Hoang-Phuong Phan, Nigel H. Lovell, and Thanh Nho Do. Smart textiles using fluid-driven artificial muscle fibers. *Scientific Reports*, 12(1), June 2022.

[152] Ben Piper, Carlo Ratti, and Hiroshi Ishii. Illuminating clay: A 3-d tangible interface for landscape analysis. In *Proceedings of the SIGCHI Conference on Human Factors in Computing Systems*, CHI '02, page 355–362, New York, NY, USA, 2002. Association for Computing Machinery.

[153] Ryan Poon and Jonathan B. Hopkins. Phase-changing metamaterial capable of variable stiffness and shape morphing. *Advanced Engineering Materials*, 21(12):1900802, 2019.

[154] Ivan Poupyrev, Tatsushi Nashida, Shigeaki Maruyama, Jun Rekimoto, and Yasufumi Yamaji. Lumen: interactive visual and shape display for calm com-

puting. In Heather Elliott-Famularo, editor, *SIGGRAPH Emerging Technologies*, page 17. ACM, 2004.

[155] Ivan Poupyrev, Tatsushi Nashida, and Makoto Okabe. Actuation and tangible user interfaces: The vaucanson duck, robots, and shape displays. In *Proceedings of the 1st International Conference on Tangible and Embedded Interaction*, TEI '07, page 205–212, New York, NY, USA, 2007. Association for Computing Machinery.

[156] S Pourazadi, Huythong Bui, and C Menon. Investigation on a soft grasping gripper based on dielectric elastomer actuators. *Smart Materials and Structures*, 28(3):035009, February 2019.

[157] Purnendu, Sasha M. Novack, Eric Acome, Christoph Keplinger, Mirela Alistar, Mark D. Gross, Carson Bruns, and Daniel Leithinger. Electriflow: Soft electrohydraulic building blocks for prototyping shape-changing interfaces. pages 1280–1290. Association for Computing Machinery, Inc, 6 2021.

[158] Isabel P. S. Qamar, Rainer Groh, David Holman, and Anne Roudaut. Hci meets material science: A literature review of morphing materials for the design of shape-changing interfaces. In *Proceedings of the 2018 CHI Conference on Human Factors in Computing Systems*, CHI '18, page 1–23, New York, NY, USA, 2018. Association for Computing Machinery.

[159] Hayes Raffle, Mitchell W. Joachim, and James Tichenor. Super cilia skin: An interactive membrane. In *CHI '03 Extended Abstracts on Human Factors in Computing Systems*, CHI EA '03, page 808–809, New York, NY, USA, 2003. Association for Computing Machinery.

[160] Raf Ramakers, Johannes Schöning, and Kris Luyten. Paddle: Highly deformable mobile devices with physical controls. In *Proceedings of the SIGCHI Conference on Human Factors in Computing Systems*, CHI '14, page 2569–2578, New York, NY, USA, 2014. Association for Computing Machinery.

[161] Majken K. Rasmussen, Esben W. Pedersen, Marianne G. Petersen, and Kasper Hornbæk. Shape-changing interfaces: A review of the design space and open research questions. In *Proceedings of the SIGCHI Conference on Human Factors in Computing Systems*, CHI '12, page 735–744, New York, NY, USA, 2012. Association for Computing Machinery.

[162] Lizette Reitsma, Andrew Smith, and Elise van den Hoven. Storybeads: Preserving indigenous knowledge through tangible interaction design. In *2013 International Conference on Culture and Computing*, pages 79–85, 2013.

[163] Devin J. Roach, Chao Yuan, Xiao Kuang, Vincent Chi-Fung Li, Peter Blake, Marta Lechuga Romero, Irene Hammel, Kai Yu, and H. Jerry Qi. Long liquid crystal elastomer fibers with large reversible actuation strains for smart textiles and artificial muscles. *ACS Applied Materials & Interfaces*, 11(21):19514–19521, 2019.

[164] Anne Roudaut, Rebecca Reed, Tianbo Hao, and Sriram Subramanian. Changibles: Analyzing and designing shape changing constructive assembly. pages 2593–2596. Association for Computing Machinery, 2014.

[165] S-muscle.co. S-muscle.co. `https://www.s-muscle.com/`. Accessed: 2022-09-3.

[166] Deepak Ranjan Sahoo, Kasper Hornbæk, and Sriram Subramanian. Tablehop: An actuated fabric display using transparent electrodes. In *Proceedings of the 2016 CHI Conference on Human Factors in Computing Systems*, CHI '16, page 3767–3780, New York, NY, USA, 2016. Association for Computing Machinery.

[167] Vanessa Sanchez, Conor J. Walsh, and Robert J. Wood. Textile technology for soft robotic and autonomous garments. *Advanced Functional Materials*, 31(6).

[168] Jessie Lee C. Santiago, Isuru S. Godage, Phanideep Gonthina, and Ian D. Walker. Soft robots and kangaroo tails: Modulating compliance in continuum structures through mechanical layer jamming. *Soft Robotics*, 3(2):54–63, June 2016.

[169] Harpreet Sareen, Udayan Umapathi, Patrick Shin, Yasuaki Kakehi, Jifei Ou, Hiroshi Ishii, and Pattie Maes. Printflatables: Printing human-scale, functional and dynamic inflatable objects. In *Proceedings of the 2017 CHI Conference on Human Factors in Computing Systems*, volume 2017-May of *CHI '17*, page 3669–3680, New York, NY, USA, 5 2017. Association for Computing Machinery.

[170] Toshiki Sato, Haruko Mamiya, Hideki Koike, and Kentaro Fukuchi. Photoelastictouch: Transparent rubbery tangible interface using an lcd and photoelasticity. In *Proceedings of the 22nd Annual ACM Symposium on User Interface Software and Technology*, UIST '09, page 43–50, New York, NY, USA, 2009. Association for Computing Machinery.

[171] Toshiki Sato, Jefferson Pardomuan, Yasushi Matoba, and Hideki Koike. Claytricsurface: An interactive deformable display with dynamic stiffness control. *IEEE Computer Graphics and Applications*, 34:59–67, 5 2014.

[172] Valkyrie Savage, Ryan Schmidt, Tovi Grossman, George Fitzmaurice, and Björn Hartmann. A series of tubes: Adding interactivity to 3d prints using internal pipes. In *Proceedings of the 27th Annual ACM Symposium on User Interface Software and Technology*, UIST '14, page 3–12, New York, NY, USA, 2014. Association for Computing Machinery.

[173] Valkyrie Savage, Carlos Tejada, Mengyu Zhong, Raf Ramakers, Daniel Ashbrook, and Hyunyoung Kim. Airlogic: Embedding pneumatic computation and i/o in 3d models to fabricate electronics-free interactive objects. In *Proceedings of the 35th Annual ACM Symposium on User Interface Software and*

Technology, UIST '22, New York, NY, USA, 2022. Association for Computing Machinery.

[174] François Schmitt, Olivier Piccin, Laurent Barbé, and Bernard Bayle. Soft robots manufacturing: A review. *Frontiers Robotics AI*, 5, 2018.

[175] Philipp Schoessler, Daniel Windham, Daniel Leithinger, Sean Follmer, and Hiroshi Ishii. Kinetic blocks: Actuated constructive assembly for interaction and display. In *Proceedings of the 28th Annual ACM Symposium on User Interface Software and amp; Technology*, UIST '15, page 341–349, New York, NY, USA, 2015. Association for Computing Machinery.

[176] Jun Shintake, Bryan Schubert, Samuel Rosset, Herbert Shea, and Dario Floreano. Variable stiffness actuator for soft robotics using dielectric elastomer and low-melting-point alloy. *2015 IEEE/RSJ International Conference on Intelligent Robots and Systems (IROS)*, 2015-December:1097–1102, 9 2015.

[177] Ali Shtarbanov. Flowio development platform – the pneumatic "raspberry pi" for soft robotics. In *Extended Abstracts of the 2021 CHI Conference on Human Factors in Computing Systems*, CHI EA '21, New York, NY, USA, 5 2021. Association for Computing Machinery.

[178] Mélina Skouras, Bernhard Thomaszewski, Peter Kaufmann, Akash Garg, Bernd Bickel, Eitan Grinspun, and Markus Gross. Designing inflatable structures. *ACM Trans. Graph.*, 33(4), jul 2014.

[179] Andrew A. Stanley, Kenji Hata, and Allison M. Okamura. Closed-loop shape control of a haptic jamming deformable surface. In *2016 IEEE International Conference on Robotics and Automation (ICRA)*, pages 2718–2724, 2016.

[180] Anthony Steed, Eyal Ofek, Mike Sinclair, and Mar Gonzalez-Franco. A mechatronic shape display based on auxetic materials. *Nature Communications*, 12(1), August 2021.

[181] Jürgen Steimle, Andreas Jordt, and Pattie Maes. Flexpad: Highly flexible bending interactions for projected handheld displays. In *Proceedings of the SIGCHI Conference on Human Factors in Computing Systems*, CHI '13, page 237–246, New York, NY, USA, 2013. Association for Computing Machinery.

[182] E. Steltz, A. Mozeika, N. Rodenberg, E. Brown, and H.M. Jaeger. Jsel: Jamming skin enabled locomotion. pages 5672–5677. IEEE, 10 2009.

[183] Evan Strasnick, Jackie Yang, Kesler Tanner, Alex Olwal, and Sean Follmer. Shiftio: Reconfigurable tactile elements for dynamic affordances and mobile interaction. In *Proceedings of the 2017 CHI Conference on Human Factors in Computing Systems*, CHI '17, page 5075–5086, New York, NY, USA, 2017. Association for Computing Machinery.

[184] Miriam Sturdee and Jason Alexander. Analysis and classification of shape-changing interfaces for design and application-based research. *ACM Comput. Surv.*, 51(1), jan 2018.

[185] Lingyun Sun, Jiaji Li, Yu Chen, Yue Yang, Zhi Yu, Danli Luo, Jianzhe Gu, Lining Yao, Ye Tao, and Guanyun Wang. Flextruss: A computational threading method for multi-material, multi-form and multi-use prototyping. In *Proceedings of the 2021 CHI Conference on Human Factors in Computing Systems*, CHI '21, New York, NY, USA, 2021. Association for Computing Machinery.

[186] Lingyun Sun, Yue Yang, Yu Chen, Jiaji Li, Danli Luo, Haolin Liu, Lining Yao, Ye Tao, and Guanyun Wang. Shrincage: 4d printing accessories that self-adapt. In *Proceedings of the 2021 CHI Conference on Human Factors in Computing Systems*, CHI '21, New York, NY, USA, 2021. Association for Computing Machinery.

[187] Ruojia Sun, Ryosuke Onose, Margaret Dunne, Andrea Ling, Amanda Denham, and Hsin-Liu (Cindy) Kao. Weaving a second skin: Exploring oppor-

tunities for crafting on-skin interfaces through weaving. In *Proceedings of the 2020 ACM Designing Interactive Systems Conference*, DIS '20, page 365–377, New York, NY, USA, 2020. Association for Computing Machinery.

[188] Ivan E. Sutherland. The ultimate display. In *Proceedings of the Congress of the Internation Federation of Information Processing (IFIP)*, volume volume 2, pages 506–508, 1965.

[189] Ryo Suzuki, Ryosuke Nakayama, Dan Liu, Yasuaki Kakehi, Mark D. Gross, and Daniel Leithinger. Lifttiles: Constructive building blocks for prototyping room-scale shape-changing interfaces. In *Proceedings of the Fourteenth International Conference on Tangible, Embedded, and Embodied Interaction*, TEI '20, page 143–151, New York, NY, USA, 2020. Association for Computing Machinery.

[190] Ryo Suzuki, Eyal Ofek, Mike Sinclair, Daniel Leithinger, and Mar Gonzalez-Franco. Hapticbots: Distributed encountered-type haptics for vr with multiple shape-changing mobile robots. In *The 34th Annual ACM Symposium on User Interface Software and Technology*, UIST '21, page 1269–1281, New York, NY, USA, 2021. Association for Computing Machinery.

[191] Ryo Suzuki, Clement Zheng, Yasuaki Kakehi, Tom Yeh, Ellen Yi-Luen Do, Mark D. Gross, and Daniel Leithinger. Shapebots: Shape-changing swarm robots. In *Proceedings of the 32nd Annual ACM Symposium on User Interface Software and Technology*, UIST '19, page 493–505, New York, NY, USA, 2019. Association for Computing Machinery.

[192] K. Suzumori, S. Iikura, and H. Tanaka. Flexible microactuator for miniature robots. *[1991] Proceedings. IEEE Micro Electro Mechanical Systems*, pages 204–209, 1991.

[193] Faisal Taher, John Hardy, Abhijit Karnik, Christian Weichel, Yvonne Jansen, Kasper Hornbæk, and Jason Alexander. Exploring interactions with physi-

cally dynamic bar charts. In *Proceedings of the 33rd Annual ACM Conference on Human Factors in Computing Systems*. ACM, April 2015.

[194] Faisal Taher, John Vidler, and Jason Alexander. A characterization of actuation techniques for generating movement in shape-changing interfaces. *International Journal of Human–Computer Interaction*, 33(5):385–398, October 2016.

[195] Yasaman Tahouni, Isabel P. S. Qamar, and Stefanie Mueller. Nurbsforms: A modular shape-changing interface for prototyping curved surfaces. In *Proceedings of the Fourteenth International Conference on Tangible, Embedded, and Embodied Interaction*, TEI '20, page 403–409, New York, NY, USA, 2020. Association for Computing Machinery.

[196] Nobuhiro Takahashi, Shinichi Furuya, and Hideki Koike. Soft exoskeleton glove with human anatomical architecture: Production of dexterous finger movements and skillful piano performance. *IEEE Transactions on Haptics*, 13:679–690, 10 2020.

[197] Yichao Tang, Yinding Chi, Jiefeng Sun, Tzu-Hao Huang, Omid H. Maghsoudi, Andrew Spence, Jianguo Zhao, Hao Su, and Jie Yin. Leveraging elastic instabilities for amplified performance: Spine-inspired high-speed and high-force soft robots. *Science Advances*, 6(19), 2020.

[198] Ye Tao, Guanyun Wang, Caowei Zhang, Nannan Lu, Xiaolian Zhang, Cheng Yao, and Fangtian Ying. Weavemesh: A low-fidelity and low-cost prototyping approach for 3d models created by flexible assembly. In *Proceedings of the 2017 CHI Conference on Human Factors in Computing Systems*, CHI '17, page 509–518, New York, NY, USA, 2017. Association for Computing Machinery.

[199] Ye Tao, Shuhong Wang, Junzhe Ji, Linlin Cai, Hongmei Xia, Zhiqi Wang, Jinghai He, Yitao Fan, Shengzhang Pan, Jinghua Xu, Cheng Yang, Lingyun

Sun, and Guanyun Wang. 4doodle: 4d printing artifacts without 3d printers. In *Proceedings of the 2023 CHI Conference on Human Factors in Computing Systems*, CHI '23, New York, NY, USA, 2023. Association for Computing Machinery.

[200] Carlos E. Tejada, Raf Ramakers, Sebastian Boring, and Daniel Ashbrook. Airtouch: 3d-printed touch-sensitive objects using pneumatic sensing. In *Proceedings of the 2020 CHI Conference on Human Factors in Computing Systems*, CHI '20, page 1–10, New York, NY, USA, 2020. Association for Computing Machinery.

[201] Shan-Yuan Teng, Tzu-Sheng Kuo, Chi Wang, Chi-huan Chiang, Da-Yuan Huang, Liwei Chan, and Bing-Yu Chen. Pupop: Pop-up prop on palm for virtual reality. In *Proceedings of the 31st Annual ACM Symposium on User Interface Software and Technology*, UIST '18, page 5–17, New York, NY, USA, 2018. Association for Computing Machinery.

[202] John Tiab, Sebastian Boring, Paul Strohmeier, Anders Markussen, Jason Alexander, and Kasper Hornbæk. Tiltstacks: Composing shape-changing interfaces using tilting and stacking of modules. In *Proceedings of the 2018 International Conference on Advanced Visual Interfaces*, AVI '18, New York, NY, USA, 2018. Association for Computing Machinery.

[203] Skylar Tibbits. 4d printing: Multi-material shape change. *Architectural Design*, 84:116–121, 1 2014.

[204] Jonas Togler, Fabian Hemmert, and Reto Wettach. Living interfaces: The thrifty faucet. In *Proceedings of the 3rd International Conference on Tangible and Embedded Interaction*, TEI '09, page 43–44, New York, NY, USA, 2009. Association for Computing Machinery.

[205] Michael T. Tolley, Robert F. Shepherd, Michael Karpelson, Nicholas W. Bartlett, Kevin C. Galloway, Michael Wehner, Rui Nunes, George M. White-

sides, and Robert J. Wood. An untethered jumping soft robot. In *2014 IEEE/RSJ International Conference on Intelligent Robots and Systems*, pages 561–566, 2014.

[206] Deepak Trivedi, Christopher D. Rahn, William M. Kier, and Ian D. Walker. Soft robotics: Biological inspiration, state of the art, and future research. *Applied Bionics and Biomechanics*, 5:99–117, 2008.

[207] Martin Tschiersky, Edsko E.G. Hekman, Dannis M. Brouwer, Just L. Herder, and Koichi Suzumori. A compact mckibben muscle based bending actuator for close-to-body application in assistive wearable robots. *IEEE Robotics and Automation Letters*, 5:3042–3049, 4 2020.

[208] Shuhei Umezu, Masaru Ohkubo, Yoshiharu Ooide, and Takuya Nojima. Hairlytop interface: A basic tool for active interfacing. In *Adjunct Proceedings of the 27th Annual ACM Symposium on User Interface Software and Technology*, UIST '14 Adjunct, page 95–96, New York, NY, USA, 2014. Association for Computing Machinery.

[209] Daniela Ghanbari Vahid, Lee Jones, Audrey Girouard, and Lois Frankel. Shape changing fabric samples for interactive fashion design. In *Proceedings of the Fifteenth International Conference on Tangible, Embedded, and Embodied Interaction*, TEI '21, New York, NY, USA, 2021. Association for Computing Machinery.

[210] Teunis van Manen, Shahram Janbaz, and Amir A. Zadpoor. Programming the shape-shifting of flat soft matter. *Materials Today*, 21(2):144–163, 2018.

[211] Marynel Vázquez, Eric Brockmeyer, Ruta Desai, Chris Harrison, and Scott E. Hudson. 3d printing pneumatic device controls with variable activation force capabilities. In *Proceedings of the 33rd Annual ACM Conference on Human Factors in Computing Systems*, CHI '15, page 1295–1304, New York, NY, USA, 2015. Association for Computing Machinery.

[212] Iddo Yehoshua Wald and Oren Zuckerman. Magnetform: A shape-change display toolkit for material-oriented designers. Association for Computing Machinery, Inc, 2 2021.

[213] Guanyun Wang, Tingyu Cheng, Youngwook Do, Humphrey Yang, Ye Tao, Jianzhe Gu, Byoungkwon An, and Lining Yao. Printed paper actuator: A low-cost reversible actuation and sensing method for shape changing interfaces. In *Proceedings of the 2018 CHI Conference on Human Factors in Computing Systems*, CHI '18, page 1–12, New York, NY, USA, 2018. Association for Computing Machinery.

[214] Guanyun Wang, Ye Tao, Ozguc Bertug Capunaman, Humphrey Yang, and Lining Yao. A-line: 4d printing morphing linear composite structures. In *Proceedings of the 2019 CHI Conference on Human Factors in Computing Systems*, CHI '19, page 1–12, New York, NY, USA, 5 2019. Association for Computing Machinery.

[215] Guanyun Wang, Kuangqi Zhu, Lingchuan Zhou, Mengyan Guo, Haotian Chen, Zihan Yan, Deying Pan, Yue Yang, Jiaji Li, Jiang Wu, Ye Tao, and Lingyun Sun. Pneufab: Designing low-cost 3d-printed inflatable structures for blow molding artifacts. In *Proceedings of the 2023 CHI Conference on Human Factors in Computing Systems*, CHI '23, New York, NY, USA, 2023. Association for Computing Machinery.

[216] Wen Wang, Lining Yao, Teng Zhang, Chin-Yi Cheng, Daniel Levine, and Hiroshi Ishii. Transformative appetite: Shape-changing food transforms from 2d to 3d by water interaction through cooking. In *Proceedings of the 2017 CHI Conference on Human Factors in Computing Systems*, CHI '17, page 6123–6132, New York, NY, USA, 2017. Association for Computing Machinery.

[217] Yifan Wang, Liuchi Li, Douglas Hofmann, José E. Andrade, and Chiara

Daraio. Structured fabrics with tunable mechanical properties. *Nature*, 596:238–243, 8 2021.

[218] Penelope Webb, Valentina Sumini, Amos Golan, and Hiroshi Ishii. Auto-inflatables: Chemical inflation for pop-up fabrication. In *Extended Abstracts of the 2019 CHI Conference on Human Factors in Computing Systems*, CHI EA '19, page 1–6, New York, NY, USA, 2019. Association for Computing Machinery.

[219] Carol Wilcox Wells. *Creative bead weaving: A contemporary guide to classic off-loom stitches*. Lark Books, 1998.

[220] Michael Wessely, Theophanis Tsandilas, and Wendy E. Mackay. Stretchis: Fabricating highly stretchable user interfaces. In *Proceedings of the 29th Annual Symposium on User Interface Software and Technology*, UIST '16, page 697–704, New York, NY, USA, 2016. Association for Computing Machinery.

[221] George M. Whitesides. Soft-robotik. *Angewandte Chemie*, 130:4336–4353, 4 2018.

[222] Sebastian Wolf, Giorgio Grioli, Oliver Eiberger, Werner Friedl, Markus Grebenstein, Hannes Höppner, Etienne Burdet, Darwin G. Caldwell, Raffaella Carloni, Manuel G. Catalano, Dirk Lefeber, Stefano Stramigioli, Nikos Tsagarakis, Michaël Van Damme, Ronald Van Ham, Bram Vanderborght, Ludo C. Visser, Antonio Bicchi, and Alin Albu-Schäffer. Variable stiffness actuators: Review on design and components. *IEEE/ASME Transactions on Mechatronics*, 21(5):2418–2430, 2016.

[223] Matheus S. Xavier, Charbel D. Tawk, Ali Zolfagharian, Joshua Pinskier, David Howard, Taylor Young, Jiewen Lai, Simon M. Harrison, Yuen K. Yong, Mahdi Bodaghi, and Andrew J. Fleming. Soft pneumatic actuators: A review of design, fabrication, modeling, sensing, control and applications. *IEEE Access*, 10:59442–59485, 2022.

[224] Junichi Yamaoka, Ryuma Niiyama, and Yasuaki Kakehi. Blowfab: Rapid prototyping for rigid and reusable objects using inflation of laser-cut surfaces. In *Proceedings of the 30th Annual ACM Symposium on User Interface Software and Technology*, UIST '17, page 461–469, New York, NY, USA, 2017. Association for Computing Machinery.

[225] Zeyu Yan and Huaishu Peng. Fabhydro: Printing interactive hydraulic devices with an affordable sla 3d printer. pages 298–311. Association for Computing Machinery, Inc, 10 2021.

[226] Yang Yang, Yazhan Zhang, Zicheng Kan, Jielin Zeng, and Michael Yu Wang. Hybrid jamming for bioinspired soft robotic fingers. *Soft Robotics*, 7(3):292–308, June 2020.

[227] Lining Yao, Ryuma Niiyama, Jifei Ou, Sean Follmer, Clark Della Silva, and Hiroshi Ishii. Pneui: Pneumatically actuated soft composite materials for shape changing interfaces. In *Proceedings of the 26th Annual ACM Symposium on User Interface Software and Technology*, UIST '13, page 13–22, New York, NY, USA, 2013. Association for Computing Machinery.

[228] Shunsuke Yoshimoto, Yuki Hamada, Takahiro Tokui, Tetsuya Suetake, Masataka Imura, Yoshihiro Kuroda, and Osamu Oshiro. Haptic canvas: Dilatant fluid based haptic interaction. In *ACM SIGGRAPH 2010 Emerging Technologies*, SIGGRAPH '10, New York, NY, USA, 2010. Association for Computing Machinery.

[229] Hye Jun Youn and Ali Shtarbanov. Pneubots: Modular inflatables for playful exploration of soft robotics. Association for Computing Machinery, 4 2022.

[230] Taylor R. Young, Matheus S. Xavier, Yuen K. Yong, and Andrew J. Fleming. A control and drive system for pneumatic soft robots: Pneusord. In *2021 IEEE/RSJ International Conference on Intelligent Robots and Systems (IROS)*, pages 2822–2829, 2021.

[231] Christopher Yu, Keenan Crane, and Stelian Coros. Computational design of telescoping structures. *ACM Trans. Graph.*, 36(4), jul 2017.

[232] Michelle C. Yuen, R. Adam Bilodeau, and Rebecca K. Kramer. Active variable stiffness fibers for multifunctional robotic fabrics. *IEEE Robotics and Automation Letters*, 1(2):708–715, 2016.

[233] Ulrich Z, Eppinger T, and Steven D. *Product Design and development*. 2016.

[234] Junshi Zhang, Lei Liu, Yuyu Chen, Mingliang Zhu, Liling Tang, Chao Tang, Jun Shintake, Junjie Zhao, Jiankang He, Xiaoyong Ren, Pengfei Li, Qiang Huang, Huichan Zhao, Jian Lu, and Dichen Li. Fiber-reinforced soft polymeric manipulator with smart motion scaling and stiffness tunability. *Cell Reports Physical Science*, 2, 10 2021.

[235] Xinlei Zhang, Ali Shtarbanov, Jiani Zeng, Valerie K. Chen, V. Michael Bove, Pattie Maes, and Jun Rekimoto. Bubble: Wearable assistive grasping augmentation based on soft inflatables. In *Extended Abstracts of the 2019 CHI Conference on Human Factors in Computing Systems*, CHI EA '19, page 1–6, New York, NY, USA, 2019. Association for Computing Machinery.

[236] Mengjia Zhu, Amirhossein H. Memar, Aakar Gupta, Majed Samad, Priyanshu Agarwal, Yon Visell, Sean J. Keller, and Nicholas Colonnese. Pneusleeve: In-fabric multimodal actuation and sensing in a soft, compact, and expressive haptic sleeve. In *Proceedings of the 2020 CHI Conference on Human Factors in Computing Systems*, CHI '20, page 1–12, New York, NY, USA, 2020. Association for Computing Machinery.